

**Development of a controller using modified Active
Disturbance Rejection Control technique**

A THESIS

submitted by

PARVATHY R

(Reg. No. 4028)

for the award of the degree

of

DOCTOR OF PHILOSOPHY



**Division of Electrical Engineering
School of Engineering
Cochin University of Science and Technology
September 2018**

THESIS CERTIFICATE

This is to certify that the thesis entitled **Development of a controller using modified Active Disturbance Rejection Control technique** submitted by **Parvathy R** to the Cochin University of Science and Technology, Kochi for the award of the degree of Doctor of Philosophy is a bonafide record of research work carried out by her under my supervision and guidance at the Division of Electrical Engineering, School of Engineering, Cochin University of Science and Technology. The contents of this thesis, in full or in parts, have not been submitted to any other University or Institute for the award of any degree or diploma.

I further certify that the corrections and modifications suggested by the audience during the pre-synopsis seminar and recommended by the Doctoral committee of **Parvathy R** are incorporated in the thesis.

Place: Kochi

5-09-2018

Dr. Asha Elizabeth Daniel

Research Guide

Professor

Division of Electrical Engineering

School of Engineering

CUSAT, Kochi - 682 022

DECLARATION

I hereby declare that the work presented in the thesis entitled **Development of a controller using modified Active Disturbance Rejection Control technique** is based on the original research work carried out by me under the supervision and guidance of Dr. Asha Elizabeth Daniel, Professor, Division of Electrical Engineering, School of Engineering, Cochin University of Science and Technology for the award of the degree of Doctor of Philosophy. I further declare that the contents of this thesis in full or in parts have not been submitted to any other University or Institute for the award of any degree or diploma.

Place: Kochi

Parvathy R

5 - 09 - 2018

DEDICATION

Dedicated to my teachers ...

ACKNOWLEDGEMENTS

At the outset I thank my research guide Dr. Asha Elizabeth Daniel, Professor, Division of Electrical Engineering, SOE, CUSAT, for her diligent guidance, scrupulous mentoring, patient listening and constant support through out the research. My heartfelt gratitude for the punctilious efforts extended during the thesis correction.

I am grateful to Dr. M.R.Radhakrishna Panicker, Principal, School of Engineering, and Dr. P. S. Sreejith, Dean, Faculty of Engineering, for providing all the necessary facilities for research. I thank Dr. Usha Nair, my Doctoral Committee Member, for her timely suggestions and support. My special regards for the valuable suggestions during the term evaluation sessions by Dr. C.A.Babu, Professor and Head of the Department, Division of Electrical Engineering, SOE, CUSAT. I thank Dr. Biju N., Professor of Mechanical Engineering, SOE for the pertinent questions during the presynopsis seminar. I thank Dr. K.S.Beena, Professor of Civil Engineering, SOE and my friend Lakshmi for their many inspiring words.

My unbounded thanks to Dr. Pailo Paul, who introduced me to my guide and helped me realise my PhD admission. I remember the “sparking” words of my Professor and mentor at I.I.T. Madras, Dr. P.A.Janakiraman, who kindled in me the idea of doing a research work. I thank Dr. Zhiqiang Gao, Professor, Cleveland State University for promptly clearing many of my doubts through emails during my research work. I take this as a golden opportunity to thank all my teachers, especially Krishna Pillai Sir, my first teacher for the conscious motivation in my studies.

FISAT management always supports for any academic improvement program for faculty. Sincere thanks for all the support extended to me. I deeply acknowledge the progressionist mind of Late Adv.P.V. Mathew who permitted me to do the re-

search work, without a second thought. My sincere thanks to Dr. K.S.M.Panicker who was always a great encouragement to pursue my higher studies. I appreciate the care and support extended to me by my PhD colleagues during the course work. I thank Mr. Bejoy Varghese, Mr. Mahesh C for their constant motivation. My colleagues in the department had helped me a lot in the department duties, which would have affected my research work many a times. I thank all of them for the constant motivation extended to me. I deeply thank Mr. Saju Kuriakose, Electrical Lab Instructor, FISAT for the help extended during my experimental studies in the Control and Power Electronics Lab and Centre for Advanced Research in Power Electronics (CARPC), FISAT. My indebted thanks to Mr. Muhamed Noufal, Assistant Professor, Department of EEE, FISAT for the seamless support and brilliant ideas during the hard times of the experimental work. This work would not have turned into this form without his relentless help.

This is a befitting opportunity to remember my grand parents for the limitless love and care extended to me. My dearest parents Mr. G.Gopalakrishna Pillai and Mrs.Rani Rajini Devi are the greatest source of motivation and inspiration for me. No words can express my thanks to them. I am deeply indebted to them. Deepest gratitude to my love and life, my husband Mr.Unni Kartha, for being an unflinching supporter for me all through my times. I remember how patiently he handled even my pestering requests in finding suitable word phrases during the thesis writing. Many thanks to my younger brother Gopi, sister Devu and little Saanvi for refrained me by their presence in many of the family functions. With deep lament, I remember the contented words and encouragements given by my father-in-law who left us during the course of my thesis work. I also thank my mother-in-law for her support during my work. I thank Janaki Chechi for sparing me from my household chores so that I could peacefully write my thesis.

Lastly I thank Shri Shirdi Sai for showering the limitless blessings upon me and my family and helped me to bring the work to this final form.

ABSTRACT

KEYWORDS: Active Disturbance Rejection Control; Extended State Observer; Critical Observer Bandwidth; Permanent Magnet DC Motor

The empirical approach of the PID presents a limitation in tuning for practicing engineers, since it requires ample experience and sound knowledge of the plant. Tuning of controllers in model based approach was challenging due to the mismatch of the actual system with approximate model. This situation demanded a model independent approach to take care of the uncertainties of the plant, including the disturbances and the unknown dynamics of the plant. Active Disturbance Rejection Control (ADRC) came up at this juncture as a robust, model less control technique in the early 21st century. This control strategy started as a potential replacement for the long flourished PID controllers, more commonly PI controllers, in industrial control sector. The thesis proposes a modification to the conventional topology of ADRC and discusses the implementation of this modified approach in the speed control of a permanent magnet dc motor. The inevitable role of Extended State Observer in the improved performance of ADRC is undoubtedly certain. A critical observer bandwidth beyond which the performance of modified ADRC wanes, due to the loss of estimation property of its integrant ESO, is brought out through this work. The discussion progresses in establishing the necessity of identifying an optimal observer bandwidth through which modified ADRC can out perform a PI controller. Finally the development of a controller based on the modified ADRC which reduces the mathematical complexity of implementation is presented.

TABLE OF CONTENTS

ACKNOWLEDGEMENTS	iii
ABSTRACT	v
ABBREVIATIONS	xiii
NOTATIONS	xiv
1 INTRODUCTION	1
1.1 Historical background	1
1.2 Motivation of the research	2
1.3 Objective and Scope	2
1.4 Organisation of the thesis	4
2 LITERATURE SURVEY	5
2.1 Control techniques - A broad classification	5
2.1.1 Error based empirical approach	5
2.1.2 Model based modern control approach	6
2.2 From automatic control to Systems Theory	7
2.3 The need for a paradigm shift	9
2.4 The evolution of the new concept of ADRC	10
2.5 A review on the theoretical justifications related to ADRC	11
2.6 A review on applications of ADRC	14
2.6.1 Motion control	14
2.6.2 MEMS gyroscope	15
2.6.3 Web tension regulators	15
2.6.4 Other applications	16

3	ACTIVE DISTURBANCE REJECTION CONTROL	17
3.1	Introduction	17
3.2	Transient profile generator	18
3.3	Tracking Differentiator (TD)	19
3.4	Nonlinear Controller	20
3.5	Extended State Observer (ESO)	23
3.6	General principle and structure of ADRC	26
3.7	Summary	30
4	EXTENDED STATE OBSERVER	32
4.1	Philosophy of observer design	32
4.2	Effect of pole location on observer characteristics - A simulation approach	34
4.3	Effect of bandwidth on the characteristics of Extended State Observer	42
	4.3.1 A simulation approach	42
	4.3.2 An experimental approach	49
4.4	Results and discussions	50
5	PERFORMANCE ANALYSIS OF PI CONTROLLER - A SIMULATION APPROACH	54
5.1	Modelling of permanent magnet dc motor	54
5.2	Motor specifications	56
5.3	Open loop response	56
5.4	Closed loop performance with Proportional Integral controller	57
	5.4.1 Tuning method	58
	5.4.2 Methodology	59
	5.4.3 Analysis of the performance of PI controller	61
5.5	Results and discussions	65
6	PERFORMANCE ANALYSIS OF MODIFIED ADRC - A SIMULATION APPROACH	70
6.1	Modifications in the topology	70

6.2	Methodology	70
6.3	Results and discussions	87
7	HARDWARE IMPLEMENTATION	89
7.1	Experimental set up	89
7.1.1	Hardware unit	90
7.1.2	Processor unit	94
7.2	Realisation of various constituents of Processor unit	95
7.3	Results and Discussions	98
8	CONCLUSIONS	102
8.1	Summary	102
8.2	Observations	104
8.3	Future scope	104
	LIST OF PAPERS BASED ON THESIS	117
	CURRICULUM VITAE	118

LIST OF FIGURES

3.1 A standard velocity and acceleration profile	18
3.2 Effect of nonlinear function on control input	21
3.3 Effect of <i>fal</i> function on control input	22
3.4 A comparison of nonlinear function and <i>fal</i> function	23
3.5 ADRC Topology initially proposed by Han	26
3.6 Modified II order ADRC topology	26
4.1 Observer based full state feedback system	33
4.2 Comparison of velocity and position estimates with actual values when poles are at $s = (-0.5, -0.5)$	38
4.3 Velocity and position error when poles are at $s = (-0.5, -0.5)$	39
4.4 Comparison of velocity and position estimates with actual values when poles are at $s = (-10, -10)$	40
4.5 Velocity and position error when poles are at $s = (-10, -10)$	41
4.6 An overview of the simulation diagram	43
4.7 The PD controller	43
4.8 DC motor	43
4.9 Effect of ω_0 on u_0	44
4.10 Effect of ω_0 on disturbance estimate	44
4.11 Effect of ω_0 on control voltage	45
4.12 u_0 Vs time when $\omega_0 = 77.1\text{rad/s}$	45
4.13 Disturbance estimate Vs time when $\omega_0 = 77.1\text{rad/s}$	46
4.14 Control voltage Vs time when $\omega_0 = 77.1\text{rad/s}$	46
4.15 u_0 Vs time when $\omega_0 = 80\text{rad/s}$	47
4.16 Disturbance estimate Vs time when $\omega_0 = 80\text{rad/s}$	47
4.17 Control voltage Vs time when $\omega_0 = 80\text{rad/s}$	48

4.18	Comparison of simulated and experimental results of estimated speed for $\omega_0 = 30\text{rad/s}$	51
4.19	Estimation error when $\omega_0 = 30 \text{ rad/s}$	51
4.20	Comparison of simulated and experimental results of estimated speed for $\omega_0 = 70\text{rad/s}$	52
4.21	Estimation error when $\omega_0 = 70 \text{ rad/s}$	52
4.22	Comparison of simulated and experimental results of estimated speed for $\omega_0 = 77.1 \text{ rad/s}$	52
4.23	Estimation error when $\omega_0 = 77.1 \text{ rad/s}$	53
5.1	A block diagram of dc motor	56
5.2	Open loop speed response for a step voltage of 12V	57
5.3	Fixing the ultimate gain during PI tuning	60
5.4	Response of PI controlled system with varied K_p and fixed T_i	63
5.5	Response of PI controlled system with fixed K_p and varied T_i	64
5.6	Response when K_p is decreased from 1.27 to 0.2	66
5.7	Response when K_p is decreased from 0.2 to 0.02	67
5.8	Response when T_i is decreased from 0.0039 to 0.002	68
5.9	Response when K_p is decreased from 0.02 to 0.007	69
6.1	Transient profile for simulation	71
6.2	Reference, actual speed for $\omega_0 = 10\text{rad/s}$	74
6.3	Reference, actual speed for $\omega_0 = 30\text{rad/s}$	74
6.4	Reference, actual speed for $\omega_0 = 60\text{rad/s}$	75
6.5	Reference, actual speed for $\omega_0 = 60\text{rad/s}$	75
6.6	Reference, actual speed for $\omega_0 = 76\text{rad/s}$	76
6.7	Reference, actual speed for $\omega_0 = 76\text{rad/s}$	76
6.8	Reference, actual speed for $\omega_0 = 77 \text{ rad/s}$	77
6.9	Reference, actual speed for $\omega_0 = 78 \text{ rad/s}$	77
6.10	Speeds Vs time when $\omega_0 = 30 \text{ rad/s}$	78
6.11	u_0 Vs time when $\omega_0 = 30 \text{ rad/s}$	79
6.12	Disturbance Vs time when $\omega_0 = 30 \text{ rad/s}$	79

6.13	Control voltage Vs time when $\omega_0 = 30$ rad/s	80
6.14	Speeds Vs time when $\omega_0 = 55$ rad/s	80
6.15	u_0 Vs time when $\omega_0 = 55$ rad/s	81
6.16	Disturbance Vs time when $\omega_0 = 55$ rad/s	81
6.17	Control voltage Vs time when $\omega_0 = 55$ rad/s	82
6.18	Speeds Vs time when $\omega_0 = 70$ rad/s	83
6.19	u_0 Vs time when $\omega_0 = 70$ rad/s	83
6.20	Disturbance Vs time when $\omega_0 = 70$ rad/s	84
6.21	Control voltage Vs time when $\omega_0 = 70$ rad/s	84
6.22	Speeds Vs time $\omega_0 = 74$ rad/s	85
6.23	Speeds Vs time when $\omega_0 = 78$ rad/s	85
6.24	u_0 Vs time when $\omega_0 = 78$ rad/s	86
6.25	Disturbance Vs time when $\omega_0 = 78$ rad/s	86
6.26	Control voltage Vs time when $\omega_0 = 78$ rad/s	87
7.1	Block schematic representation of the test set up	89
7.2	Hardware setup	90
7.3	Circuit setup for the experimental study	91
7.4	Permanent magnet DC motor	92
7.5	Buck converter circuit	93
7.6	Voltage sensing circuit	93
7.7	Speed sensing components	94
7.8	Speed sensing circuit	94
7.9	Simulation result when $\omega_0 = 70$ rad/s	99
7.10	Experimental result when $\omega_0 = 70$ rad/s	99
7.11	Error in speed in simulation when $\omega_0 = 70$ rad/s	100
7.12	Error in speed in experiment when $\omega_0 = 70$ rad/s	100
7.13	Control voltage Vs time	101

LIST OF TABLES

2.1	A consolidated review of the studies on ADRC conducted so far	13
3.1	A comparison of steady state error	21
4.1	Time chart with different observer gains	36
4.2	Time of estimation for different values of ω_0 with an accuracy of 0.1%	49
5.1	DC motor parameters	55
5.2	Motor specifications	56
5.3	Zeigler Nichols tuning table	58
5.4	Effect of PI parameters in system behaviour	62
6.1	% error for different values of ω_0 at 10.07s	73
6.2	Settling time with an accuracy of 0.1% when a constant torque of 0.6Nm is applied at 15s	88
8.1	A performance comparison of ADRC and PI controller	103
8.2	Design Results	103

ABBREVIATIONS

ADRC	Active Disturbance Rejection Control
DOB	Disturbance Observer
EKF	Extended Kalman Filter
ESO	Extended State Observer
IBE	Input Based Estimator
IOBO	Input and Output Based Observer
KF	Kalman Filter
LADRC	Linear ADRC
LESO	Linear ESO
MIMO	Multiple Input Multiple Output
NLADRC	Nonlinear ADRC
NESO	Nonlinear Extended State Observer
OBE	Output Based Estimator
ODE	Ordinary Differential Equations
PID	Proportional-Integral-Derivative
PIO	Proportional Integral Observer
POB	Perturbation Observer
SISO	Single Input Single Output System
TD	Tracking Differentiator
UIO	Unknown Input Observer

NOTATIONS

σ	Attenuation constant
ω_c	Controller bandwidth
ζ	Damping ratio
K_d	Derivative gain constant
T_d	Derivative time constant
K_i	Integral gain constant
T_i	Integral time constant
ω_0	Observer bandwidth
ϕ	Phase shift
K_p	Proportional gain constant
K_u	Ultimate gain
T_u	Ultimate period

CHAPTER 1

INTRODUCTION

1.1 Historical background

Inventions are cumulations of small advancements that reach a critical point. This statement has significant relevance in the history of control systems. The developments in control systems date back to third century BC when a Greek mathematician Ktesibios invented a self regulating valve. A new phase for control theory was marked by the contributions of Maxwell *et al.* (1868), where they highlight the stability issues related to governors, using the concept of differential equations. It was during World War II that the discipline of *feedback control systems* emerged as a result of the interdisciplinary research of mathematicians and engineers from various specialisations. This opened a new era which showed the merging of control theory and mathematics: the era of *Systems Theory*. A significant progress in the development of control system happened when Minorsky (1922) proposed a clear theoretical analysis for the automatic steering of ships using a three term controller called Proportional-Integral-Derivative (PID) controller. The original tuning technique of the classical PID was developed by Ziegler and Nichols (1942). Later on, this very technology spearheaded the industrial revolution.

Though many advances occurred in the field of feedback controllers, classical PID controller continues to rule the industry, since its inception, many decades back. This is mainly due to its constant and simple structure, that requires only repeated tuning to solve various problems. However, PID controllers suffer the major drawback of *repeated tuning* using a trial and error approach. Also, there are situations with ramp set point changes which require considerable performance specifications.

The reactive nature of PID controllers always posed a limitation to its performance in such cases (Sung and Lee, 1996). There are other instances where dynamic response of systems change with operating conditions. These changing operating conditions make it difficult to tune a PID controller to achieve acceptable performance over a broader range of operating conditions (Marlin, 1995). Furthermore, PID controllers exhibit certain limitations in handling disturbances and time delays in systems (Åström and Hägglund, 2001). As experience in tuning played a key role in all the above mentioned situations, control engineers in industry, started demanding a novel robust control technique. It was at this juncture that Han (1999) came up with a promising concept called Active Disturbance Rejection Control (ADRC) which had started gaining significant popularity amongst industrial control engineers since the beginning of 21st century.

1.2 Motivation of the research

The formulation of the control technique called Active Disturbance Rejection Control marked a paradigm shift in the domain of industrial control. This novel concept is capable enough to replace classical PID control from control industry. This had motivated for a research, after identifying certain research gaps, to analyse the performance of ADRC, when applied to a permanent magnet DC motor.

1.3 Objective and Scope

As mentioned earlier, mathematical modelling is an inevitable part of control design. But unfortunately, the non availability of accurate mathematical descriptions for physical plants created design predicaments among practicing engineers. Though robust control strategies emerged as a solution to handle these uncertainties (Chandrasekharan, 1996), they could solve it only to a limited extent. Handling un-

wanted external disturbances creeping into the system was another challenge faced by control design engineers. Many researchers proposed that disturbance estimators could appropriately estimate and eliminate the unwanted disturbances (Brandin, 1988; Profeta *et al.*, 1990; Epstein *et al.*, 1989). Among the many disturbance estimators, Extended State Observer (ESO) stands apart, as it plays a key role in the control approach called Active Disturbance Rejection Control (Gao *et al.*, 2001*b*). This control strategy extracts the required information and then cancels out the effect of unknown internal plant dynamics and external disturbances.

A systematic design approach for Extended State Observer, in the context of ADRC is rarely reported in literature. To validate the design approach, a detailed analysis through simulation and hardware is required.

The objective of this dissertation is to

1. analyse the effect of observer bandwidth on the performance of Extended State Observer and come up with a critical observer bandwidth.
2. analyse the performance of the modified control technique pertaining to changes in observer bandwidth.
3. develop a controller based on the modified Active Disturbance Rejection Control technique, keeping an eye on the critical observer bandwidth, which is a key factor affecting the performance of ADRC and its allied ESO.

The scope of the study is limited to the performance analysis of this control technique from the perspective of a permanent magnet dc motor, which is a fundamental motor. This study can then be extended to any other motor.

1.4 Organisation of the thesis

A literature survey on different control techniques, evolution of the concept of Active Disturbance Rejection Control and its applications are included in **Chapter 2**.

A detailed description of the main theme of the research, *i.e.*, Active Disturbance Rejection Control (ADRC), is given in **Chapter 3**.

Chapter 4 discusses the study conducted to analyse the effect of bandwidth on the performance of the Extended State Observer using simulation approach.

As mentioned in the previous section PI controller suffers a major drawback of repeated tuning of the two controller gains. The tuning method and the challenges faced in tuning are elaborated in **Chapter 5** with a series of simulations. This brings out the need for a novel approach in industrial control domain.

As the Extended State Observer is a key constituent of this controller unit, we can notice that the controller bandwidth and observer bandwidth are intensely related. **Chapter 6** reports a performance evaluation of ADRC in this frame of reference. This lays the foundation for conducting the experimental analysis.

Various aspects of hardware implementation of the modified ADRC are examined in **Chapter 7**.

Finally the thesis concludes with **Chapter 8** which brings out the contributions of the research work and recommendations of probable future work that could be taken forward, gathering the apprehensions gained through this dissertation.

CHAPTER 2

LITERATURE SURVEY

The present chapter narrates an overall classification of the control techniques prevailing in practice and how a transition occurred from classical control to mathematically enriched Systems Theory. A brief note on the need for a shift in the existing control strategy is mentioned here. A survey on the concept of evolution of Active Disturbance Rejection Control, its analysis and engineering applications that utilised this notion are also reported in this chapter.

2.1 Control techniques - A broad classification

Existing control techniques can be broadly classified into

1. Error based technique (Empirical Approach)
2. Model based technique (Modern Control Approach)

2.1.1 Error based empirical approach

The design of such controllers is *not based* on any information of the dynamics of the system. *i.e.*, a mathematical model of the system is not required for its design. The controller design is purely based on observation of the behaviour of the plant. Practitioners in control industry follow such an error based approach for control of processes. They tune these controllers using lookup tables and trial and error techniques which they gained from their vast industrial experience. Hence the name empirical approach. Here the practical design aims in developing a control law that

minimises the error between the process variable and reference tracking signal. The control action largely depends on the present error, the accumulated errors over an interval of time and the prediction of the error variations in the future. PID controller belongs to this category of controllers. The mathematical equations that describe the operation of the established PID controller is empirically deduced without a mathematical system model.

$$u = \mathbf{K}_p e + \mathbf{K}_i \int e dt + \mathbf{K}_d \frac{de}{dt} \quad (2.1)$$

The three parameters of Equation 2.1 are manually tuned to achieve the desired performance. However, it requires tuning of three parameters and the tuning process need to be repeated for varied operating conditions.

2.1.2 Model based modern control approach

The control law for these controllers is designed to suit the model devised for the system. State feedback controllers belong to this category. Their performance primarily depends on the extent to which the mathematical model matches with the actual system. Though the design of these controllers results in acceptable range of performance, they do not often exhibit optimal operating behaviour, primarily due to this model mismatch.

Consider a mathematical relation governing an electromechanical system as given below.

$$\ddot{y} = f(y, \dot{y}, w, t) + bu \quad (2.2)$$

In this model based design, we assume that the required dynamics of the plant is

$$\ddot{y} = g(y, \dot{y}) \quad (2.3)$$

Assuming the system as a disturbance free and linearised one, we can write

$$f(y, \dot{y}, w, t) \approx \bar{f}(y, \dot{y}) \quad (2.4)$$

This reduces equation (2.2), resulting in the control law of (2.5)

$$u = \frac{-\bar{f}(y, \dot{y}) + g(y, \dot{y})}{b} \quad (2.5)$$

In equation (2.5), the effectiveness of the control law u depends much on the closeness of the term $-\bar{f}(y, \dot{y})$, to the actual dynamics of the system. In short, modern control paradigm can be summarised in the following steps:

1. An accurate mathematical model is required to describe the process (2.2).
2. Another mathematical model is required to define the design requirements (2.3). This can even be a cost function to be minimised.
3. A control law is formulated combining the above two (2.5).

2.2 From automatic control to Systems Theory

Most of the early engineering processes were naturally described by Ordinary Differential Equations (ODE). Hence the classical approaches in control theory mainly relied on Linear Ordinary Differential Equations, with constant coefficients. Mathematical control theory had its origin when people started using many mathematical techniques to a large extent, to put the principles of control theory into practice. This is true in all the control systems developed till date: beginning from Watt's steam engine governor to present day autopilots in air planes. By the middle of 20th century, the world of mathematical control theory opened appreciably for researchers. In this context, we cannot forget the remarkable contributions made by a few great mathematicians. These include Dynamic Programming by Richard E. Bellman (1954),

Pontryagin's principle by Lev.S. Pontryagin (2018) and Linear System Theory by Rudolf E. Kalman *et al.* (1969). During the development of modern control theory, it was noticed that the real world was too complex and the mathematical models in use till then, failed to accurately describe the dynamics of the system. Modelling of complex, nonlinear, uncertain, real world systems were beyond the scope of studies till then. Researchers concentrated on bringing a solution to this issue, and many responses to this problem can be found in the literature. Among these are the remarkable contributions of modern control era,

1. Robust Control - A control technique that requires a priori information of the plant dynamics and the bound of uncertainties (Vesely, 2013). In this case, the control law is not changed. The contributions of the Russian control theorist Vladimir Kharitonov (1979) marked a turning point for the developments in robust control. Some examples of robust control techniques are high gain feedback control, Sliding Mode Control (SMC), Variable Structure Control (VSC), loop transfer recovery technique, H_∞ control etc.
2. Adaptive Control - A control technique that does not require a priori information of the plant dynamics and the bound of uncertainties (Landau *et al.*, 2011). In this case, the control law automatically gets adapted to system variations. Some examples of adaptive control techniques commonly used in practice are Deterministic and Stochastic Adaptive Controls, Feedback and Feed-forward Adaptive Controls and Model Reference Adaptive Control. Apart from this, different state-of-the-art adaptive control methods are also reported in literature (Anavatti *et al.*, 2015).

Control theory, thus, started under the name "Automatic Control" gradually moved to a mathematically enriched new phase under the name "Systems Theory". Modern control presumed that mathematical models could be used to effectively describe the dynamics of the plant. Subsequently, the control law was formulated from mathematical descriptions of the plant/process. Obviously, the performance and accuracy

of the controller depend much on the extent to which the mathematical model resembles the system. Thus, the performance of the controller was adversely affected by the uncertainties that were not included in the system model. This made researchers think in the direction of developing some method by which the uncertainties of the system could be adequately tracked. They wanted to make easily tunable, robust and model independent controllers that could compensate unknown dynamics of the plant and the actual disturbances in real time. The conflict between the established modern control theories and primordial practices led to the unabating theory Vs practice hassle. It was this irritating theory-practice gap that kindled the minds of Jingqing Han and triggered him to answer the question of “need for a paradigm shift” (Gao, 2006a).

2.3 The need for a paradigm shift

It was Thomas Kuhn, the American historian and philosopher of science who introduced the term “paradigm shift” for scientific revolutions. According to Kuhn, “paradigms prove to be constitutive of the research activity”. He ascertained that “when paradigms change, there are usually significant shifts in the criteria determining the legitimacy, both of problems and of proposed solutions” (Kuhn and Hawkins, 1963). Mathematics is all about manipulation of abstracts. Hence, as long as we fail to develop a perfect mathematical model of the system under study, the precision of mathematics fails. The words of Albert Einstein perfectly match this context -“As far as the laws of mathematics refer to reality, they are not certain; and as far as they are certain, they do not refer to reality”.

Modern Control Paradigm depended too much on mathematical models, whereas the Empirical Design Paradigm proved inappropriate in uncertain environments, as it is rather an intuitive approach. In short, model-based and error based techniques had their limitations in solving the cardinal issue of *uncertainties* in feedback con-

trol systems. This reinforced the need for a paradigm shift in control theory.

2.4 The evolution of the new concept of ADRC

Unmodelled dynamics, parameter variations due to failure in components and external disturbances largely exist in the processes in nature. These demanded “disturbance rejection” and “control of systems with uncertainty” as a fundamental issue to be solved by researchers working in the field of control systems in recent years. Active Disturbance Rejection Control (ADRC) evolved as a fruitful control technique, that could handle uncertainties of any nature, be it internal or external. Here, the *total disturbances* are included in an extended state variable which is estimated using an Extended State Observer (ESO). The control mechanism, thereby, remains unaffected by any discrepancies in the modelling, as it includes all uncertainties as the extended state variable. Uncertainty reduction and a kind of robustness make this method an interesting solution to problems, in cases where full knowledge of the system is not available.

The concept of ADRC was pioneered by Jingqing Han and contributed through many of his Chinese transcripts, before his last publication (Han, 2009). The term Active Disturbance Rejection Control was systematically used for the first time in English literature and opened to the research world by Zhiqiang Gao in the year 2001 (Gao *et al.*, 2001*b*). Active Disturbance Rejection Control (ADRC) is a robust control strategy, which encompasses the features of, error driven PID and state observer. Here the observer model of the system is extended with a new state variable, which includes all parameter variations, disturbances and internal dynamics that are left unnoticed in the normal plant description. The key idea behind this principle lies in the canonical representation of the Extended State Observer (ESO). The online estimation of this new state is performed using a state observer called ESO, which is used to separate the system and uncertainties, which in turn indirectly

simplifies the closed loop system to a large extent. Due to the real time compensation of the uncertainty, issues in modelling are satisfactorily eliminated. Thus the control mechanism, more or less remains unaffected even in the presence of model discrepancies, parameter variations and external disturbances.

2.5 A review on the theoretical justifications related to ADRC

In the early days of its progress, analysis of ADRC took a slow pace due to its very structure with nonlinear gains. However, studies on convergence of nonlinear ADRC for Single Input Single Output systems (Zhao and Guo, 2016) and Multiple Input Multiple Output systems (Guo and Zhao, 2013) are reported in literature. In the initial years, research attempts resulted only in approximate frequency response of nonlinear ADRC to analyse the extent of disturbance rejection (Gao *et al.*, 2001a). A frequency response analysis of Nonlinear ADRC (NLADRC) was carried out using describing function approach. These studies show that NLADRC exhibited higher control efficiency for linear plants, but with lesser stability (Wu and Chen, 2013).

The linear reduction and gain parameterisation of ADRC by Gao (2006b) simplified the approach and paved the way for many justifications on its potential capabilities. Later, the stability analysis of the ADRC with this linear topology was studied (Zheng *et al.*, 2007c,b). This paper gives an analytical approach that establishes the performance of Linear ADRC (LADRC) achieved in varied classes of plants like nonlinear, time-varying and plants with unknown dynamics. Two extreme cases are considered here.

1. For plants with accurate mathematical model, asymptotic stability is detailed and derived.

2. For plants with unknown dynamics, upper bounds of tracking error and estimation error are defined.

The exponential stability of nonlinear time variant systems with LADRC (Zhou *et al.*, 2009) is dealt with by decomposing the original one into slow subsystem and a fast subsystem. Zhao and Huang (2012) discuss the performance of LADRC in linear time invariant Single Input Single Output minimum phase systems with unknown orders, uncertain relative degrees, and unknown input disturbances. Investigations had been extended to study the performance of LADRC in systems with long dead time and with right half-plane zeros, unstable and of distributed parameters (Chai *et al.*, 2011).

However, a frequency response analysis was inevitable for ADRC to be appreciated by practicing engineers. An initial step in this line on analysing the extent of stability and performance of linear ADRC, through frequency response using a transfer function approach, on highly uncertain linear time invariant systems was justified by Tian and Gao (2007). Csank and Gao (2008) used frequency response approach to explore the disturbance rejection property of linear ADRC. The reports of Xue and Huang (2013a) give a better insight on frequency response analysis of ADRC for uncertain systems. The discussion on the link between time domain and frequency domain characteristics of ADRC solidifies its capability for engineering applications (Xue and Huang, 2013b; Zheng and Gao, 2016). An overall time domain and frequency domain performance analysis of LADRC for plants with uncertain dynamics proves the extent of robustness and ability of disturbance rejection of this promising concept (Xue and Huang, 2015).

It is noticed that the design framework of ADRC applies to all categories of systems like linear, nonlinear, time invariant, time variant, Single Input Single Output (SISO) as well as Multiple Input Multiple Output(MIMO) Systems. The review reports of Huang and Xue (2014) consolidate all facets of the methodology and theoretical aspects of ADRC .

Table 2.1: A consolidated review of the studies on ADRC conducted so far

Type of plant	Objective of study	Topology		Nature of study	
		NLADRC	LADRC	Time domain	Frequency domain
SISO	convergence	x		x	
MIMO	convergence	x		x	
Nonlinear plants	stability, tracking performance	x			x
Nonlinear time varying with unknown dynamics	stability		x	x	
Nonlinear plants	exponential stability		x	x	
Linear SISO minimum phase systems with unknown order	performance and stability		x	x	
Linear time invariant	performance and stability		x		x
Linear time invariant	robustness			x	x
	Critical bandwidth				

The research gap was identified after consolidating the above review. The study is tabulated in Table 2.1. The blank spaces represents the research gaps, while ‘x’ represents the availability of literature.

Along with the developments of ADRC, its various constituents were also the subject of interest for researchers. Theoretical research on the convergence for a second order linear tracking differentiator with any differentiable input signal and nonlinear tracking differentiator is discussed in literature (Guo *et al.*, 2002). The studies by Yang and Huang (2009) and Yoo *et al.* (2007) show significant performance level of Extended State Observer pillaring ADRC. Some simulation studies on the convergence of Linear ESO (LESO) associated with ADRC for nonlinear systems are reported in discrete time domain by Yoo *et al.* (2006) as well as in continuous time domain by Guo and Zhao (2011).

A procedure based tuning method for a second order LADRC for a variety of systems like low order and high order was also developed by taking settling time as the performance specification (Chen *et al.*, 2011). Rather than time domain specifications, frequency domain specifications are the matter of interest for practicing engineers. Since ADRC was developed as a transformative control strategy for industrial control applications, tuning based on frequency specifications is highly recommended. But elaborate studies in this perspective are hardly noted in literature.

In short, the major highlights of this intuitive technology are robustness and uncertainty reduction. It is understood that ADRC is a potential replacement for the deeply rooted PID technology in industries and had become an attractive area for applied researchers. In the next section some applications are reported where the principle of ADRC is tried and implemented in engineering applications by various research groups across the globe.

2.6 A review on applications of ADRC

Even though there are some gaps in the theoretical aspects of ADRC, it had been effectively implemented in some major industrial applications. This section lists a few of this kind.

2.6.1 Motion control

The research group of The Applied Control Research Laboratory of Cleveland State University initiated the studies on ADRC based motion control systems (Gao *et al.*, 2001a). The search for the best control law for a motion control problem converged to Linear ADRC (LARDC) among control algorithms like PID control, PID with leadlag compensation, PID with velocity feedforward control, parameterized loop

shaping control and LADRC (Zheng and Gao, 2005; Goforth, 2004). The results of about 168 benchmark tests on an industrial motion control platform that characterises the performance of both ADRC and existing industrial controllers show the prospective future of ADRC as a feasible solution in manufacturing industry (Tian and Gao, 2009).

2.6.2 MEMS gyroscope

Automotive industry and navigation systems largely rely on gyroscopes. With the advent of microelectromechanical systems (MEMS), the conventional gyroscopes were replaced by MEMS gyroscopes. Eventually, the control techniques of MEMS gyroscopes too invaded the research field of control theory. A major challenge in the control aspect of MEMS gyroscopes is its time varying rate of rotation which is normally discarded in studies. Researchers took this as an opportunity to apply the technique of Active Disturbance Rejection Control, to handle this issue in the model dynamics of MEMS gyroscopes. It is found that ADRC could successfully eliminate the vibrations in the sense axis of MEMS gyroscopes resulting in an easier and precise estimation of the rotation rate. This establishes the high tracking performance of ADRC (Zheng *et al.*, 2007a). An economic solution for counteracting the structural and fabrication imperfections and improving the rotation rate sensing of MEMS gyroscopes was addressed by (Dong *et al.*, 2008b). The stability analysis with encouraging results proves the theoretical establishment of ADRC in MEMS gyroscopes where the underlying issue is disturbance rejection (Dong *et al.*, 2008a; Zheng *et al.*, 2008; Zheng and Gao, 2011).

2.6.3 Web tension regulators

The web tension control problem is a highly dynamic and complex case due to large amount of uncertain parameter variations, which requires special concern in

industrial control situations. Different control techniques were tried to solve the issue of rejecting changing dynamics due to “tension transfer” between nearby web spans, changes in working temperature, defects in physical framework etc. ADRC provided an encouraging solution in this case too (Hou *et al.*, 2001; Zhou and Gao, 2007).

2.6.4 Other applications

Apart from the areas mentioned above, the concept of ADRC had been successfully applied in solving a variety of interesting issues related to human postural sway (Kotina *et al.*, 2011), the disturbances and unmeasured dynamics associated with chemical processes (Chen *et al.*, 2007), load changes and system uncertainties in power system containing both thermal and hydraulic turbines (Dong and Zhang, 2010), integrated flight-propulsion control scheme (Wang *et al.*, 2010) and the like. Zheng *et al.* (2011) address the disturbance rejection as the key annoying issue in thermal power plants and proposes ADRC as a meaningful solution. It is found that this control strategy gives convincing results in the field of power electronics (Sun and Gao, 2005), space power management (Ping and Gao, 2005), electric power assist steering system (Dong *et al.*, 2010), iron and steel processes (Wang *et al.*, 2011) and airships under uncertain wind disturbances (Kim *et al.*, 2003). The areas of application can be extended to systems whose accurate mathematical models are not fully demystified like high precision machining processes, high altitude flight control problems, uncertain power plant contingencies etc.

CHAPTER 3

ACTIVE DISTURBANCE REJECTION CONTROL

3.1 Introduction

The idea of ADRC had its origin when Jinqing Han (2009) wondered whether a true mathematical model for a system was ever obtained and if modern control theory is all about controlling mathematical models or the actual physical systems. Researchers were in the direction of developing some methods by which the uncertainties of the system model and external disturbances can be properly tracked as they adversely affect the controller performance. This was always a matter of serious discussion among the theoreticians and practising engineers. Unfortunately, practising engineers handle the plant uncertainties empirically, while theoreticians neglect them in their model dynamics. Han thought of combining these uncertainties too as a disturbance parameter and there originated the work related to Active Disturbance Rejection Control better known as ADRC, way back in 1999. The fundamental idea of ADRC is to treat the process/plant as a series of integrators and eliminate the internal and external, uncertainties and disturbances, which Han called as “total disturbances hitting the process/plant”. Though, with a glaring demand, PID control deep rooted in process industry, Jinqing Han raised four fundamental issues for this topology.

1. *“Set point is often given as a step function, not appropriate for most dynamics systems because it amounts to asking the output and, therefore, the control signal, to make a sudden jump”*
2. *“PID is often implemented without the D part because of the noise sensitivity”*

3. *“The weight sum of the three terms of PID, while simple, may not be the best control law based on the current and the past of the error and its rate of change”*
4. *“The integral term, while critical to rid of steady-state error, introduces other problems such as saturation and reduced stability margin due to phase lag”*

To overcome the above mentioned issues, Han proposed the idea of Active Disturbance Rejection Control (ADRC) which included a transient profile generator, Tracking Differentiator (TD), Nonlinear Controller and an Extended State Observer (ESO).

3.2 Transient profile generator

A major concern mentioned by engineers in feedback control is the set point jump of reference signals, especially the step input. A sensible transient profile that can be smoothly tracked by the output is used to solve the above issue (Figure 3.1).

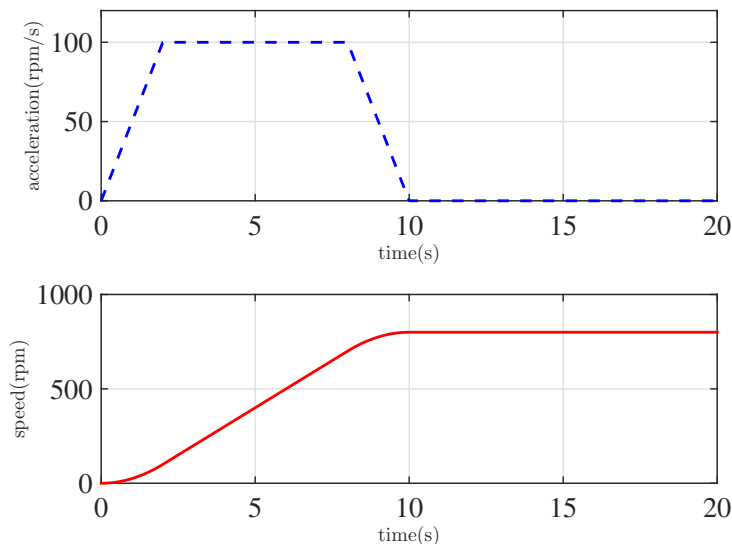


Figure 3.1: A standard velocity and acceleration profile

3.3 Tracking Differentiator (TD)

A tracking differentiator is one that produces two signals $x_1(t)$ and $x_2(t)$ from a given signal $x(t)$, such that

$$x_1(t) = x(t) \quad (3.1)$$

$$x_2(t) = \dot{x}(t) \quad (3.2)$$

Tracking differentiators have found to enhance the performance of PID controllers. The role of tracking differentiators is two-fold in the design of PID controller, *i.e.*, in both the feedback measurement and reference generation. In any feedback control system, the selection of the sensor that measures the feedback signal has utmost significance. For e.g., the position measurement has always exhibited better performance over velocity measurement due to the increased interference of noise signals in the latter one. A tracking differentiator proves to be an appealing solution to this issue. It can reconstruct high-quality velocity signal numerically from the available position measurement. Also, it can be used to provide the *derivative* in PID control. They can be used in generating non differentiable or discontinuous reference signals too. A generalised form of the tracking differentiator used in the conventional ADRC topology (Su *et al.*, 2005) originally developed by Han is given in Equation 3.3.

$$\begin{aligned} \dot{x}_1 &= x_2 \\ \dot{x}_2 &= -R_1 \operatorname{sgn}(x_1 - x_{ref}) + \frac{x_2 |x_2|}{2R_1} \end{aligned} \quad (3.3)$$

where x_1 is the parameter to be tracked, x_2 is its reconstructed derivative and R_1 is the maximum attainable value of \dot{x}_2 .

3.4 Nonlinear Controller

The control law of a PID controller with linear gains is given in Equation 3.4. Though the linear gain PID controller is simple and easily manageable, it is found that there are certain limitations as mentioned in Section 1.1. Gain scheduling of controllers was a possible solution for this problem, though restricted with slow variations in scheduling variables. Shamma and Athans (1992) discuss the potential threats of gain scheduling and suggest possible remedies. But the solution was more or less problem dependent.

$$u = K_p e + K_i \int e dt + K_d \frac{de}{dt} \quad (3.4)$$

Along with the development of ADRC, Han had proposed an ingenious change in the structure of PID, which he called a Nonlinear Controller. The Nonlinear Controller suggested by Han acts along with the tracking differentiator, gives the control law as in Equation 3.5.

$$u = K_p |e|^{\alpha_p} \text{sgn}(e) + K_i |e_i|^{\alpha_i} \text{sgn}(e_i) + K_d |e_d|^{\alpha_d} \text{sgn}(e_d) \quad (3.5)$$

where $e_i = \int_0^t e(t) dt$ and e_d is the error in actual and reference, derivative signals. The idea behind a Nonlinear Controller is the use of nonlinear gains and $\text{sgn}()$ function in PID structure.

Gao *et al.* (2001b) gives a concrete example that brings out the concept of Nonlinear Controller. A comparison of the steady state error for a single integrator system with a linear controller (Equation 3.6a) and a nonlinear controller (Equation 3.6b) is tabulated in Table 3.1. This clearly explains the effectiveness of this approach.

$$u = -K_p e \quad (3.6a)$$

$$u = -K_p |e|^\alpha \text{sgn}(e) \quad (3.6b)$$

Table 3.1: A comparison of steady state error

Type of controller	α	Steady state error
Linear	NA	< 0.1
Nonlinear	0.5	< 0.01
Nonlinear	0.33	< 0.001

It is found that for the same gain $K_p = 10$, a linear controller (Equation 3.6a) gives a steady state error less than 0.1, while a non-linear controller (Equation 3.6b) gives a steady state error less than 0.01 for an $\alpha = \frac{1}{2}$. This gets still reduced to less than 0.001, when $\alpha = \frac{1}{3}$. The improved performance is due to the mathematical nature of the non-linearity (Figure 3.2).

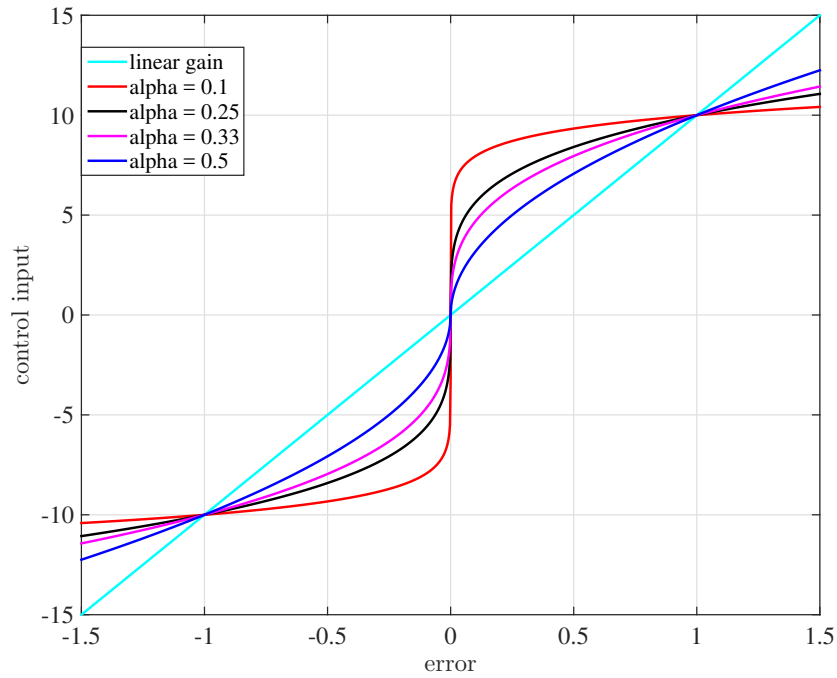


Figure 3.2: Effect of nonlinear function on control input

Also, for the Nonlinear Controller, when $\alpha_i < 1$, the integral action is improved for smaller errors, for which its action should be significant. This also prevents saturation effect at larger errors. On the other hand a selection of $\alpha_d > 1$, makes

the differential action significant for larger errors like transients. This term has negligible effect when the output is close to steady state. For $\alpha < 1$, Equation 3.6b gives a higher gain for lower error (e) and lower gain for higher error (e), in comparison with Equation 3.6a.

Another nonlinear function was also proposed by Gao *et al.* (2001b) that can be used in implementing Nonlinear PD controller (Figure 3.3). Here $|e|^\alpha \text{sgn}(e)$ is replaced with a mathematical relation (Equation 3.7) that generates a linear control input for a smaller range of error.

$$fal(e, \alpha, \delta) = \begin{cases} |e|^\alpha \text{sgn}(e), & |e| > \delta. \\ \frac{e}{\delta^{1-\alpha}}, & |e| \leq \delta. \end{cases}, \delta > 0 \quad (3.7)$$

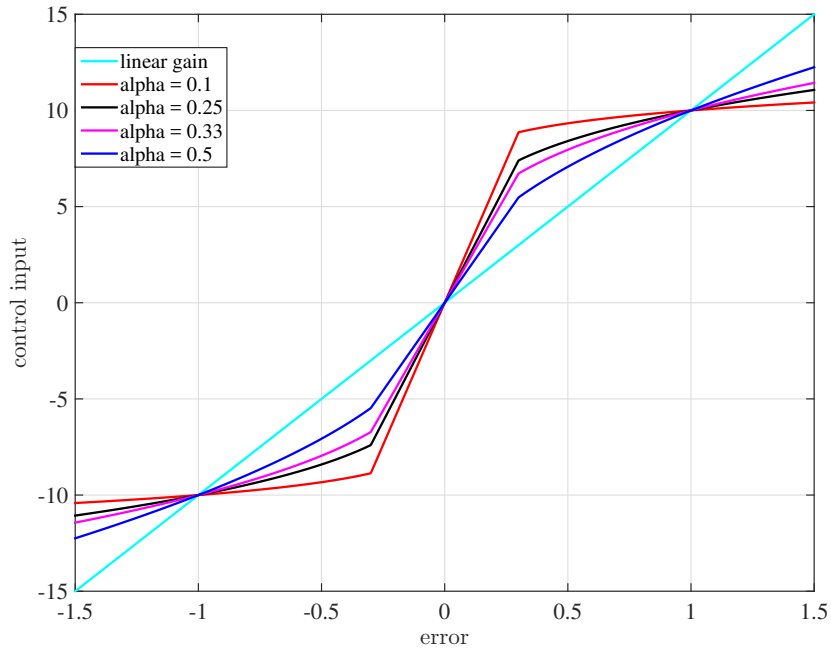


Figure 3.3: Effect of fal function on control input

A comparison of nonlinear function and fal function for $\alpha = 0.1, 0.25, 0.33$ and 0.5 is given in Figure 3.4. It is noted that nonlinear function results in smooth change in control input while fal function results in linear control input for a range

of small error. This is similar to gain scheduling of controllers. Gain scheduling by inexperienced control engineers can lead to severe unpredictable situations in industrial control processes.

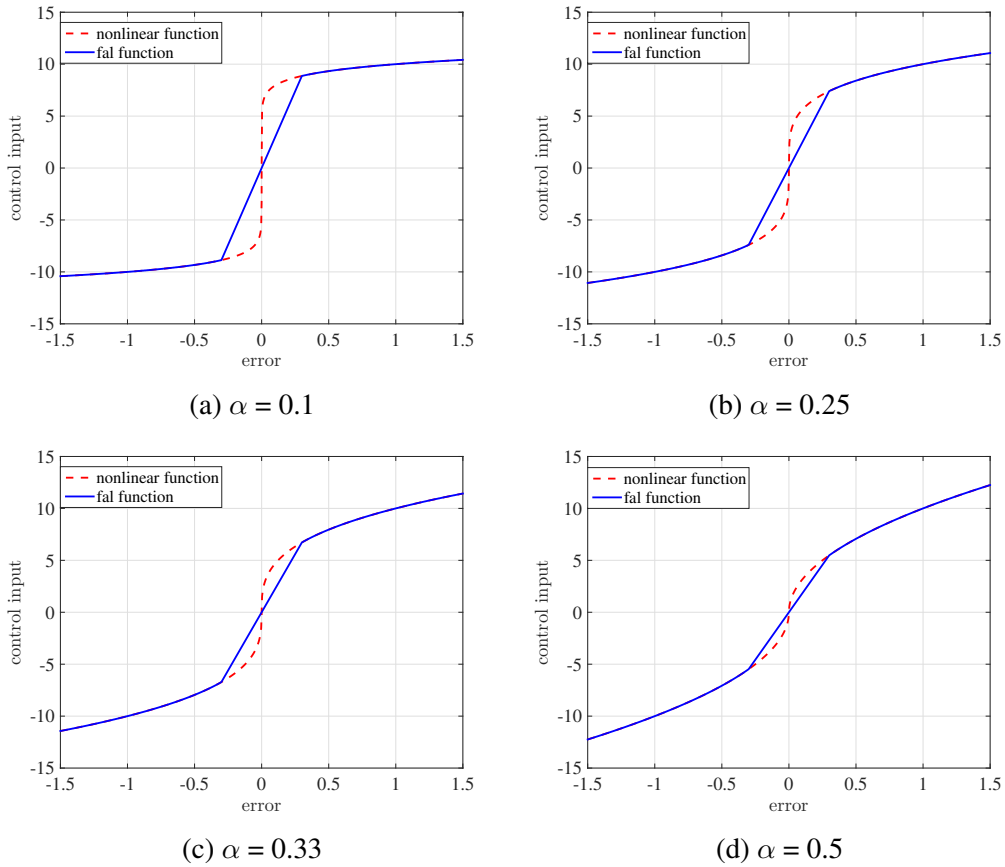


Figure 3.4: A comparison of nonlinear function and *fal* function

3.5 Extended State Observer (ESO)

Over the time, “observers” or “estimators” have become a key element in engineering design and implementation. In control design, we often come across unmeasurable parameters. Observers are programs that derive information of the state of a system from some plant information, in real time. The concept of the observer was first introduced by Luenberger (1964) in his seminal paper, where it was shown that the state of a linear system can be reconstructed from observation of input and out-

put of the system. One can find many modifications of state observer in literature. A closer look at the different observer designs like high gain observer by Esfandiari and Khalil (1992), sliding mode observer by Slotine *et al.* (1987) and Utkin (2013) and the like, points to a common fact that majority of the observer designs depend on the mathematical model of the system. It was Han (2009) who introduced the concept of Nonlinear Extended State Observer (NESO), one which is independent of the mathematical model. The NESO, was used for disturbance estimation in ADRC developed by J.Han. In Extended State Observer the uncertainties of the plant and the external disturbances are accounted in a single term. Literature gives detailed analysis with rigorous mathematical proof on the convergence of ESO, which is the backbone of ADRC (Guo and Zhao, 2011).

The design methods of observers fall into two categories:

- (a) Observer design for *state estimation* based on the mathematical model of the plant.
- (b) Observer design for *disturbance estimation* based on input-output data from the plant.

Observers for state estimation rely on a plant model. Hence the scope of exactness of the plant model gets reflected in the state estimation. Thus, practising engineers were reluctant in accepting these estimators. This resulted in the development of disturbance observers, which helped to identify the uncertainties in plant modelling. This disturbance estimation invariably improved the accuracy of the state estimation.

Estimators can be broadly classified into early estimators, modern estimators and disturbance estimators based on their evolution (Radke and Gao, 2006).

Early estimators: The observers that used the input, output and initial conditions come under this category. Some of the early estimators are

- (i) Plant Output Based Estimator (OBE)
- (ii) Plant Input Based Estimator (IBE)
- (iii) Input and Output Based Observer (IOBO)
- (iv) Proportional Integral Observer (PIO)

Modern estimators: They were developed in line with the advances in modern control theory, which mathematically formulates a cost function to minimise the disturbances in systems under modelling. The following are some of the key modern estimators.

- (i) Kalman Filter (KF)
- (ii) Extended Kalman Filter (EKF)
- (iii) H_∞ Estimator

Disturbance Estimators: Although modern estimators took into account the disturbances affecting the plant being modelled, the practising engineers could not easily understand the complexities involved in them. Thus disturbance estimators developed as a separate school of thought. The underlying concept of these estimators is that uncertainties and disturbances are estimated along with the states and they were used in formulating the control law. Literature gives detailed descriptions of disturbance estimators. Some of them are listed below.

- (i) Disturbance Observer (DOB) (Umeno and Hori, 1991; Lee and Tomizuka, 1996; Schrijver and Van Dijk, 2002; Choi *et al.*, 2003; Yang *et al.*, 2005)
- (ii) Unknown Input Observer (UIO) (Basile and Marro, 1969; Johnson, 1971; Hostetter and Meditch, 1973; Gourishankar *et al.*, 1977; Müller, 1990; Profeta *et al.*, 1990)

tion (3.8)

$$\ddot{y} + a_1\dot{y} + a_0y = bu + w \quad (3.8)$$

where y , u and w are the output, control signal and external disturbances respectively.

$$\begin{aligned} \ddot{y} &= -a_1\dot{y} - a_0y + bu + w \\ &= -a_1\dot{y} - a_0y + bu + w + b_0u - b_0u \\ &= -a_1\dot{y} - a_0y + (b - b_0)u + w + b_0u \end{aligned} \quad (3.9)$$

$$\ddot{y} = f + b_0u \quad (3.10)$$

where

$$f = -a_1\dot{y} - a_0y + (b - b_0)u + w \quad (3.11)$$

The term f (Equation 3.11) denotes the total disturbance which includes the unknown plant dynamics and external disturbances. In order to make it more of a control problem rather than a model problem, f is properly estimated as z_3 , the third state of ESO (Figure 3.6). The closeness of z_3 to the actual dynamics of the system (Equation 2.4) determines the extent to which the plant can be reduced to a simple double integrator (Equation 3.12), when the control law of Equation 3.13 is applied. This makes the control solution easier.

$$\ddot{y} = u_0 \quad (3.12)$$

$$u = \frac{u_0 - z_3}{b_0} \quad (3.13)$$

The theme idea behind ADRC is given by equations 3.12 and 3.13. The relevance of this paradigm lies in the fact that the mathematical expression for f is absent in (Equation 3.12). The method is very systematic and at the same time, little knowledge of the plant dynamics, will not hinder the control process. This allows the use of this control mechanism in a varied set of plants like linear, non-linear, time

invariant and time variant systems. All that one needs to know is the order of the system obtained from the fundamental laws governing the system.

The concept of Extended State Observer (ESO) is used in the estimation of f , denoted as z_3 . A canonical approach is used to mathematically model the system and the Extended State Observer. Apparently, this reduces the number of parameters to be known in advance for modelling the system. For the system represented by Equation 3.10, the state variables are selected as in Equation 3.14 to form the state model of the system.

$$\begin{aligned}x_1 &= y \\x_2 &= \dot{x}_1 \\x_3 &= f\end{aligned}\tag{3.14}$$

Here f is appended as a third state for the basic second order system. The augmented state model (Equation 3.16) is obtained by selecting $\dot{f} = h$. Its equivalent matrix expanded form is Equation 3.15. This model does not include any of the plant parameters, which makes this canonical technique a model less approach.

$$\begin{aligned}\begin{bmatrix} \dot{x}_1 \\ \dot{x}_2 \\ \dot{x}_3 \end{bmatrix} &= \begin{bmatrix} 0 & 1 & 0 \\ 0 & 0 & 1 \\ 0 & 0 & 0 \end{bmatrix} \begin{bmatrix} x_1 \\ x_2 \\ x_3 \end{bmatrix} + \begin{bmatrix} 0 \\ b_0 \\ 0 \end{bmatrix} u + \begin{bmatrix} 0 \\ 0 \\ 1 \end{bmatrix} h \\ y &= \begin{bmatrix} 1 & 0 & 0 \end{bmatrix} \begin{bmatrix} x_1 \\ x_2 \\ x_3 \end{bmatrix}\end{aligned}\tag{3.15}$$

$$\begin{aligned}\dot{X} &= AX + Bu + Eh \\ y &= CX\end{aligned}\tag{3.16}$$

Similarly, the Extended State Observer is modelled as Equation 3.17.

$$\begin{aligned}
\dot{Z} &= AZ + Bu + G(y - \hat{y}) \\
&= (A - GC)Z + Bu + Gy \\
\hat{y} &= CZ
\end{aligned} \tag{3.17}$$

The the matrix expanded form of Equation 3.17 is obtained (Equation 3.18) by selecting $G = \{g_1, g_2, g_3\}$.

$$\begin{aligned}
\dot{Z} &= \begin{bmatrix} -g_1 & 1 & 0 \\ -g_2 & 0 & 1 \\ -g_3 & 0 & 0 \end{bmatrix} \begin{bmatrix} z_1 \\ z_2 \\ z_3 \end{bmatrix} + \begin{bmatrix} 0 & g_1 \\ b_0 & g_2 \\ 0 & g_3 \end{bmatrix} \begin{bmatrix} u \\ y \end{bmatrix} \\
\hat{Y} &= \begin{bmatrix} 1 & 0 & 0 \\ 0 & 1 & 0 \\ 0 & 0 & 1 \end{bmatrix} \begin{bmatrix} z_1 \\ z_2 \\ z_3 \end{bmatrix}
\end{aligned} \tag{3.18}$$

Only two inputs u and y are required to implement the ESO. Defining the error state vector as $\tilde{X} = X - Z$, the error state model is obtained as Equation 3.19.

$$\dot{\tilde{X}} = (A - GC)\tilde{X} + Eh \tag{3.19}$$

The roots of $|sI - (A - GC)| = 0$ determines the characteristics of ESO (Equation 3.17) as well as the error state model (Equation 3.19). The poles of the error state model can be suitably located by proper selection of G . In order to reduce the complexity of design of the observer and controller, the observer gain vector G is selected such that all the observer poles are located at $-\omega_0$. Using Equation 3.20, the gain matrix (Equation 3.21) is obtained as

$$\begin{aligned}
|sI - (A - GC)| &= (s + \omega_0)^3 \\
s^3 + g_1s^2 + g_2s + g_3 &= s^3 + 3\omega_0s^2 + 3\omega_0^2s + \omega_0^3
\end{aligned} \tag{3.20}$$

$$G = \begin{bmatrix} g_1 \\ g_2 \\ g_3 \end{bmatrix} = \begin{bmatrix} 3\omega_0 \\ 3\omega_0^2 \\ \omega_0^3 \end{bmatrix} \quad (3.21)$$

A reasonably faster observer poles resulting in larger observer bandwidth gives improvement in estimation accuracy. However, it increases noise sensitivity (Yoo *et al.*, 2007). Thus a judicious selection of ω_0 is a trade-off between accuracy and noise sensitivity.

With a suitable choice of ω_0 , the ESO accurately estimates all the states. z_1 , z_2 and z_3 are the estimated states of x_1 , x_2 and x_3 (Figure 3.6). The control equation 3.22 of PD controller generates a control signal u_0 .

$$u_0 = K_p(r - z_1) - K_d(z_2) \quad (3.22)$$

The PD controller, if isolated is a second order system (Equation 3.23).

$$\frac{\omega_c^2}{s^2 + 2\zeta\omega_c s + \omega_c^2} = \frac{K_p}{s^2 + K_d s + K_p} \quad (3.23)$$

This reduces the number of parameters in the controller design to ω_c alone. Selecting proper ζ as per the design specification, the controller gains are obtained as $K_p = \omega_c^2$ and $K_d = 2\zeta\omega_c$. The entire design is reduced to a single parameter ω_0 using a frequently used rule of thumb *i.e.*,

$$\omega_0 = 4 \text{ to } 10 \text{ times } \omega_c$$

3.7 Summary

This chapter discussed the concept of the control technique called Active Disturbance Rejection Control. The constituents of the topology is detailed with sufficient reviews on its developments. It is seen that the performance of ADRC mostly de-

depends on the accurate design of ESO, as it estimates and cancels the “total disturbances” even before acting upon the system. The next chapter discusses the performance analysis of the Extended State Observer in the speed control of a permanent magnet dc motor.

CHAPTER 4

EXTENDED STATE OBSERVER

4.1 Philosophy of observer design

The time domain characteristics of a linear time invariant system are completely governed by the position of the closed loop poles. The unit step response of a generalised second order underdamped system (Equation 4.1)

$$\frac{C(s)}{R(s)} = \frac{\omega_n^2}{s^2 + 2\zeta\omega_n s + \omega_n^2} \quad (4.1)$$

is given by Equation 4.2.

$$c(t) = 1 - \frac{e^{-\sigma t}}{\sqrt{1 - \zeta^2}} \text{Sin}(\omega_d t + \phi) \quad (4.2)$$

where, ω_d represents the damped natural frequency of oscillation. The rate at which the response tracks the reference signal depends on the value of $\sigma (= \zeta\omega_n)$, the attenuation factor, which also corresponds to the real part of the dominant closed loop pole. The location of the closed loop poles decides the performance and in turn the stability of this linear closed loop system. The closed loop poles should be relocated to achieve a remarkable improvement in the system performance of stable systems or to achieve stability, in the case of unstable systems. A proper relocation of closed loop poles is achieved through state feedback, more precisely, through full state feedback with control law $u = -KX$. Full state feedback requires the availability of all the states of the system. This is made available using observers. A block diagram representing an observer based full state feedback is shown in Figure 4.1 in which dark lines represent vectors and light lines represent signals. The

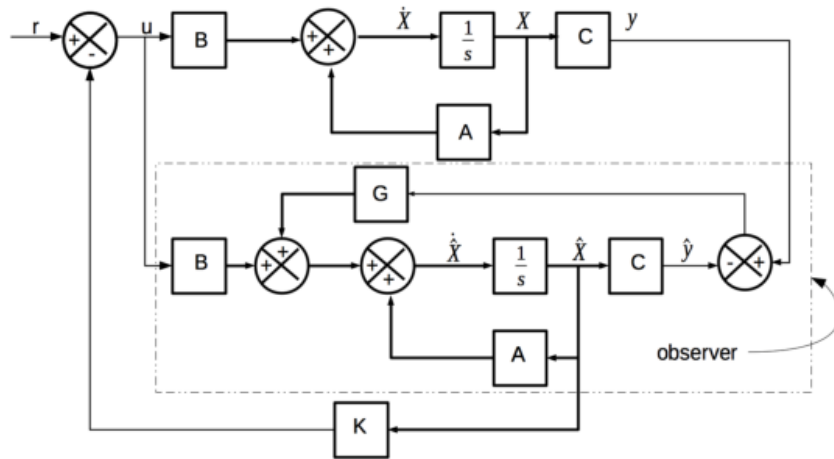


Figure 4.1: Observer based full state feedback system

design of observer first involves building a model of the given system. The model and the original system are driven by the same input u . The dynamic behaviour of the observer is assumed to be identical with that of the system it observes. For a linear state model (Equation 4.3),

$$\begin{aligned}\dot{X} &= AX + Bu \\ y &= CX\end{aligned}\quad (4.3)$$

the state estimate \hat{X} is given by Equation 4.4,

$$\begin{aligned}\dot{\hat{X}} &= A\hat{X} + Bu + G(y - \hat{y}) \\ \hat{y} &= C\hat{X}\end{aligned}\quad (4.4)$$

where $G = \begin{bmatrix} g_1 \\ g_2 \end{bmatrix}$ is the gain matrix corresponding to the observer for a second order system. Defining the error state vector (Equation 4.5),

$$\tilde{X} = (X - \hat{X})\quad (4.5)$$

the error state model is obtained as Equation 4.6,

$$\dot{\tilde{X}} = (A - GC)\tilde{X} \quad (4.6)$$

4.2 Effect of pole location on observer characteristics

- A simulation approach

An observer is said to have tracked the states properly when, the error between the actual and observed states, becomes zero. If initial conditions are not set properly, or, if there are slight disturbances, the model generally recovers slowly to provide an estimate suitable for control. This requires a proper selection of the observer gains g_1 and g_2 (Equation 4.4). The observer gains are so selected, such that the roots of the characteristic equation $|sI - (A - GC)| = 0$, which otherwise represents the poles of the error state model, lie away from the original plant poles.

Literature points to the well known fact that farther poles result in faster response for low noise level systems (Ogata and Yang, 2002). Luenberger (1966) ascertained that noise is not a critical design factor when the noise level is low. However, reviews on observers reveal that much theory is not devoted to the choice of observer pole locations from this perspective. There lacks the 'extent' to which the poles can be relocated and the threats resulting from farther poles.

A double integrator (Equation 4.7), for which the open loop plant poles are at the origin, is selected for the analysis as the ADRC reduces the system into a series of integrators. The state model is formed (Equation 4.8) with x_1 as position and x_2 as velocity.

$$G(s) = \frac{2}{s^2} \quad (4.7)$$

$$\begin{aligned}\dot{x} &= \begin{bmatrix} 0 & 1 \\ 0 & 0 \end{bmatrix} x + \begin{bmatrix} 0 \\ 2 \end{bmatrix} u \\ y &= \begin{bmatrix} 1 & 0 \end{bmatrix} x\end{aligned}\quad (4.8)$$

The position of the characteristic roots of the error state model (Equation 4.6) is varied over a wide range to notice the effect of the location of poles of the error state model on the speed of state estimation.

The initial values of the plant model are selected as $x_1(0) = 10$ and $x_2(0) = 20$ and that of the observer is fixed as $\hat{x}_1(0) = 0$ and $\hat{x}_2(0) = 0$. Combining Equation 4.8 of the plant, Equation 4.4 of the observer and G , we get Equation 4.9 for simulation. The simulation is carried out in MATLAB/SIMULINK with fixed step sampling time of 0.1s using ode3 (Bogacki-Shampine) as the solver.

$$\begin{aligned}\dot{\hat{x}}_1 &= -g_1\hat{x}_1 + \hat{x}_2 + g_1x_1 \\ \dot{\hat{x}}_2 &= -g_2\hat{x}_1 + g_2x_1 + 2u\end{aligned}\quad (4.9)$$

Equation 4.10 reveals that g_1 and g_2 are related to both observer pole locations and characteristic roots of the error state model (Equation 3.17 and 3.19).

$$\begin{aligned}|sI - (A - GC)| &= (s + p_1)(s + p_2) \\ s^2 + g_1s + g_2 &= (s + p_1)(s + p_2)\end{aligned}\quad (4.10)$$

The open loop plant poles are at $s = (0, 0)$. By rule of thumb, the position of the observer error poles can be 2 to 5 times away from the closed loop plant poles. Simulations were carried out for various error pole locations from $s = (-0.5, -0.5)$ to $s = (-10, -10)$, which corresponds to observer gain variation from $(1, 0.25)$ to $(20, 100)$ respectively.

The pole locations, corresponding observer gains, and the time taken by the observer to estimate velocity and position with an accuracy of 0.1% are tabulated in Table 4.1. Here t_1 and t_2 represent the time taken for estimating velocity and position respectively, p_1 and p_2 are the poles of the error state model and g_1 and g_2 are the observer gains.

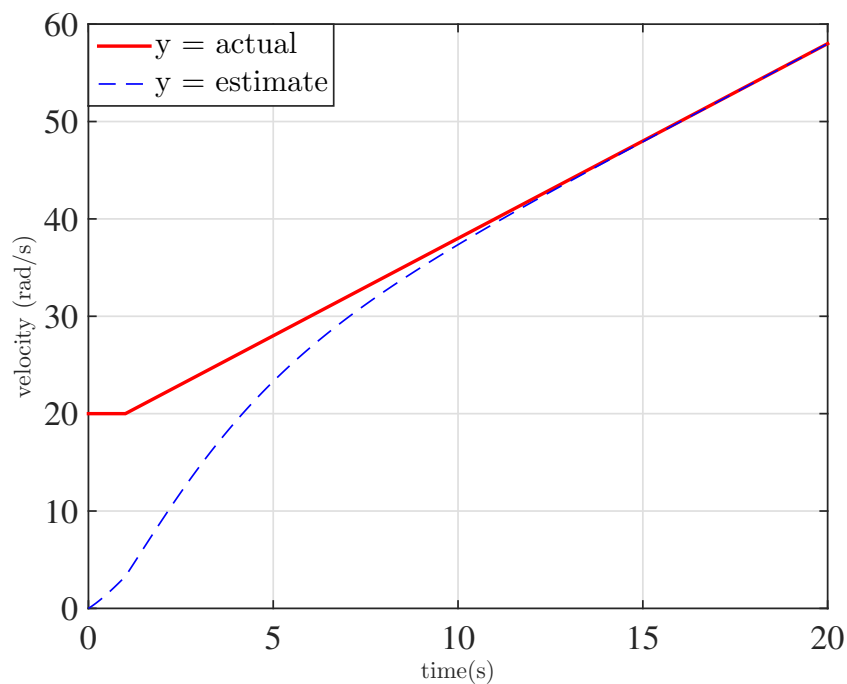
Table 4.1: Time chart with different observer gains

p_1	p_2	g_1	g_2	$t_1(s)$	$t_2(s)$
-0.5	-0.5	1	0.25	25.2	26.4
-1	-1	2	1	12.5	12.3
-2	-2	4	4	6	5.3
-3	-3	6	9	3	2.3
-4	-4	8	16	3.1	2.5
-5	-5	10	25	2.7	2.1
-6	-6	12	36	2.4	1.8
-7	-7	14	49	2.1	1.6
-8	-8	16	64	1.9	1.2
-9	-9	18	81	3.7	3.2
-10	-10	20	100	not converging	not converging

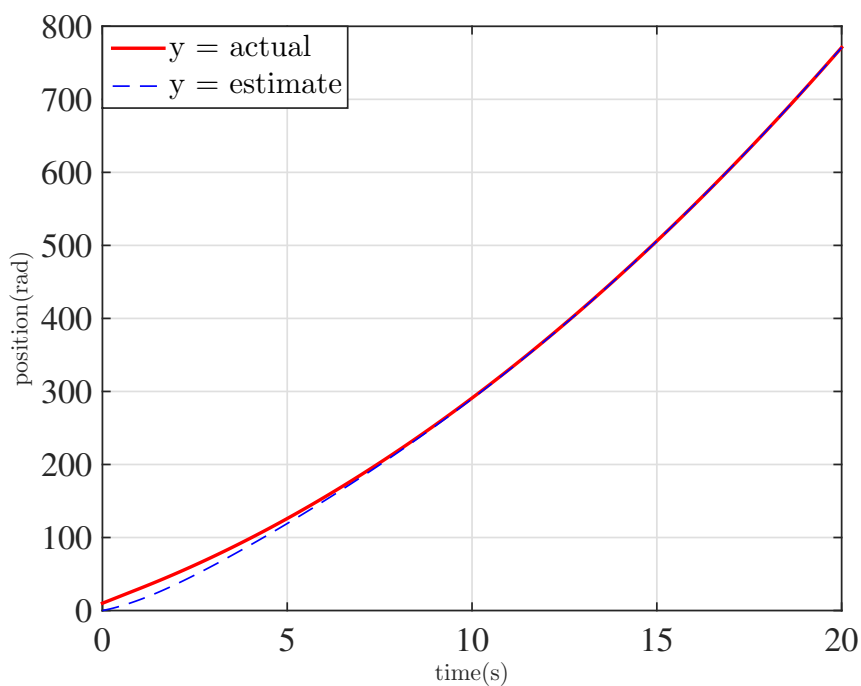
It is observed that as the location of the observer poles moves away from plant poles, the speed of estimation increases. This continues till pole locations are $s = (-9, -9)$. This is because farther poles of the error state model, i.e, characteristic roots of $|sI - (A - GC)| = 0$, have faster response and their effects decay faster. When $s = (-9, -9)$, the speed of estimation decreases from the previous value. This indicates a performance degradation of the observer. When pole locations move still away from the plant poles, it is noted that estimation is not converging.

Figure 4.2 gives a comparison of the actual velocity and position with its corresponding estimated values for $(g_1, g_2) = (1, 0.25)$ i.e, when $s = (-0.5, -0.5)$, while

Figure 4.3 shows its velocity error and position error Vs time. As the poles are placed at $s = (-10, -10)$, there is significant error in the estimated values of velocity and position (Figure 4.4). There is a sustained swing in the error plots (Figure 4.5).

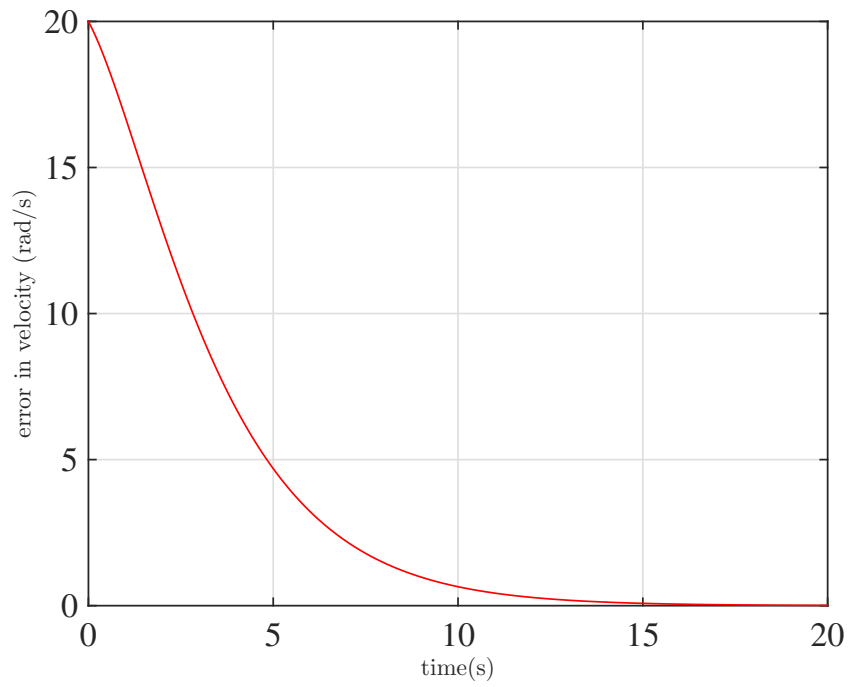


(a) Velocity Vs time

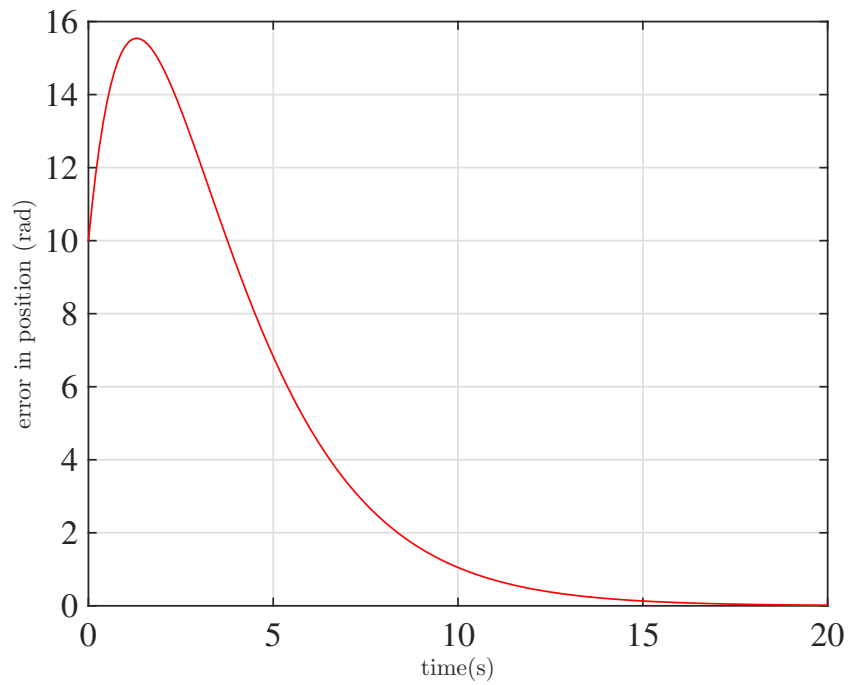


(b) Position Vs time

Figure 4.2: Comparison of velocity and position estimates with actual values when poles are at $s = (-0.5, -0.5)$

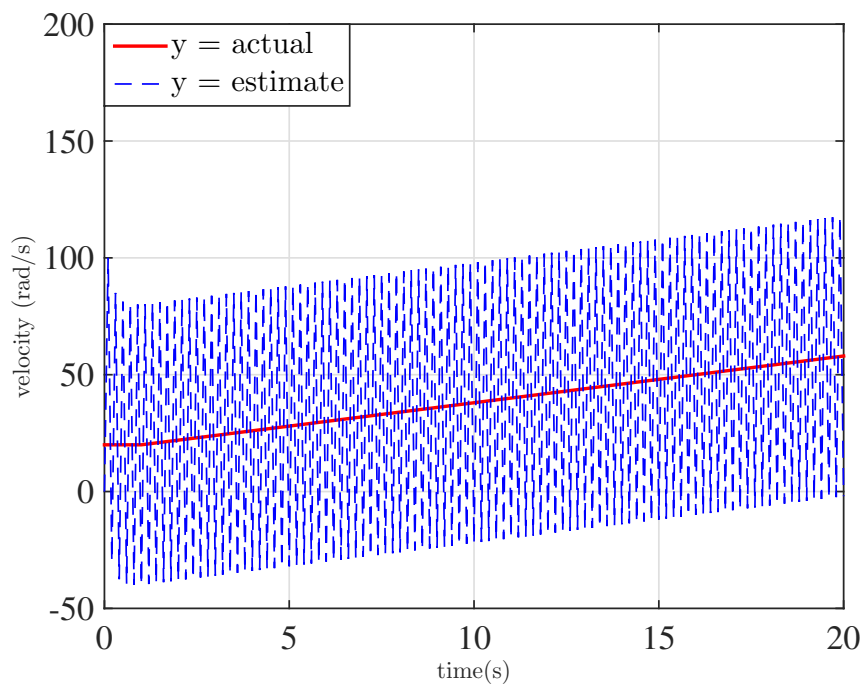


(a) Velocity error Vs time

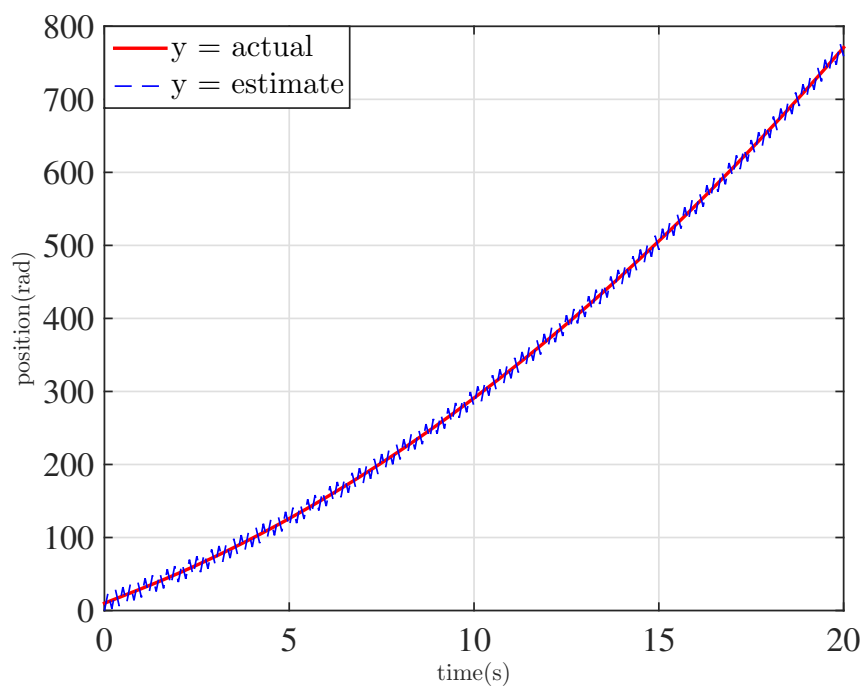


(b) Position error Vs time

Figure 4.3: Velocity and position error when poles are at $s = (-0.5, -0.5)$

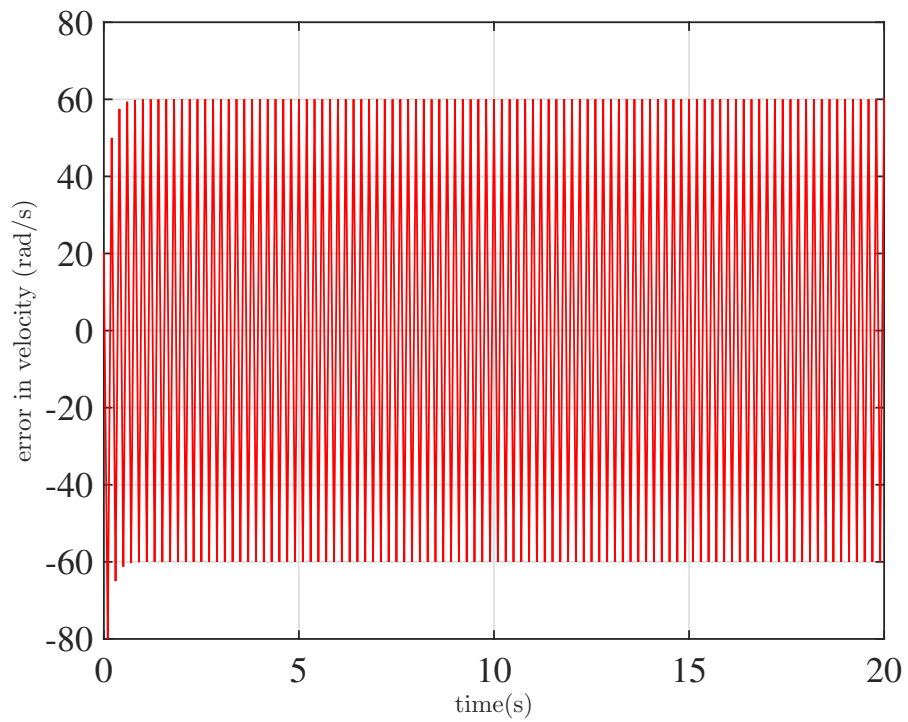


(a) Velocity Vs time

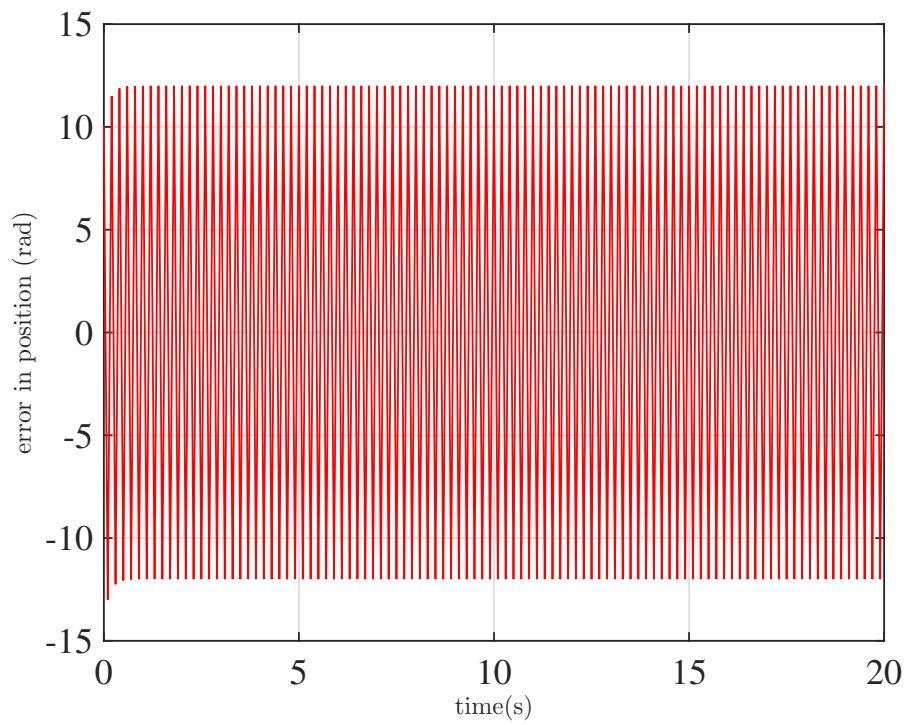


(b) Position Vs time

Figure 4.4: Comparison of velocity and position estimates with actual values when poles are at $s = (-10, -10)$



(a) Velocity error Vs time



(b) Position error Vs time

Figure 4.5: Velocity and position error when poles are at $s = (-10, -10)$

Instead of a converging error, the error swings about a value, when the poles are at $s = (-10, -10)$. Thus $\omega_0 = 10\text{rad/s}$ represents the critical observer bandwidth for the given system. As the position of the observer poles move farther from the original plant poles, the bandwidth of the observer increases, making the system more sensitive to noise. Thus, this anomalous swing can be attributed to increased speed of estimation resulting from increased bandwidth of the observer. This points to a marked conclusion that the selection of poles of the state error model needs to be a trade-off between accuracy and fastness of estimation. In the design of Extended State Observer associated with ADRC, similar characteristics were observed in simulations as well as experimental studies. The next section discusses the effect of bandwidth on the characteristics of Extended State Observer.

4.3 Effect of bandwidth on the characteristics of Extended State Observer

4.3.1 A simulation approach

Simulations were carried in MATLAB/SIMULINK with fixed step sampling time of 0.0001s using ode3 (Bogacki-Shampine) as the solver for 100s. The details of modelling and parameters of the dc motor are given in Chapter 5. The design of ESO was carried out based on the discussions in Section 3.6. The performance of ESO was studied using different values of ω_0 ranging from 5 rad/s to 80 rad/s. This study was carried out to notice the effect of observer bandwidth on the characteristic performance of ESO. Simulation diagrams are shown below (Figure 4.6 - Figure 4.8). Figure 4.9, Figure 4.10 and Figure 4.11 show the variations of u_0 , disturbance estimate and control voltage for some typical cases $\omega_0 = 30\text{rad/s}$, $\omega_0 = 70\text{rad/s}$ and $\omega_0 = 77\text{rad/s}$ respectively.

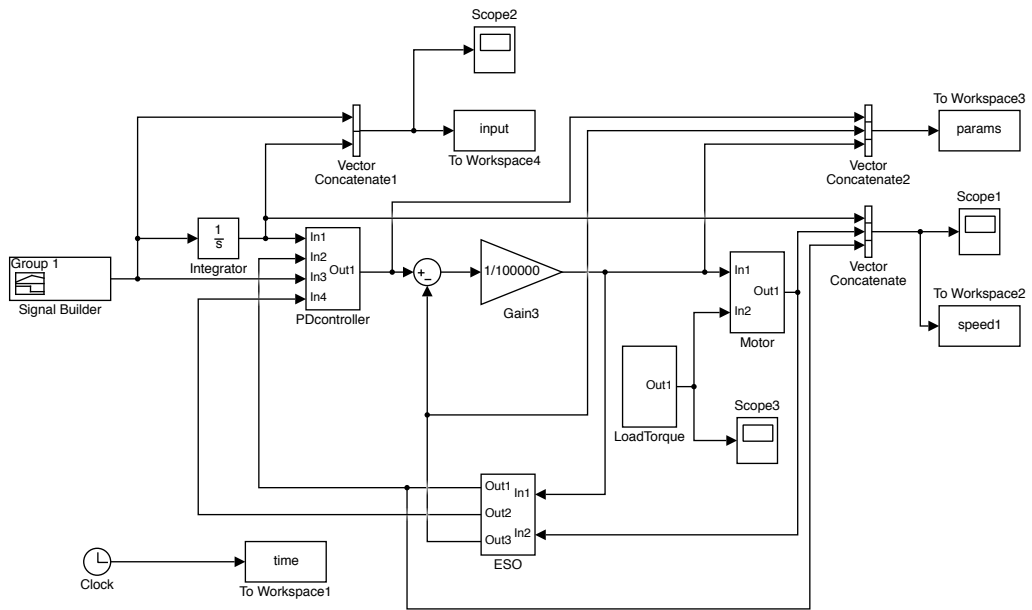


Figure 4.6: An overview of the simulation diagram

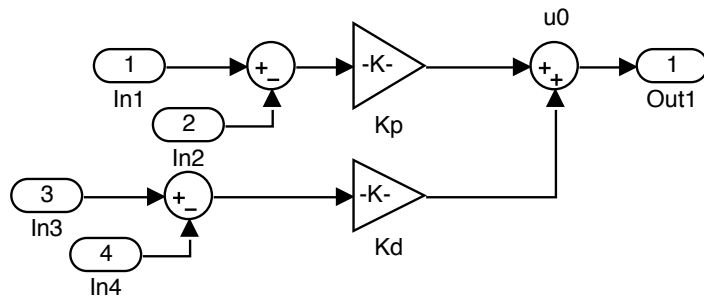


Figure 4.7: The PD controller

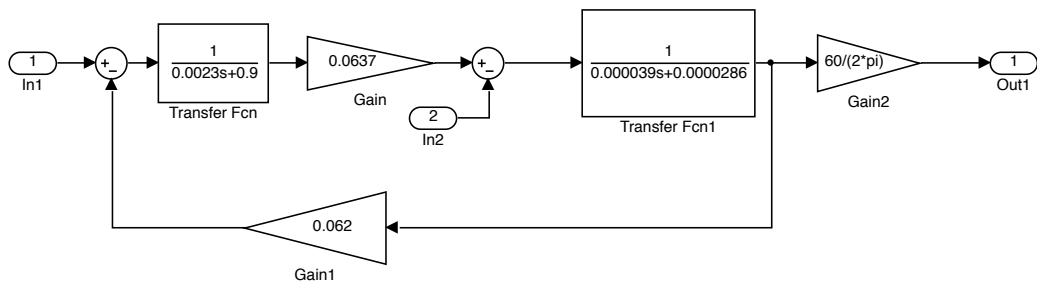


Figure 4.8: DC motor

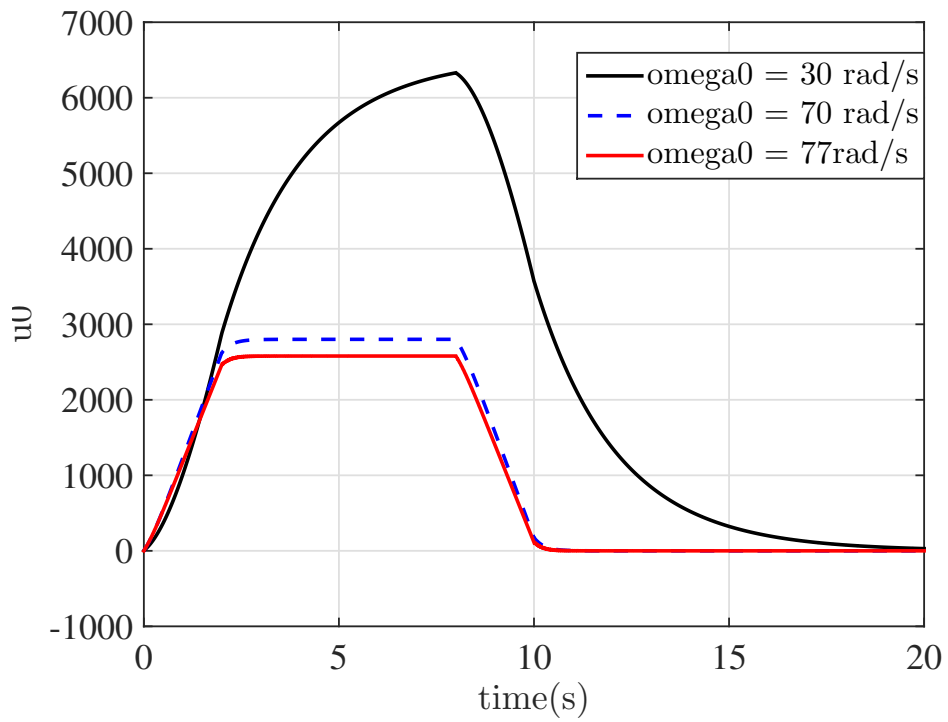


Figure 4.9: Effect of ω_0 on u_0

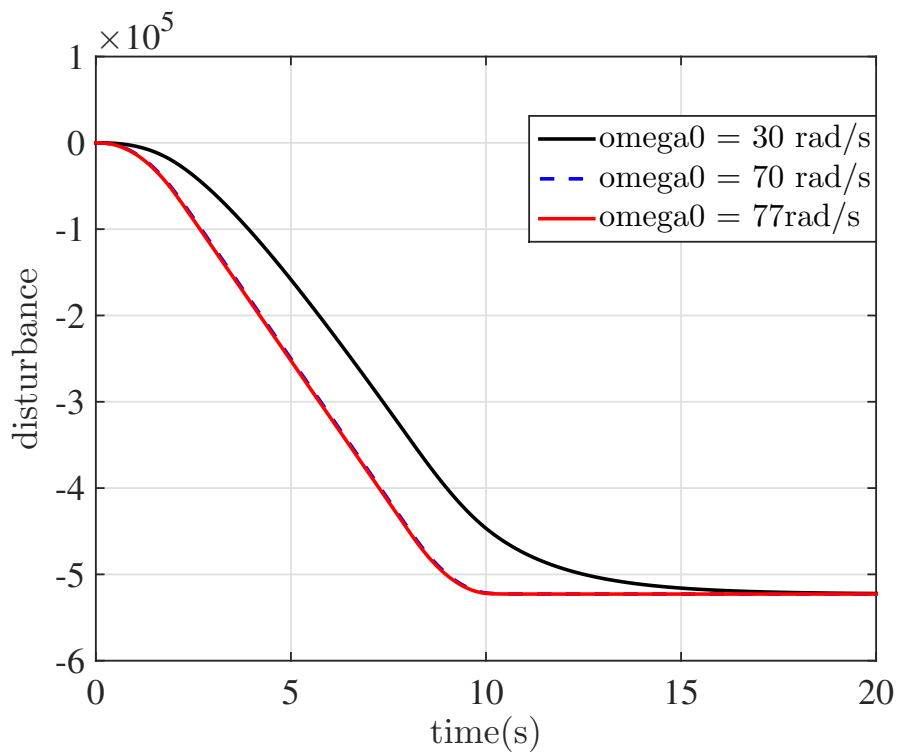


Figure 4.10: Effect of ω_0 on disturbance estimate

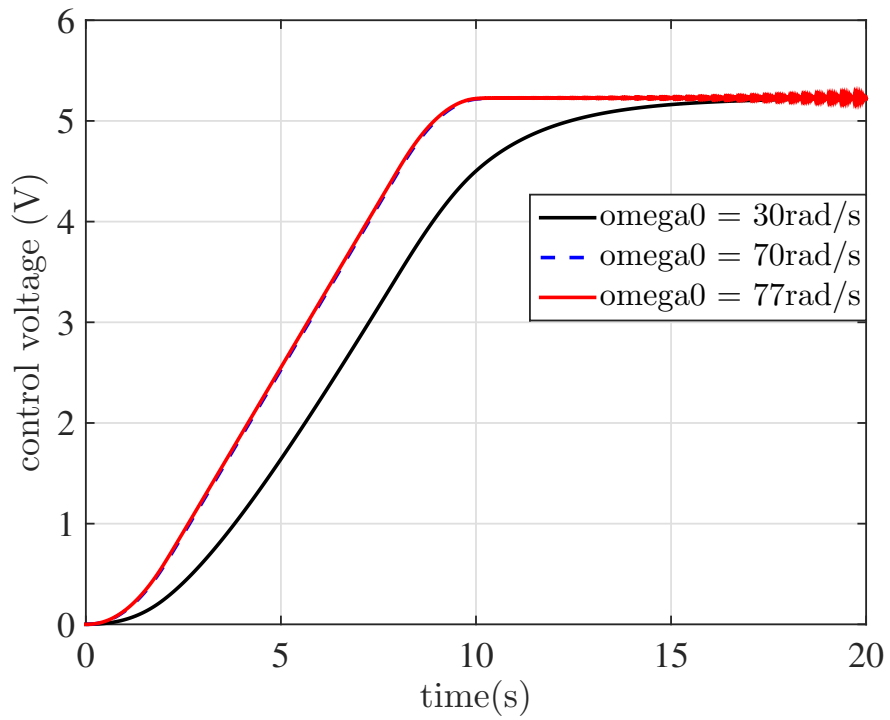


Figure 4.11: Effect of ω_0 on control voltage

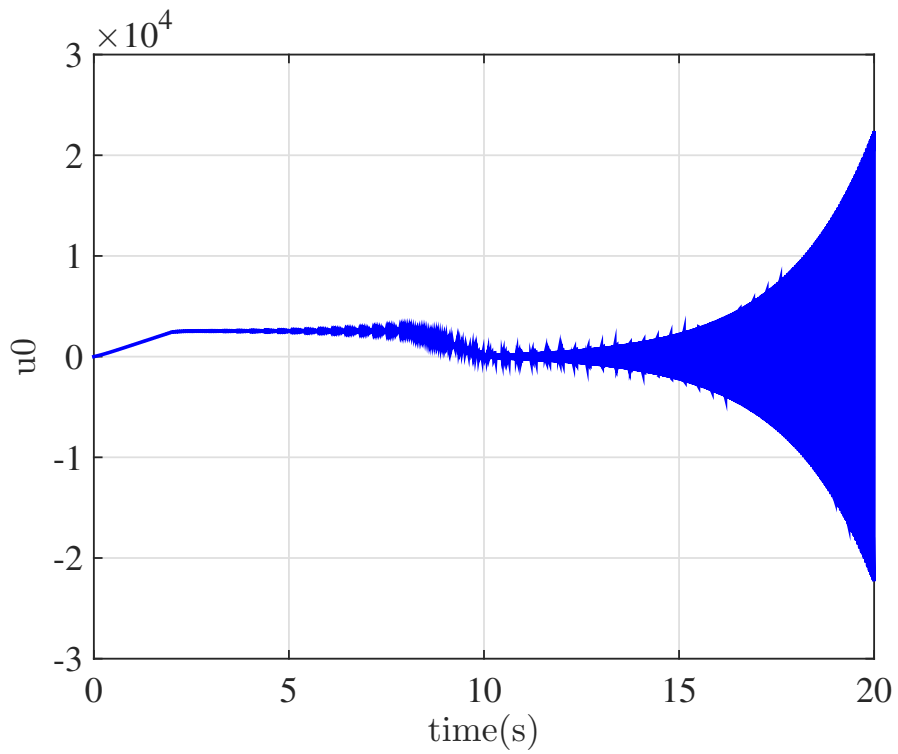


Figure 4.12: u_0 Vs time when $\omega_0 = 77.1$ rad/s

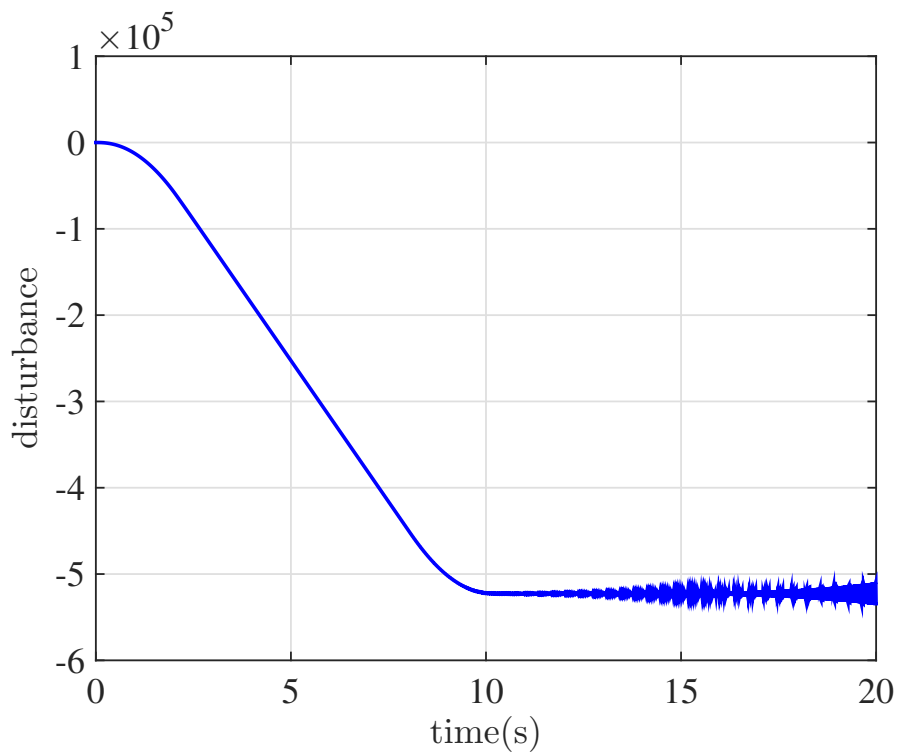


Figure 4.13: Disturbance estimate Vs time when $\omega_0 = 77.1\text{rad/s}$

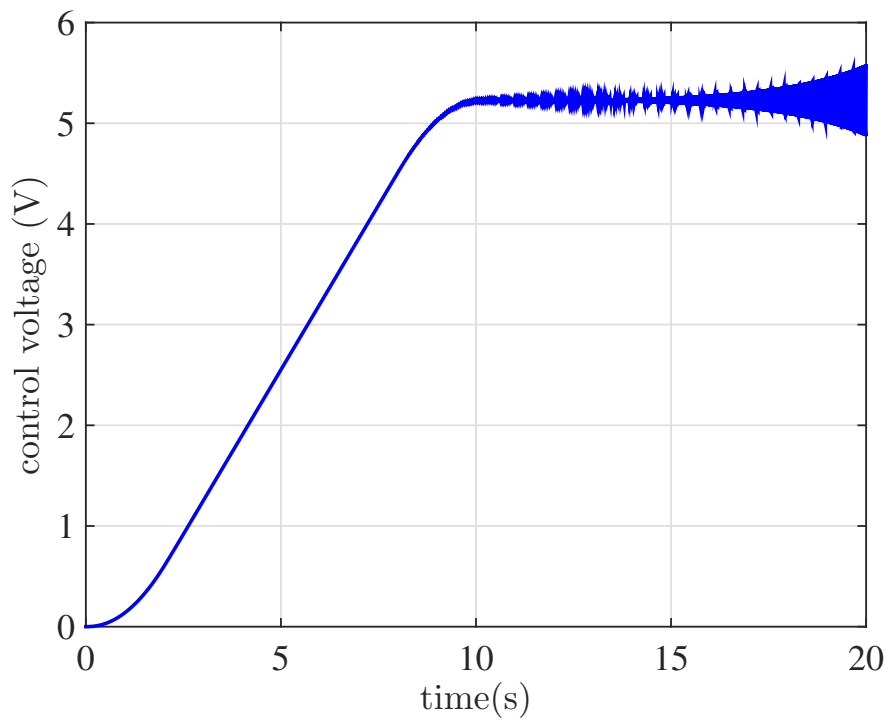


Figure 4.14: Control voltage Vs time when $\omega_0 = 77.1\text{rad/s}$

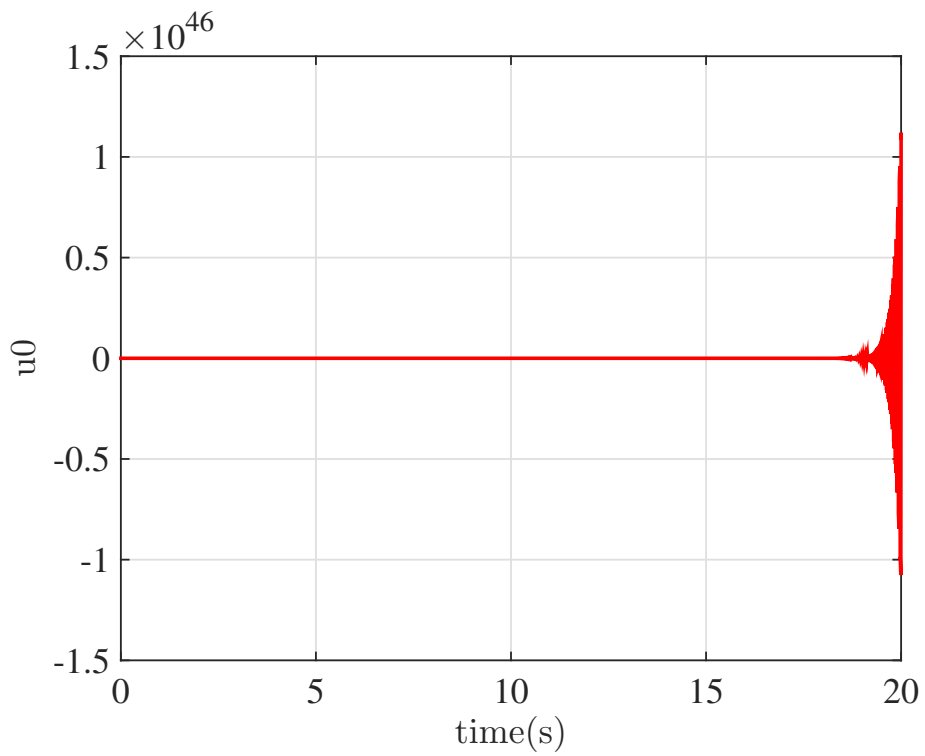


Figure 4.15: u_0 Vs time when $\omega_0 = 80\text{rad/s}$

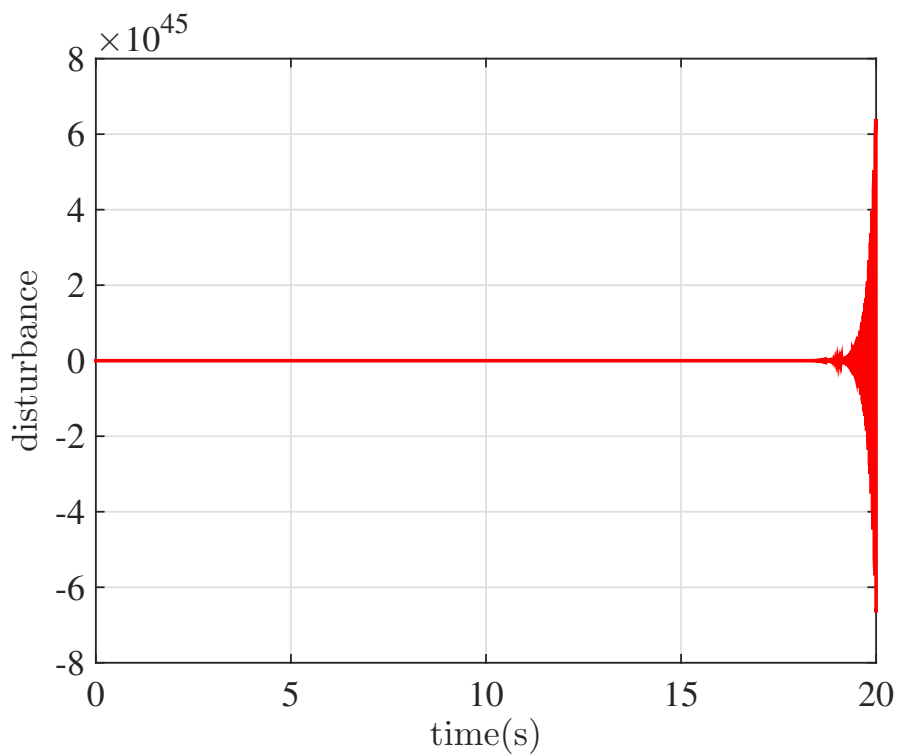


Figure 4.16: Disturbance estimate Vs time when $\omega_0 = 80\text{rad/s}$

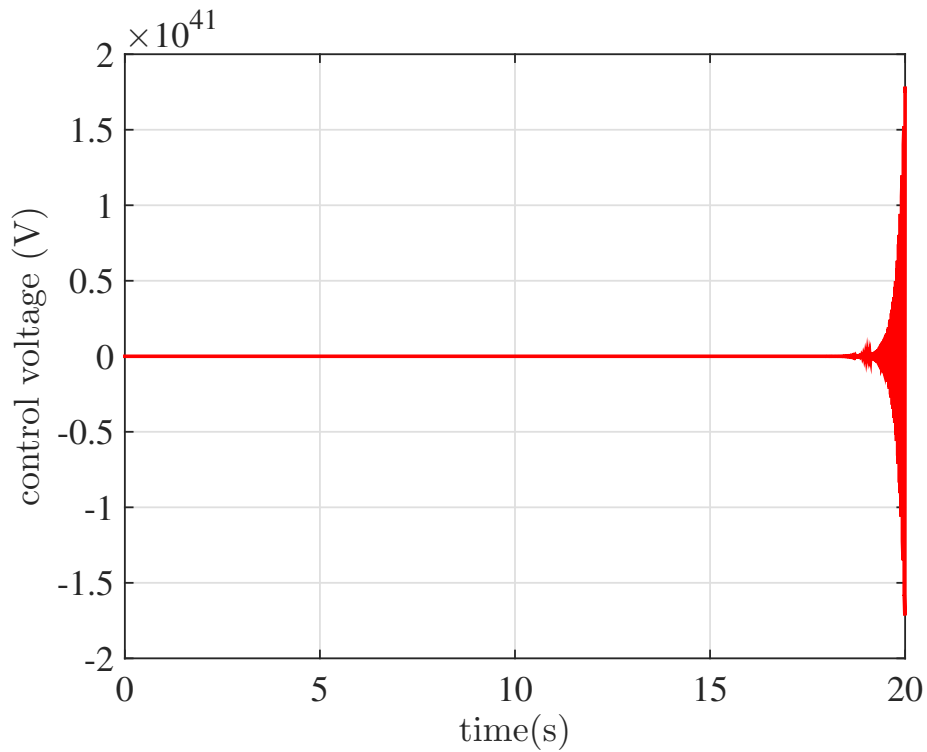


Figure 4.17: Control voltage Vs time when $\omega_0 = 80\text{rad/s}$

It is noticed in simulations that the ESO loses its estimation totally for higher values of ω_0 . The simulation results for $\omega_0 = 77.1\text{rad/s}$ (Figure 4.12, 4.13, 4.14) show that the critical observer bandwidth is $\omega_0 = 77\text{rad/s}$. Here, $\omega_0 = 80\text{rad/s}$ is considered as a case, that exceeds the critical value. Figure 4.15, 4.16 and 4.17 show the variations of u_0 , disturbance estimate and control voltage respectively for $\omega_0 = 80\text{rad/s}$. When ω_0 exceeds the critical limit, the estimation goes unbounded. The estimation time was calculated for various values of ω_0 . Table 4.2 shows the improvements in estimation time with increase in the value of ω_0 . The simulation was carried out for 100s. The estimation accuracy was fixed as 0.1%. As mentioned in Section 6.2, the reference signal is not a set jump but a smooth profile which attains its final value of 800 rpm in 10s. Hence the % error is discussed for the time after 10s. Henceforth an estimation time of 10.07s corresponds to 0.07s. The results show that as the observer poles move farther, from the plant poles, faster response is achieved. But once the poles cross a critical limit, the accuracy of estimation is

Table 4.2: Time of estimation for different values of ω_0 with an accuracy of 0.1%

omega0 (rad/s)	time of estimation (s)
5	>100
10	>100
15	>100
20	49.42
25	29.09
30	20.35
35	15.91
40	13.56
45	12.23
50	11.42
55	10.91
60	10.57
65	10.34
70	10.19
75	10.08
76	10.07
77	10.06
78	cannot be measured

lost. This in turn affects the performance of the controller which will be discussed in the following chapters.

4.3.2 An experimental approach

In the previous section we have seen the effect of critical observer bandwidth on accuracy of estimation and time of estimation. Experimental studies were also performed to validate the results. This section describes a brief account on the experimental setup for analysing the effect of observer bandwidth on the performance of ESO. A detailed description of the entire experimental setup is given in Chapter 7.

A testbed was developed to experimentally validate the performance of ESO in the speed control of a permanent magnet dc motor. It consists of the dc motor as the drive system, sensor units, converter unit and a processor unit. A hall sensor A1104 constitutes the speed sensor circuit, that measures the speed of the dc motor. The control voltage is measured using a simple potential divider setup. These sensor

circuits provide necessary inputs to the Extended State Observer (ESO) (Figure 3.6). The sampling period was set as 8ms as it requires ample calculations in every sampling period. The development platform is a processor unit of ARM Cortex - A8 32 bit processor with an operating speed of 1GHz. The estimated outputs z_1 , z_2 , z_3 (Figure 3.6) were used by the linear controller to implement the control law (Equation 3.13). The mathematical calculations for the solution of state equation of ESO (Equation 3.18) were realized in Python with the support of numpy and scipy libraries.

4.4 Results and discussions

A comparison of the simulated and experimental results of estimated speed for $\omega_0 = 30\text{rad/s}$, $\omega_0 = 70\text{rad/s}$ and $\omega_0 = 77.1\text{rad/s}$ are shown in Figure 4.18, Figure 4.20, Figure 4.22 respectively. Proper estimation does not occur for ω_0 less than 20rad/s. As the value of ω_0 increases, the estimation time decreases for an accuracy of 0.1% (Table 4.2). It is noted that estimation is improved for $\omega_0 = 70\text{ rad/s}$ (Figure 4.20), both in simulation and experiment.

In the experimental results, the accuracy of estimation decreases as the value of ω_0 was still increased (Figure 4.22b), though an improved simulation time was noticed in simulation studies (Table 4.2). To establish the performance of the ESO quantitatively, the estimation error is plotted for various values of ω_0 (Figure 4.19, 4.21, 4.23).

The present chapter discussed the effect of bandwidth on the performance of ESO which is a key constituent that enhances the overall performance of the control algorithm of ADRC. The results demonstrate that bandwidth of the observer restricts the design of ESO. An inspection of Figure 4.10 and Figure 4.11 shows that an increase in observer bandwidth results in a faster estimation of uncertainties which improves the performance of the control algorithm. But when ω_0 crosses the critical

bandwidth limit (Figure 4.16), the speed of estimation becomes too high that proper estimation of disturbance does not happen which impedes the implementation of the control law (Equation 3.13). A reasonable bandwidth for observer is hence proposed to obtain the best performance of ESO and ADRC, as the ESO can act like a filter for noises in such cases. It is suggested that a judicious selection of ω_0 is a trade-off between accuracy and noise sensitivity for the effective implementation of the modified topology.

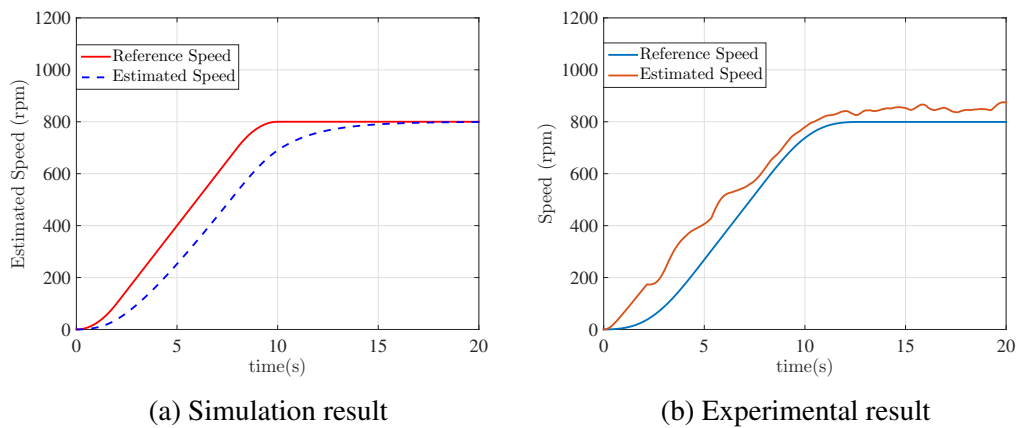


Figure 4.18: Comparison of simulated and experimental results of estimated speed for $\omega_0 = 30\text{rad/s}$

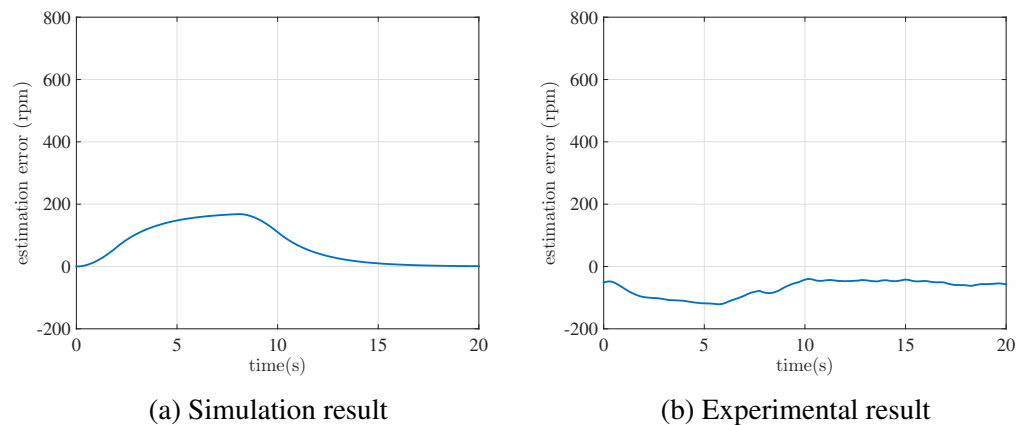
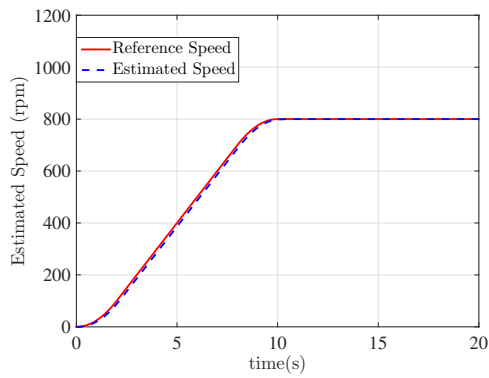
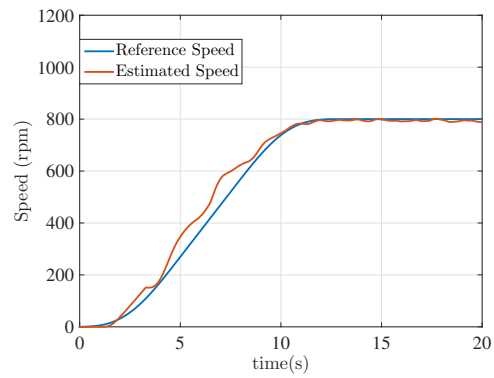


Figure 4.19: Estimation error when $\omega_0 = 30\text{ rad/s}$

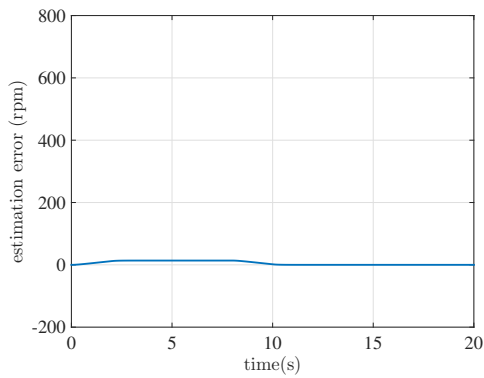


(a) Simulation result

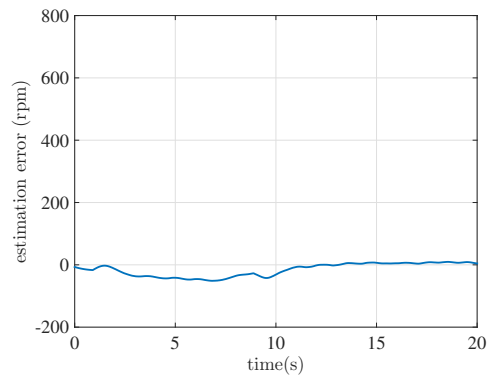


(b) Experimental result

Figure 4.20: Comparison of simulated and experimental results of estimated speed for $\omega_0 = 70\text{rad/s}$

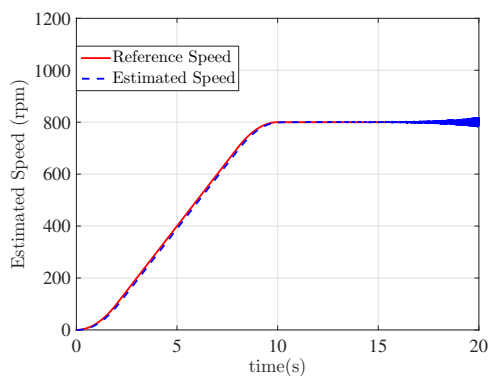


(a) Simulation result

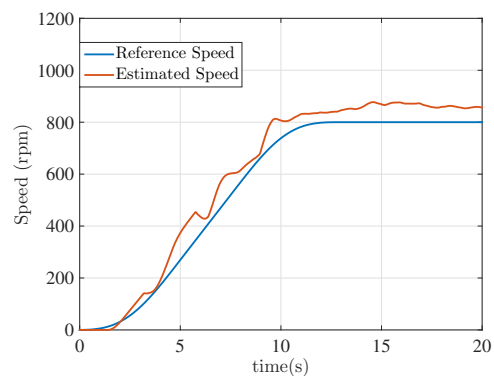


(b) Experimental result

Figure 4.21: Estimation error when $\omega_0 = 70\text{ rad/s}$

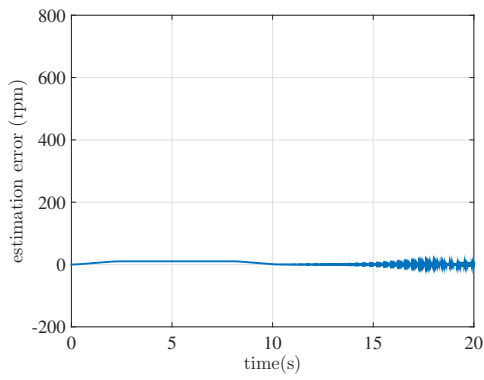


(a) Simulation result

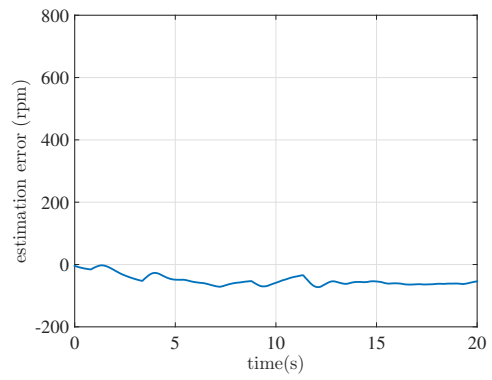


(b) Experimental result

Figure 4.22: Comparison of simulated and experimental results of estimated speed for $\omega_0 = 77.1\text{ rad/s}$



(a) Simulation result



(b) Experimental result

Figure 4.23: Estimation error when $\omega_0 = 77.1$ rad/s

CHAPTER 5

PERFORMANCE ANALYSIS OF PI CONTROLLER - A SIMULATION APPROACH

Simulation is a cost-effective approach of imitating a real process in a computer so that one can study the working of a process in detail. Simulations play a major role in research owing to the fact that, a researcher can evaluate even the effect of minor parameter variations, in simulation experiments, without much disastrous situations. In the context of ADRC, it is required to highlight the challenges in two term tuning of a PI controller and the effect of variation of controller parameters on the time domain specifications. This chapter discusses the simulations carried out on a permanent magnet dc motor whose speed is controlled by a PI controller and reports a qualitative analysis.

5.1 Modelling of permanent magnet dc motor

The parameters used for developing the mathematical model are given in Table 5.1. The armature resistance and inductance are represented as lumped parameters.

A dc motor is mathematically modelled by Equation 5.1 as a linear, time invariant second order system with angular position as the output and current as input (Dorf and Bishop, 2011).

$$J \frac{d\omega}{dt} + B\omega + T_L = K_t i_a \quad (5.1)$$

The present study concentrates on the armature control used for speed regulation. Moreover, for a permanent magnet dc motor one can provide only armature control method. Hence a different selection is done for input and output of the model. Here,

Table 5.1: DC motor parameters

Specification	Symbol	Unit
Armature resistance	R_a	Ω
Armature inductance	L_a	H
Armature voltage	V_a	V
Armature current	i_a	A
Back emf	E_b	V
Angular speed	ω	rad/sec
Angular velocity	N	rpm
Equivalent moment of inertia	J	kg.m ²
Equivalent viscous friction coefficient	B	N.m.s
Load torque on motor	T_L	N.m
Developed magnetic torque by motor	T_m	N.m
Back emf constant	K_b	V/rad/s
Torque constant	K_t	Nm/A

voltage applied to the dc motor(V_a) is selected as input and angular velocity(ω) is selected as the output. The governing equations are given below. The electromagnetic torque developed by the motor is given by Equation 5.2 and back emf developed in the motor by Equation 5.3

$$T_m = K_t * i_a \quad (5.2)$$

$$E_b = K_b * \omega \quad (5.3)$$

The dynamic equation of the armature circuit is expressed by Equation 5.4 and that of the mechanical system comprising armature and load is given by Equation 5.5

$$V_a = L_a \frac{di_a}{dt} + R_a i_a + E_b \quad (5.4)$$

$$J \frac{d\omega}{dt} + B\omega + T_L = T_m \quad (5.5)$$

The above equations are incorporated in the block diagram (Figure 5.1). Using these fundamental equations, the dynamic characteristics of the permanent magnet dc motor is written, with speed as a function of voltage, as in Equation 5.6.

$$\ddot{\omega} + \left(\frac{JR_a + BL_a}{JL_a} \right) \dot{\omega} + \left(\frac{R_a B + K_t K_b}{JL_a} \right) \omega = \left(\frac{K_t}{JL_a} \right) V_a \quad (5.6)$$

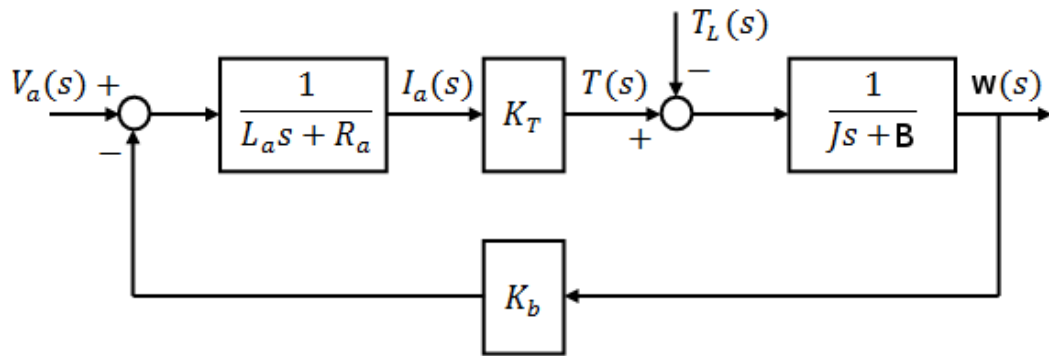


Figure 5.1: A block diagram of dc motor

5.2 Motor specifications

The specifications of the motor under study are tabulated in Table 5.2.

Table 5.2: Motor specifications

Specification	Value
J	$0.39 * 10^{-4} kgm^2$
B	$2.86 * 10^{-5} Nms/rad$
R_a	0.9Ω
L_a	$2.3mH$
K_t	$6.37 * 10^{-2} Nm/A$
K_b	$0.062Vs/rad$
Rated voltage	12V
Rated speed	1500rpm (157rad/s)

5.3 Open loop response

The motor parameters are validated by simulating the open loop response. A no load speed of 1834 rpm which turns as 192 rad/s is obtained for an input voltage of 12V. The response time of the motor is found to be 0.032s (Figure 5.2).

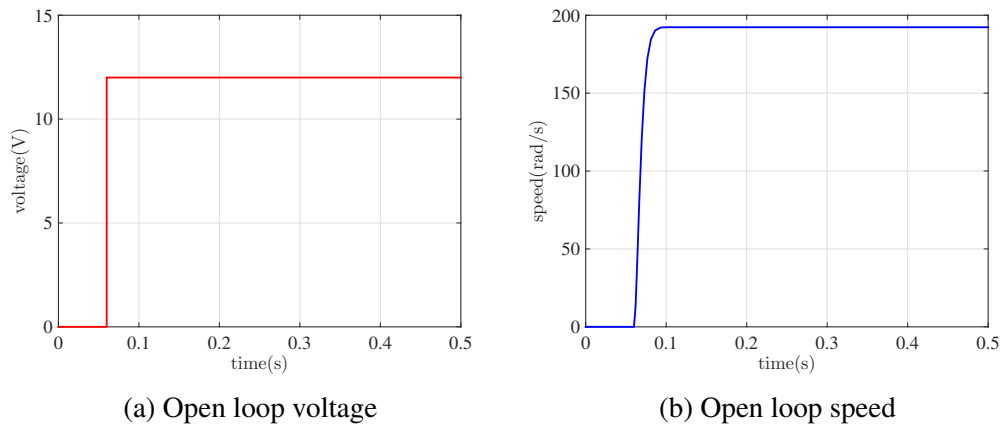


Figure 5.2: Open loop speed response for a step voltage of 12V

5.4 Closed loop performance with Proportional Integral controller

Proportional Integral Derivative (PID) controllers are widely used in industries and its popularity is attributed to its simple model and implementation by practising engineers. Each term of the PID controller has its own significance. In any industrial process, the proportional term sufficiently pushes the actuator to bring the process variable to the set point. But in doing so, this may result in unwanted oscillations if the coefficient exceeds the required value. Also, its effect deteriorates as the error decreases. ie, the control effort due to proportional term decreases as the error decreases. This causes a steady state error. An integral term helps to solve the problem of steady state error. It sums up all the previous errors and accordingly generates the control effort. Thus all the steady errors occurred till then, will be added up and extra push will be generated by the integral term, reducing the steady state error. In its course of action, this can result in overshoots. This phenomenon of overshoot is accounted by the derivative term and results in smooth settling response with an improved settling time. But the derivative controller causes much fluctuations in noisy environment. Hence in noisy situations where the speed of response is not a matter of fact one goes for PI controller. In such cases, the P and I terms are so

tuned that it also accommodates the effort put forward by the derivative term if it would have been present. As always said “a well tuned PI controller is always better than a moderately tuned PID controller”. A Proportional Integral(PI) controller is mathematically represented as Equation 5.7.

$$y(t) = K_p \left\{ e(t) + \frac{1}{T_i} \int e(t) dt \right\} \quad (5.7)$$

where K_p is the proportional error constant and T_i is the integral time constant.

5.4.1 Tuning method

From the above discussions it is clear that the controller gains should be properly selected to attain the required specifications. Tuning of controllers involve setting the suitable gains for the controller. In practical systems the objective of controller tuning is always “Acceptable stability, and medium fastness of response”. A systematic procedure is required for the tuning of all controllers. There are different approaches for the tuning of controllers mentioned in literature. In closed loop tuning methods (Krishnaswamy *et al.*, 1987), controller tuning takes place in automatic state while the plant works in closed loop. But in open loop tuning methods (Dreinhofer, 1988), the controller tuning takes place manually while the plant works in open loop. Once the coefficients are fixed, the plant is put in closed loop mode. The parameters of the controller can be fixed by other machine learning algorithms too (Zhu and Azar, 2015), that takes into account several factors like robustness, optimality, cost etc.

The present simulation is based on Zeigler Nichols tuning technique. In this method,

Controller	K_p	T_i	T_d
P	$K_u/2$		
PI	$K_u/2.2$	$T_u/1.2$	
PID	$K_u/1.7$	$P_u/2$	$P_u/8$

Table 5.3: Zeigler Nichols tuning table

the system being in closed loop, the integral term is set to zero. On increasing the proportional gain the step response becomes faster. The proportional gain is increased until steady oscillations are obtained as a response for unit step change. This gain is called the ultimate gain K_u and the period of oscillation is termed as the ultimate period T_u . The controller gains are then derived as per Table 5.3.

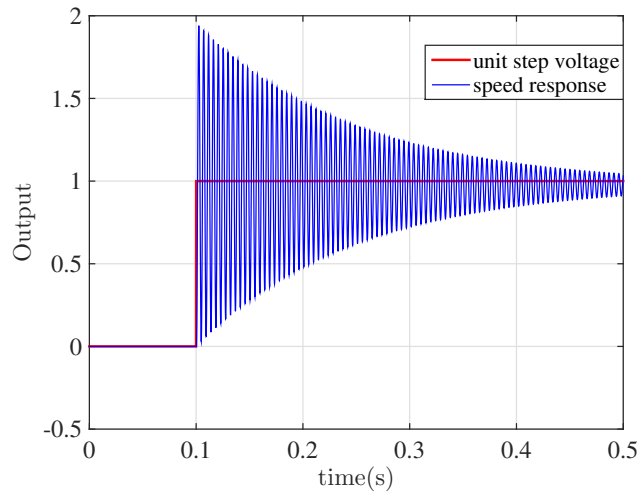
5.4.2 Methodology

Simulations were carried out in MATLAB/SIMULINK with fixed step sampling time of 0.0001s using ode3 (Bogacki-Shampine) as the solver for 25s. In order to take into account the real sense of a dc motor, a transport delay is included in the system. The best results were obtained when the delay time is greater than the step size used in simulation. As the simulation step size was 0.0001s, the delay time of the transport delay was selected as 0.0002s. The dc motor system given in Figure 5.1 was tuned using the Zeigler Nichols tuning approach in the closed loop mode using the specifications mentioned in Sec.5.2. The simulation was carried out to a longer duration to ensure that the resulting oscillations are sustained for the ultimate gain. The ultimate gain K_u was found to be 2.8 where the system gave a sustained oscillation at the output for unit step change in reference. For a gain of 2.7 and 2.9 the system outputs have decreasing and increasing envelopes respectively in unit step response (Figure 5.3). The ultimate period was found to be $T_u = 0.0047s$.

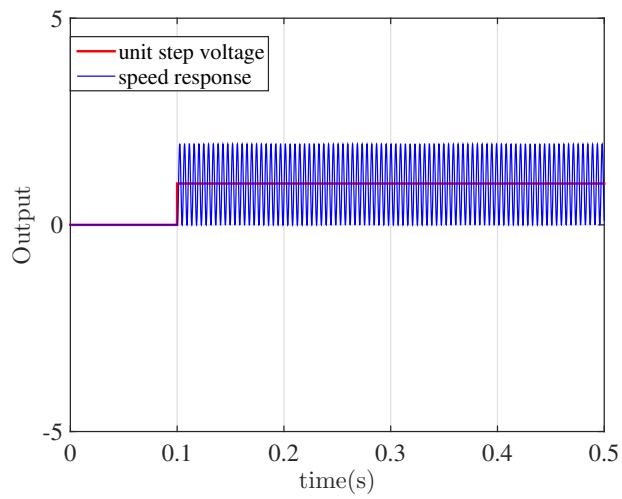
Validation of Ultimate gain

Using the specifications in Sec.5.2 the transfer function of motor was obtained as Equation 5.8.

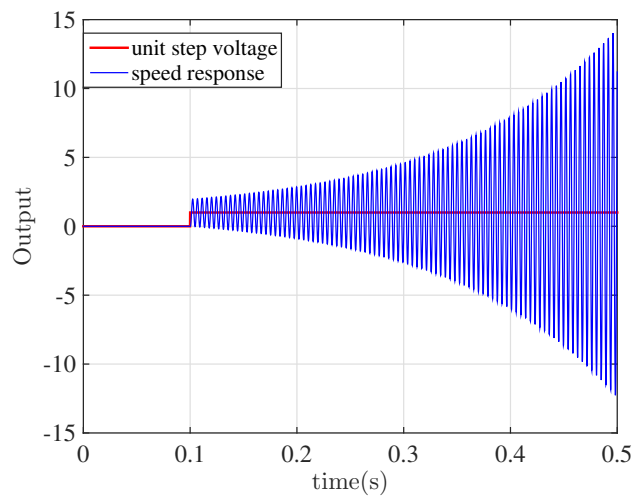
$$\frac{\omega(s)}{V(s)} = \frac{715730.33}{s^2 + 395.05s + 44606.74} \quad (5.8)$$



(a) $K_u=2.7$



(b) $K_u=2.8$



(c) $K_u=2.9$

Figure 5.3: Fixing the ultimate gain during PI tuning

By including ultimate gain K_u and transport delay of 0.0002s, the open loop transfer function becomes Equation 5.9

$$\frac{\omega(s)}{V(s)} = \frac{715730.33 * K_u * (1 - 0.0002s)}{s^2 + 395.05s + 44606.74} \quad (5.9)$$

and equivalent closed loop transfer function will be Equation 5.10

$$\frac{\omega(s)}{V(s)} = \frac{715730.33 * K_u - 143.15 * K_u * s}{s^2 + 395.05s + 44606.74 + 715730.33 * K_u - 143.15 * K_u * s} \quad (5.10)$$

This can give a sustained oscillatory response for step input only when the coefficient of the s term in the denominator becomes zero.

$$\begin{aligned} 395.05 &= 143.15 * K_u \\ K_u &= 2.76 \end{aligned} \quad (5.11)$$

The value of K_u was thus obtained as 2.76 mathematically (Equation 5.11), which validates the simulated result of 2.8 as discussed in Section 5.4.1.

5.4.3 Analysis of the performance of PI controller

Simulations were carried out for the permanent magnet dc motor (Section 5.2), for a set speed of 157rad/s. The PI parameters were calculated based on the tuning table (Table 5.3). The values were obtained as $K_p = 1.27$ and $T_i = 0.0039$ for a PI controller. The parameters tuned using Zeigler Nichols tuning approach may not give satisfactory results in the beginning. It can be used as a starting point for choosing the PI parameters. Hence the parameters were further tuned to meet the specifications. The effect of PI parameters in system behaviour is tabulated in Table 5.4. The effect of variation of K_p when T_i is kept constant is discussed below (Figure 5.4). As the value of K_p increases the system loses its stability (Figure 5.4d). With reduced value of K_p , there is reduction in overshoot and the system

Table 5.4: Effect of PI parameters in system behaviour

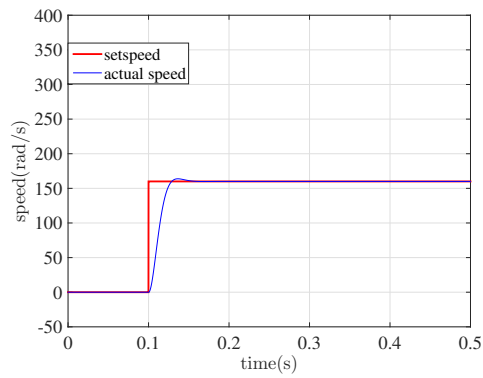
Controller Parameters	Rise Time	Overshoot	Settling Time	Steady State Error	Stability
K_p	Decrease	Increase	Slight Change	Decrease	Degrade
K_i	Decrease	Increase	Increase	Eliminate	Degrade

gains stability (Figure 5.4a). The effect of variation of T_i is also noted when K_p is kept constant (Figure 5.5). The integration effect increases with decrease in the value of T_i . This results in subsequent reduction in steady state error (Figure 5.5c). On the other hand, a higher reduction in T_i , results in an unstable response (Figure 5.5b, Figure 5.5a). Hence, care should be taken while tuning the integral time constant T_i , to avoid unstable system responses, while one aims at reducing the steady state error.

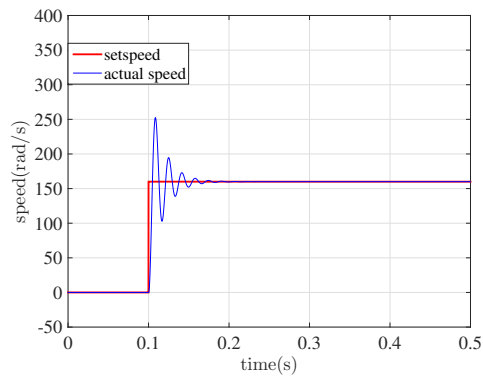
As the effects of variation of both parameters K_p and T_i are analysed, controller gains can be further tuned till required specifications are met. The value of T_i is fixed at 0.0039 and K_p is decreased to 0.2 and the response is noted (Figure 5.6). Now the response has settled with very low steady state error and considerable overshoot (Figure 5.6b). The proportional term K_p is reduced to 0.02 to further decrease the overshoot. However, reduction in overshoot is achieved at the cost of increased rise time (Figure 5.7).

To reduce the rise time, T_i is decreased without changing K_p (Figure 5.8). However, the reduction in rise time is achieved at the cost of increased overshoot.

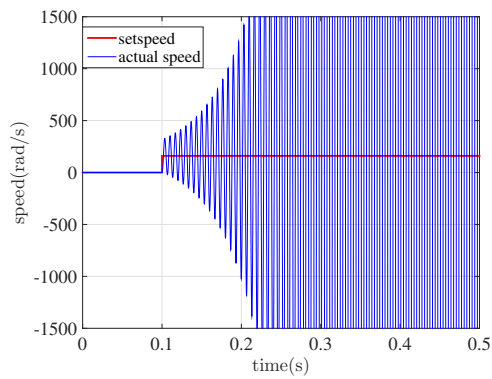
Further reduction in K_p results in increase of rise time (Figure 5.9). The designer has to tune the two parameters K_p and T_i by a trial and error approach until a satisfactory response as per the required specification is achieved.



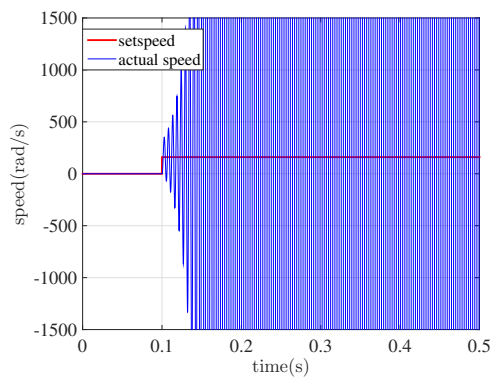
(a) $K_p = 0.02, T_i = 0.0039$



(b) $K_p = 0.2, T_i = 0.0039$

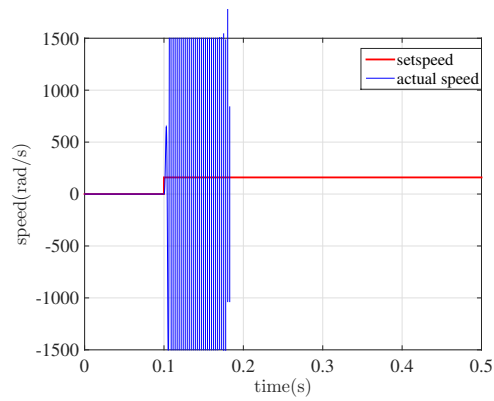


(c) $K_p = 1.27, T_i = 0.0039$

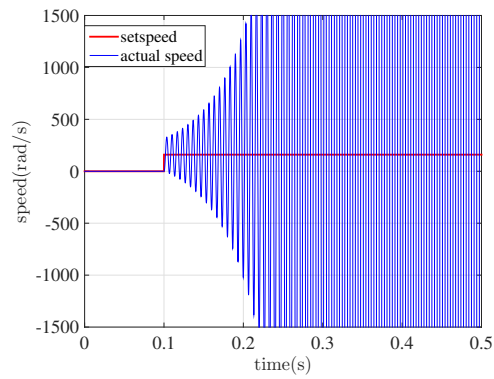


(d) $K_p = 2, T_i = 0.0039$

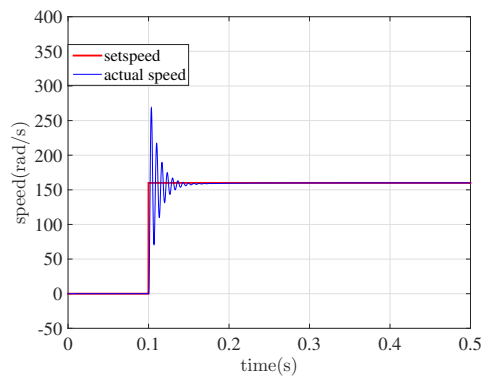
Figure 5.4: Response of PI controlled system with varied K_p and fixed T_i



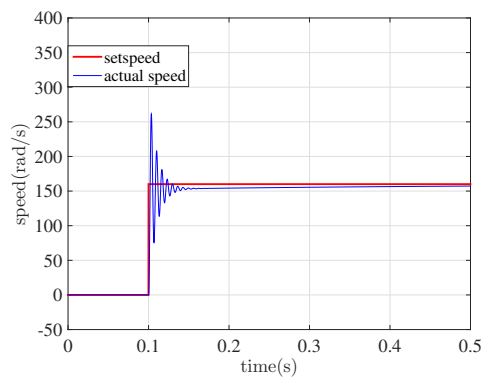
(a) $K_p = 1.27, T_i = 0.00039$



(b) $K_p = 1.27, T_i = 0.0039$



(c) $K_p = 1.27, T_i = 0.039$

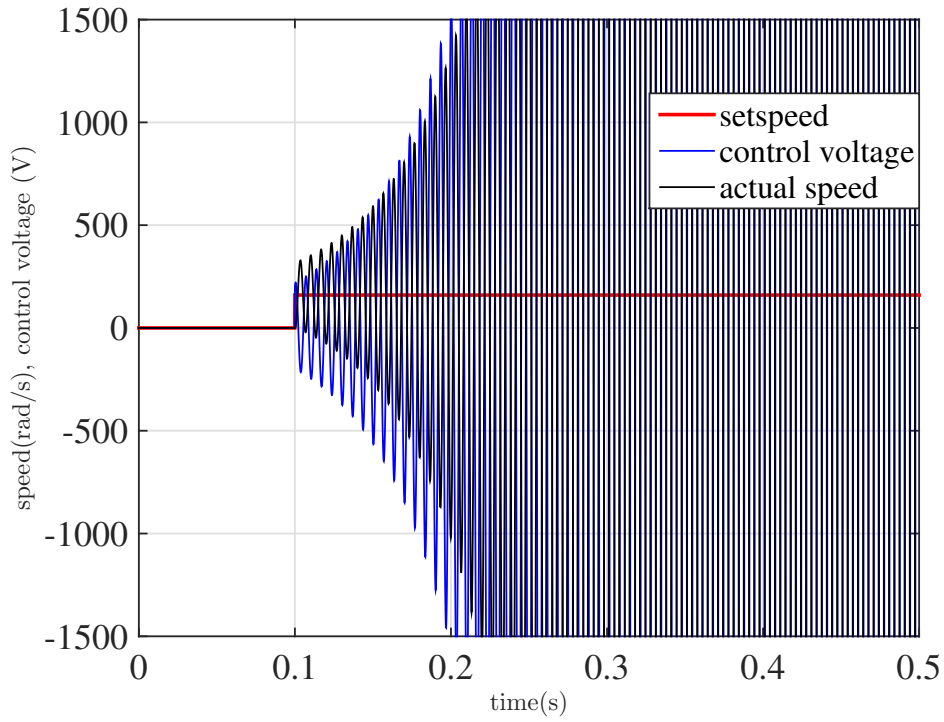


(d) $K_p = 1.27, T_i = 0.39$

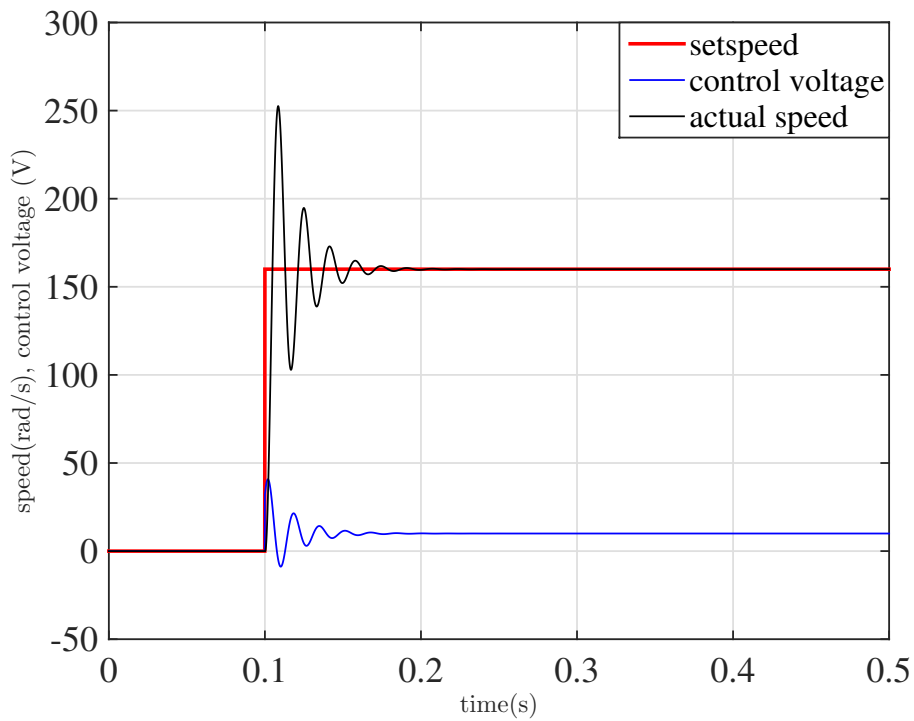
Figure 5.5: Response of PI controlled system with fixed K_p and varied T_i

5.5 Results and discussions

This chapter discussed a qualitative analysis of the performance of PI controller and the challenges in tuning. It was observed that in a PI controller, keeping T_i constant, an increase in K_p decreases rise time, along with a prominent overshoot while, a decrease in K_p , decreases the overshoot but at the cost of increased rise time. Keeping K_p constant, an increase in T_i reduces overshoot, degrades steady state error and increases rise time, where as decrease in T_i results in increased overshoot, even though steady state error and rise time are improved. Thus improved performance of a closed loop control system is the result of a judicious trial and error approach from the part of the control engineer which he gains from vast practical experience. This also results in a trade off between many specifications as we include more time domain specifications. The challenges in tuning becomes more evident in a PID controller as it is a three term controller. The merit of ADRC upon PI controller is that it is a single parameter tuning controller. The next chapter discusses the simulation analysis of performance of ADRC based system in the speed control of a permanent magnet dc motor.

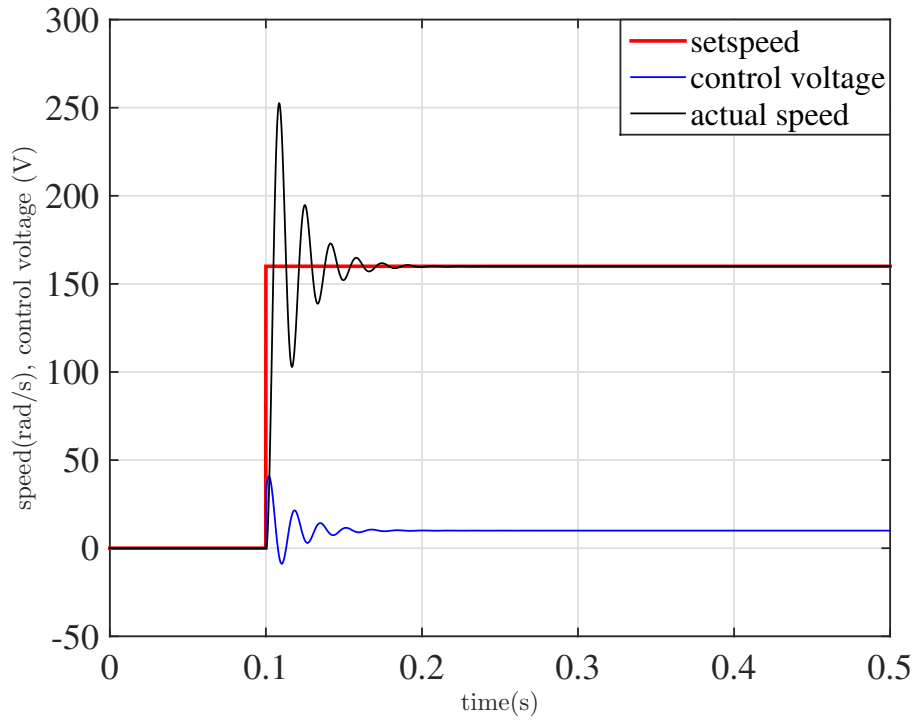


(a) $K_p = 1.27, T_i = 0.0039$

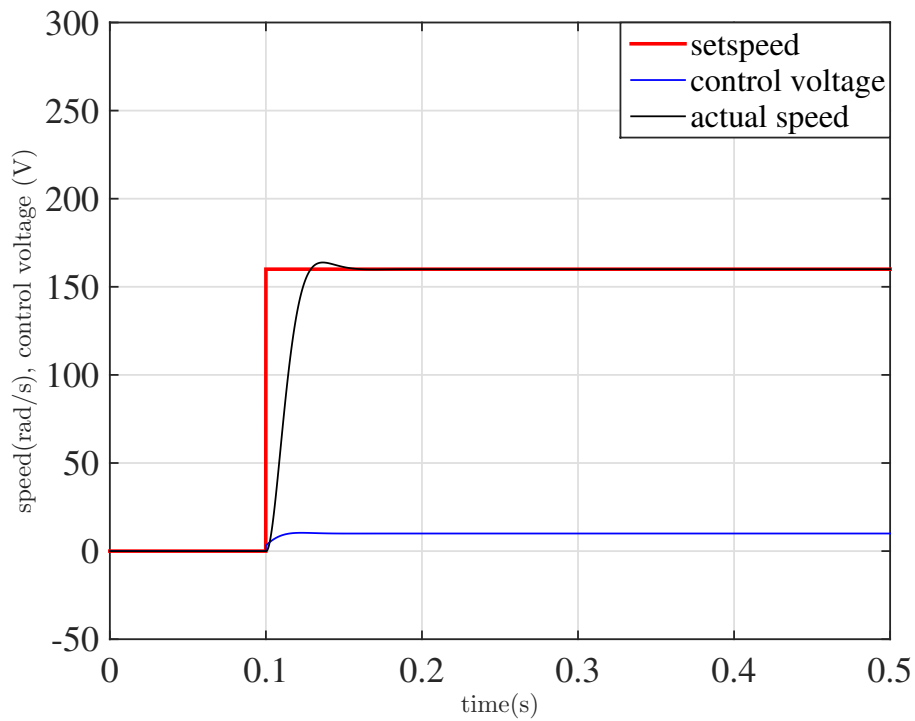


(b) $K_p = 0.2, T_i = 0.0039$

Figure 5.6: Response when K_p is decreased from 1.27 to 0.2

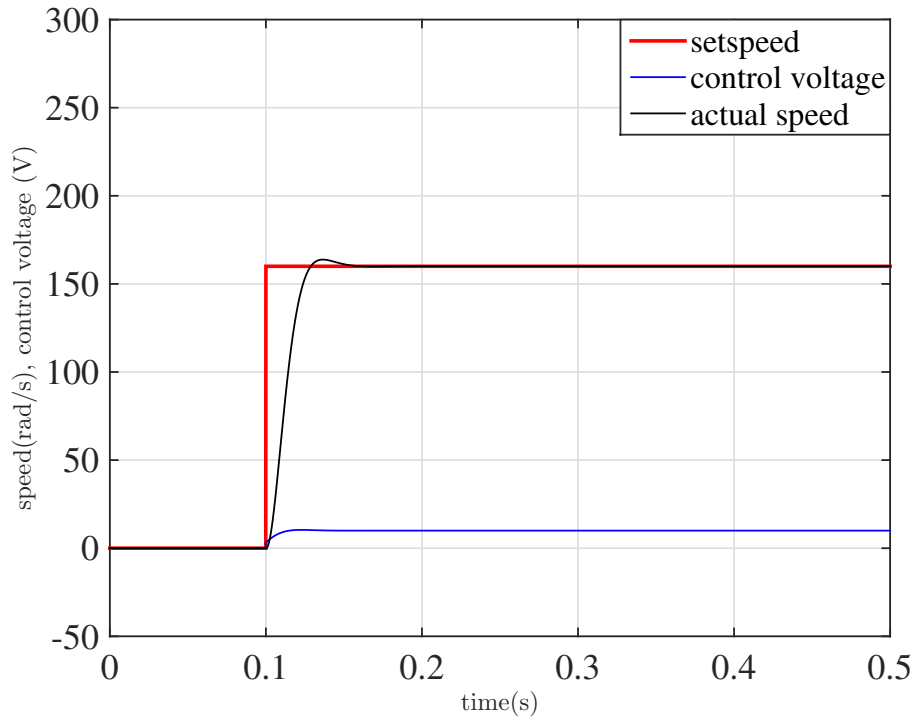


(a) $K_p = 0.2, T_i = 0.0039$

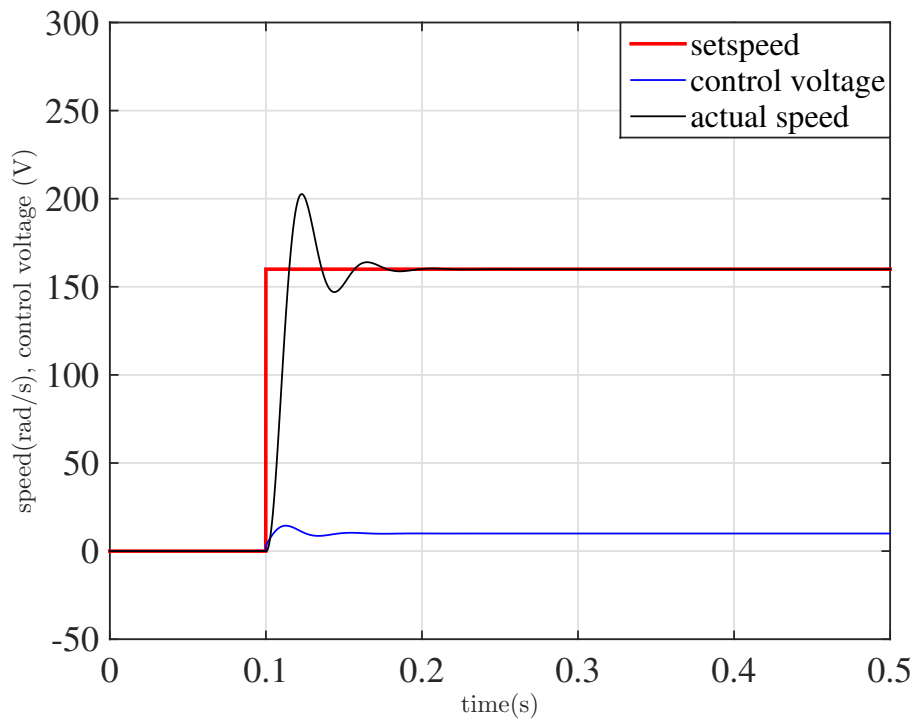


(b) $K_p = 0.02, T_i = 0.0039$

Figure 5.7: Response when K_p is decreased from 0.2 to 0.02

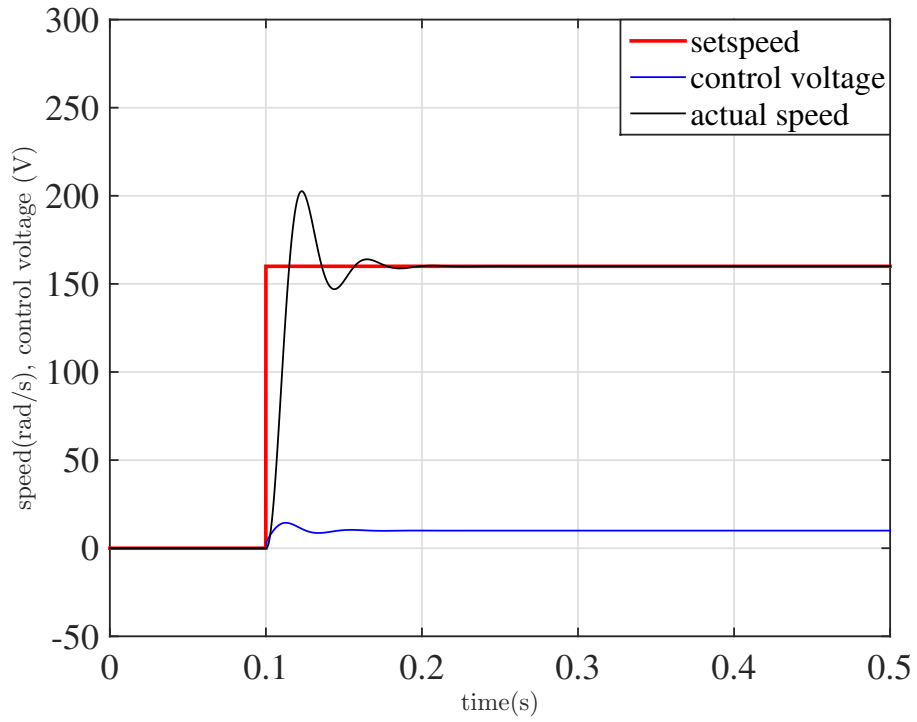


(a) $K_p = 0.02$, $T_i = 0.0039$

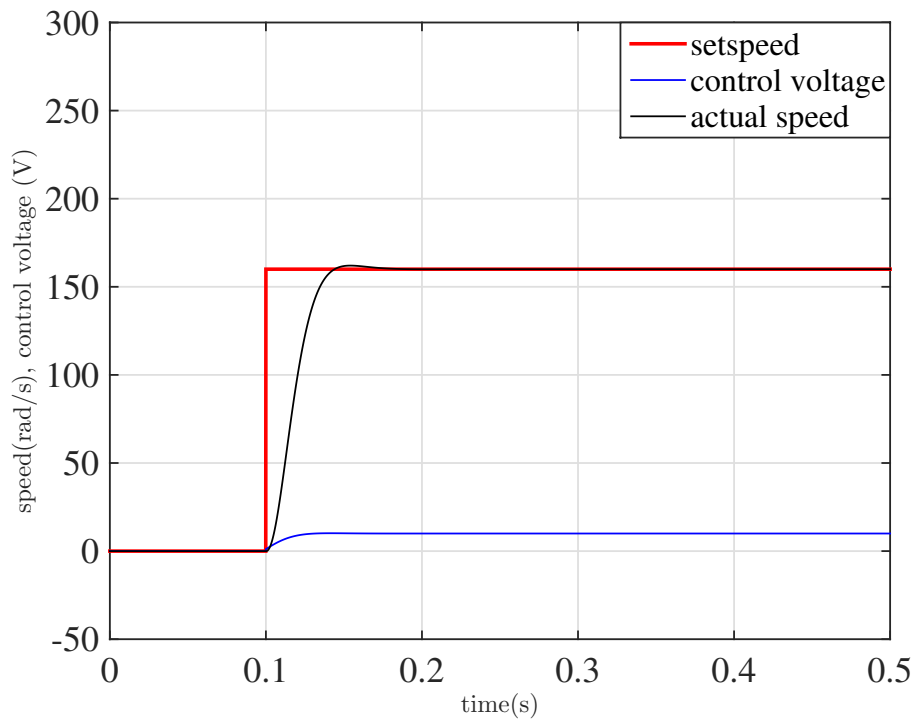


(b) $K_p = 0.02$, $T_i = 0.002$

Figure 5.8: Response when T_i is decreased from 0.0039 to 0.002



(a) $K_p = 0.02, T_i = 0.002$



(b) $K_p = 0.007, T_i = 0.002$

Figure 5.9: Response when K_p is decreased from 0.02 to 0.007

CHAPTER 6

PERFORMANCE ANALYSIS OF MODIFIED ADRC - A SIMULATION APPROACH

This chapter reports the studies performed in evaluating the performance of modified ADRC topology in the context of speed control of permanent magnet dc motor. The effect of the critical bandwidth, which is the major focus of this research work, on the performance of controller and its uncertainty reduction are also elaborated.

6.1 Modifications in the topology

Tracking differentiator was one of the constituents of ADRC proposed by Han (2009). The conventional ADRC topology used a tracking differentiator in profile generation. However, in this modified approach a smooth speed profile is generated by integrating a trapezoidal acceleration signal formed using simple mathematical relations (Equation 6.1). Thus the generation of tracking profile is made easier avoiding the complexity of the mathematical equation (Equation 3.3). In most cases, position sensors are used and eventually tracking differentiator had a role in the feedback loop also, to generate the actual speed signal from the sensed position. In this approach, the speed is directly feedback. Apparently, this approach eliminates the tracking differentiator in the feedback loop, thus simplifying the system.

6.2 Methodology

Simulations were performed in MATLAB/SIMULINK with a fixed step sampling time of 0.0001s using ode3 (Bogacki- Shampine) as the solver for 20s. Simulation

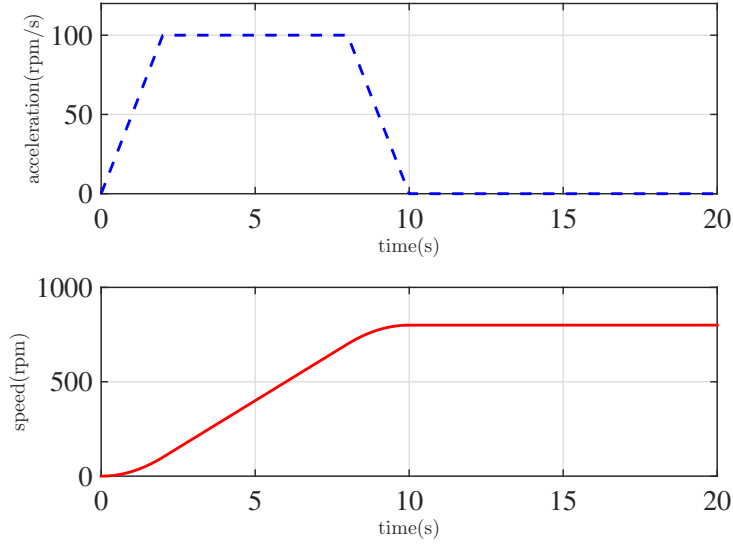


Figure 6.1: Transient profile for simulation

diagrams are shown in Figure 4.6, 4.7 and 4.8. A transient profile shown in Figure 6.1 was generated as the tracking signal. The Equation 6.1 for acceleration was integrated to get a steady reference speed of 800 rpm in 10s.

$$a(t) = \begin{cases} 50t, & 0 < t < 2 \\ 100, & 2 \leq t < 8 \\ 500 - 50t, & 8 \leq t < 10 \end{cases} \quad (6.1)$$

In Equation 3.9 if $-a_1\dot{y} - a_0y + w$ is chosen as f , then the exact value of b must be known in implementing ADRC, which makes the model less concept of ADRC meaningless. Hence in Equation 3.9 a new constant b_0 is used, to avoid knowing b a priori. The mismatch between b and b_0 , is accounted as an “uncertainty” and will be included in estimated state variable z_3 of ESO. In the simulation of ADRC based system in order to implement the control law (Equation 3.13) the value of b_0 is required and it is randomly selected as 100000. Any value of b_0 will not alter the performance of the system as the mismatch between b and b_0 will be estimated and cancelled by the control action.

However, for simulation, a model is required though it does not include all aspects of the dynamics of the system. Equation 6.2 is obtained as the transfer function of the permanent magnet dc motor using the specifications mentioned in Section 5.2 and Equation 5.6.

$$\frac{\omega(s)}{V(s)} = \frac{715730.33}{s^2 + 395.05s + 44606.74} \quad (6.2)$$

Equation 6.3 gives the criteria for selecting observer gains as discussed in detail in Sec.3.6. It can be noticed that ω_0 is the only deciding factor in the performance of ADRC.

$$G = \begin{bmatrix} g_1 \\ g_2 \\ g_3 \end{bmatrix} = \begin{bmatrix} 3\omega_0 \\ 3\omega_0^2 \\ \omega_0^3 \end{bmatrix} \quad (6.3)$$

As discussed in Sec.4.1, ω_0 , the observer bandwidth decides how fast the estimation takes place. A higher bandwidth results in faster estimation but at the same time increases noise sensitivity which in turn affects accuracy of estimation. Hence the choice of ω_0 is crucial in the design of ADRC. Here it is found that poles of the second order system are $(-197.525 \pm j 74.7)$ with the known parameters of the system. But the inclusion of ADRC into this system, reduces it to a simple double integrator. In order to accommodate larger amount of uncertainties of the system model, the bandwidth of the observer must be kept high (Figure 4.10).

The design of controller was done as mentioned in Section 3.6. With

$$\omega_0 = 4\omega_c \quad (6.4)$$

the value of $K_p = \omega_c^2 = \frac{\omega_0^2}{16}$ and $K_d = 2\zeta\omega_c = \frac{\omega_0}{2}$, with $\zeta =$ selected as 1, to avoid overshoots in response.

The analysis was carried out with various values of ω_0 starting from $\omega_0 = 5$ rad/s. From the studies on Extended State Observer in Chapter 4, it is seen that the critical value for observer bandwidth is $\omega_0 = 77$ rad/s for this system. As mentioned

Table 6.1: % error for different values of ω_0 at 10.07s

ω_0 rad/s	% error
5	98.17
10	88.36
15	68.71
20	45.09
25	25.64
30	13.48
35	6.99
40	3.70
45	2.02
50	1.46
55	0.67
60	0.41
65	0.26
70	0.17
75	0.11
76	0.1
77	0.09
78	response blows up

in Section 6.2, the reference signal is not a set jump but a smooth profile which attains its final value in 10s. Hence the % error is discussed for the time after 10s. Henceforth an estimation time of 10.07s corresponds to 0.07s. Hence to get a reasonable estimation, ω_0 is selected as 70rad/s, for which the estimation time (Table 4.2) is found to 10.19s. In other words, the steady state error of the estimate is only 0.1% (Table 4.2) and the estimation time is 0.19s. In the perspective of a controller, the specification selected under study are steady state error, overshoot and settling time. However, overshoot is avoided by the selection of $\zeta=1$ in the controller design. From Table 6.1 it can be observed that as the observer bandwidth is increased from 5 rad/s to 77 rad/s, the % error in the actual speed decreases from 98.17% to 0.09%. Also it is noted that the % error becomes too large when ω_0 is 78rad/s as the response blows up. Eventually, the optimal value of observer bandwidth is selected as $\omega_0=70$ rad/s.

Plots of reference speed and actual speed for $\omega_0 = 10$ rad/s and $\omega_0 = 30$ rad/s are shown in Figure 6.2 and Figure 6.3 respectively. In this case the %error decreases

from 88.36% to 13.48% at time 10.07s.

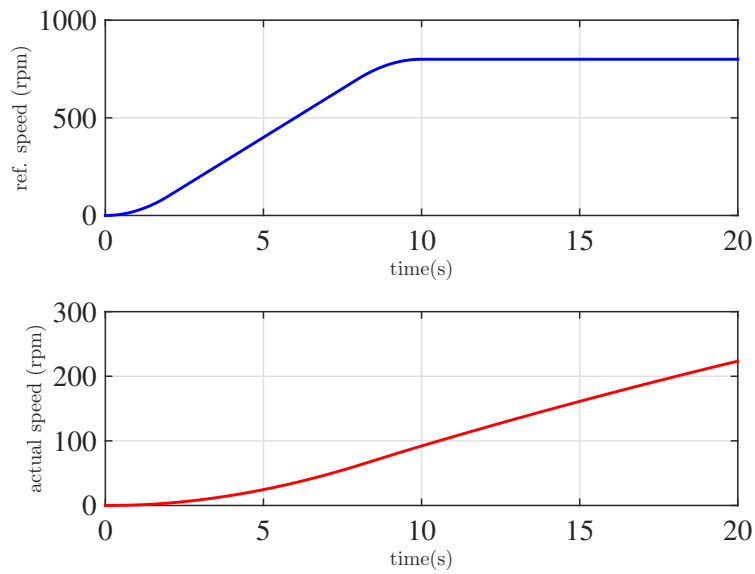


Figure 6.2: Reference, actual speed for $\omega_0 = 10\text{rad/s}$

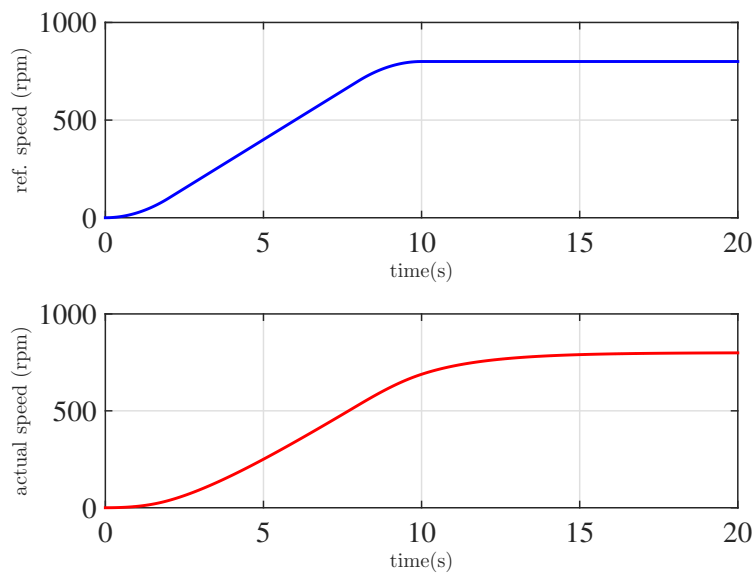


Figure 6.3: Reference, actual speed for $\omega_0 = 30\text{rad/s}$

Another case, when $\omega_0 = 60 \text{ rad/s}$ is shown in Figure 6.4. Figure 6.5 shows the speed variation in a smaller interval of time which shows that the % error is 0.41 at $\omega_0 = 60 \text{ rad/s}$.

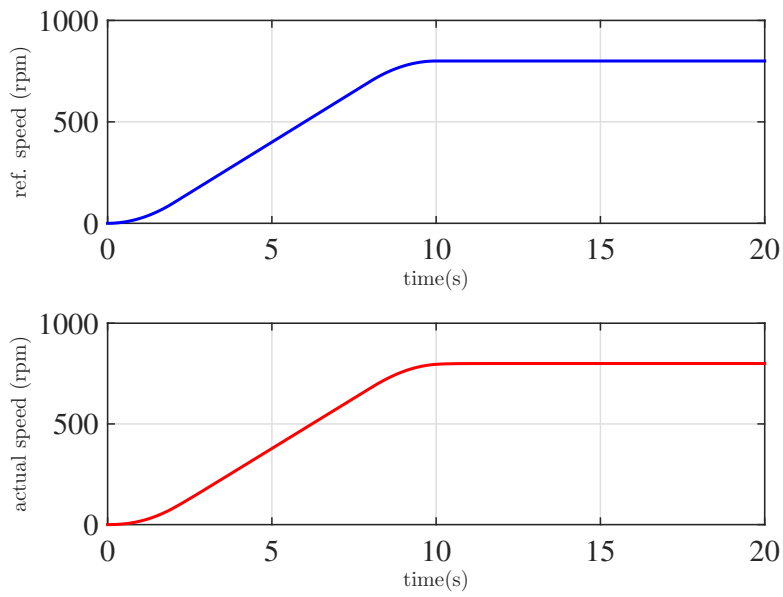


Figure 6.4: Reference, actual speed for $\omega_0 = 60\text{rad/s}$

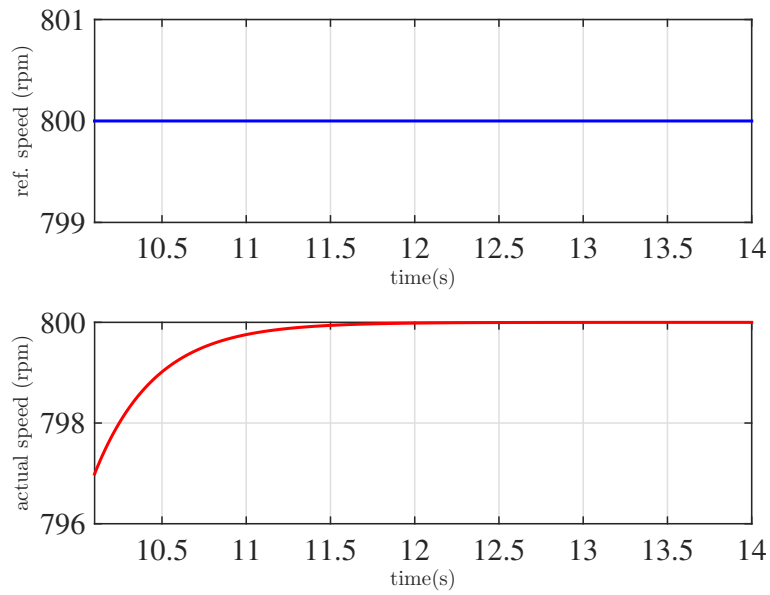


Figure 6.5: Reference, actual speed for $\omega_0 = 60\text{rad/s}$

Figure 6.6 shows the speed tracking when ω_0 is 76 rad/s. A smaller interval of time is selected to highlight the steady state error of 0.1%, when $\omega_0 = 76$ rad/s (Figure 6.7).

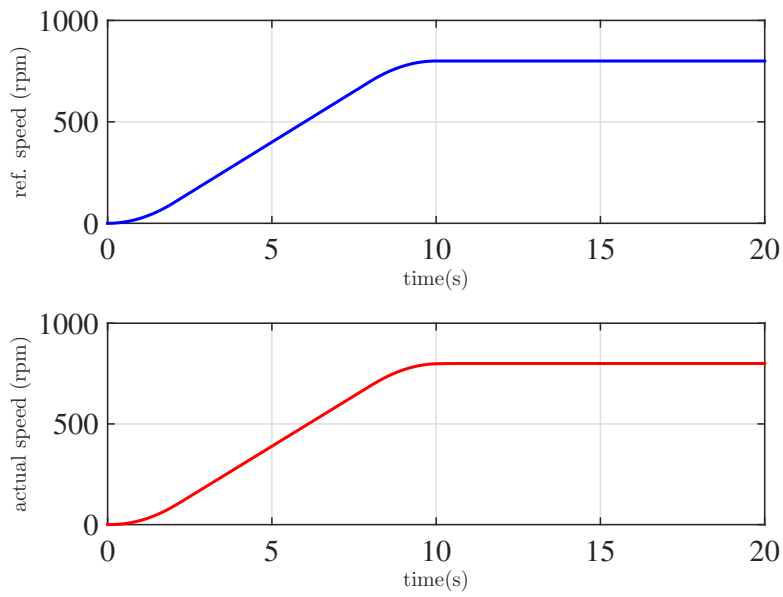


Figure 6.6: Reference, actual speed for $\omega_0 = 76\text{rad/s}$

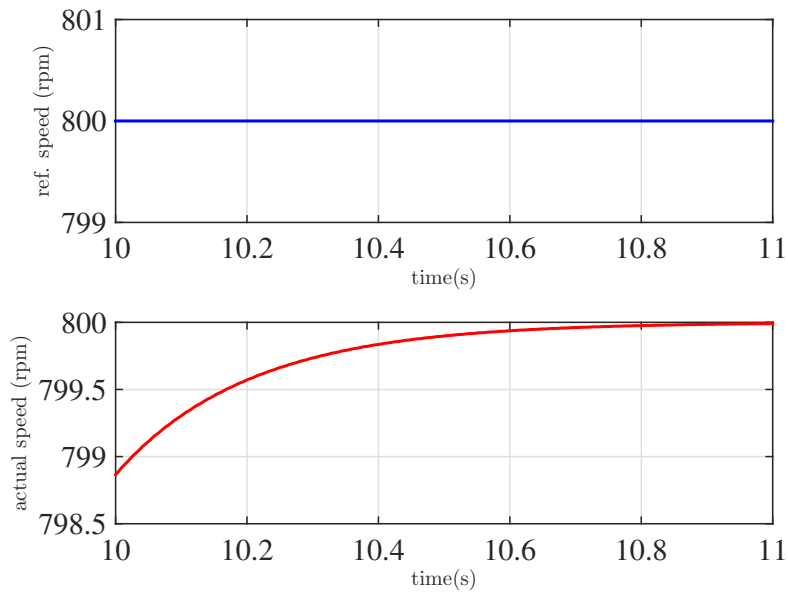


Figure 6.7: Reference, actual speed for $\omega_0 = 76\text{rad/s}$

When $\omega_0 = 77 \text{ rad/s}$, it is seen that the response is oscillating (Figure 6.8) about the reference value which indicates that the response is about to blow up on further increase in ω_0 . Thus this can be treated as the critical bandwidth.

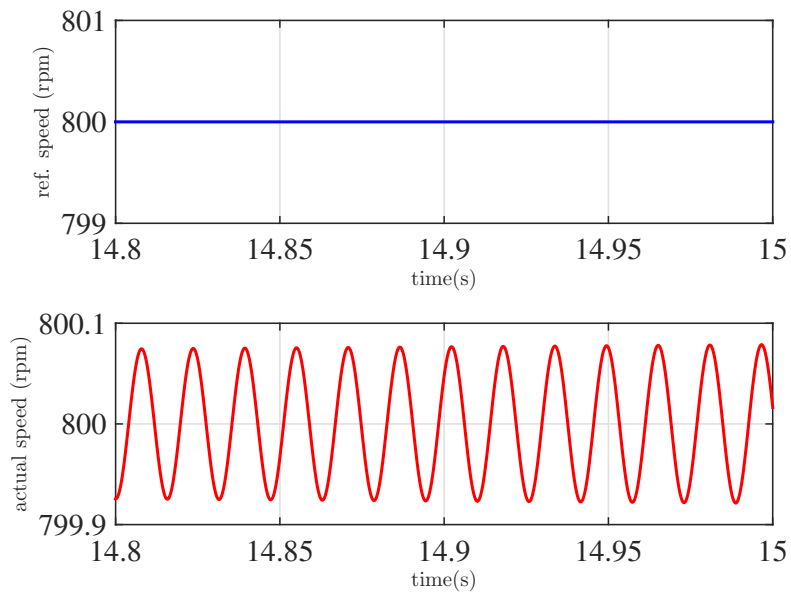


Figure 6.8: Reference, actual speed for $\omega_0 = 77$ rad/s

It is noticed that, a further increase in ω_0 to 78 rad/s, results in total lose of estimation and henceforth tracking.

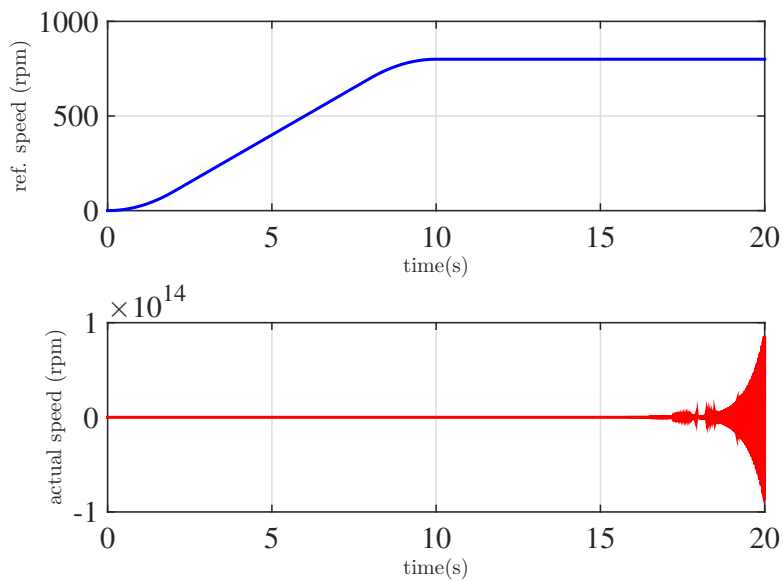


Figure 6.9: Reference, actual speed for $\omega_0 = 78$ rad/s

A detailed analysis on the performance of the controller with variations in observer bandwidth and thereby the controller bandwidth (Equation 6.4) is done till now.

Simulation was extended to analyse the performance of the controller when load is included. A constant torque of 0.6 Nm is applied at $t=15s$ and simulation is carried for 20s. ADRC shows similar performance in tracking even when load is included. In this analysis also, settling time is selected as the parameter under study for an accuracy of 0.1%. The speed tracking is shown when $\omega_0 = 30\text{rad/s}$ in Figure 6.10). The variation u_0 , disturbance estimation and control voltage are also given in Figure 6.11, 6.12 and 6.13 respectively. Here the settling time is greater than 20 s.

When $\omega_0 = 55\text{rad/s}$ (Figure 6.14) the settling time is obtained as 3.09s (Table 6.2), for an accuracy of 0.1%. The settling time has reduced. For this value of ω_0 , the plots of u_0 Vs time (Figure 6.15), disturbance estimation Vs time (Figure 6.16) and control voltage Vs time (Figure 6.17) are also obtained.

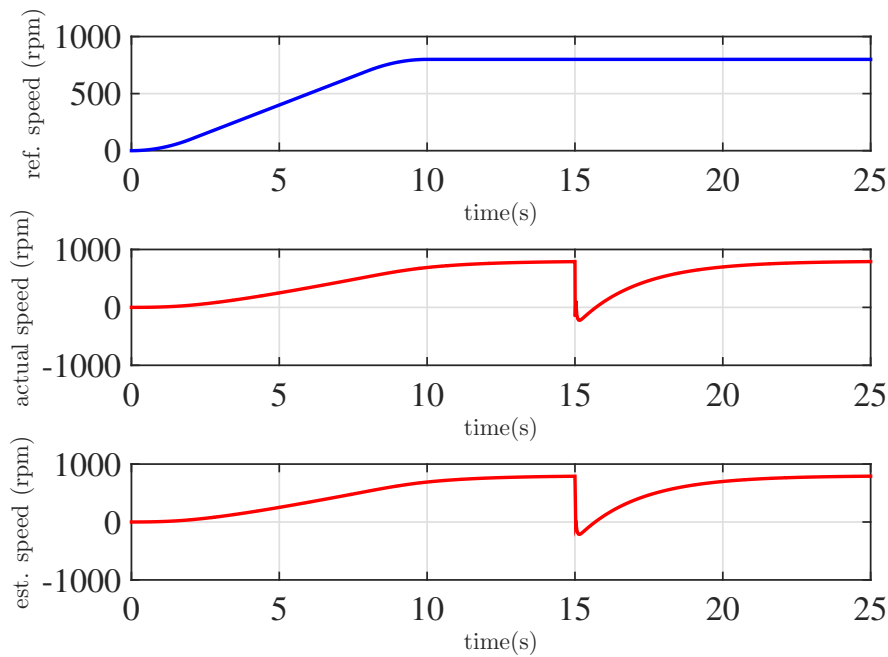


Figure 6.10: Speeds Vs time when $\omega_0 = 30 \text{ rad/s}$

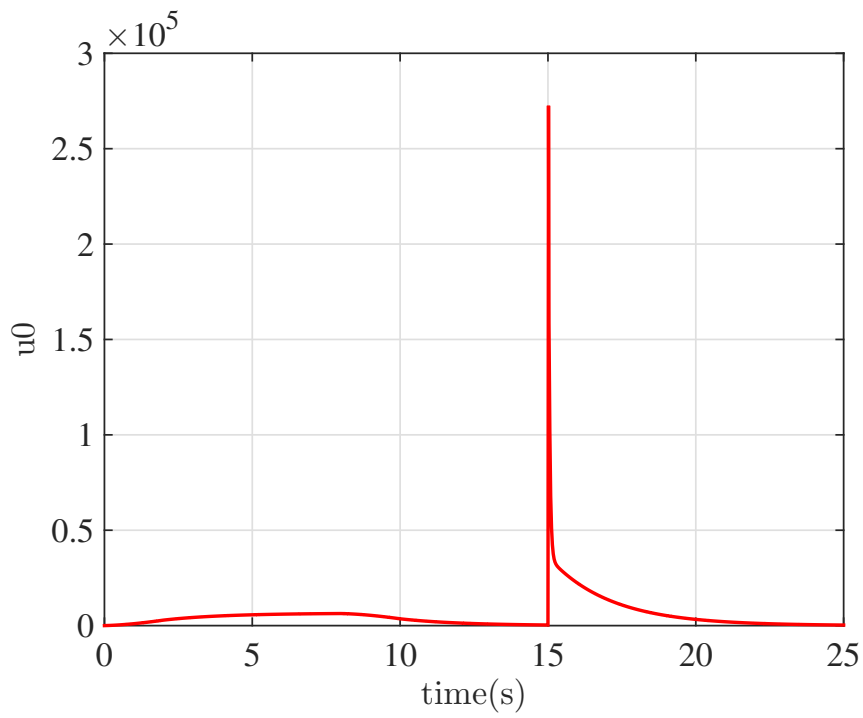


Figure 6.11: u_0 Vs time when $\omega_0 = 30$ rad/s

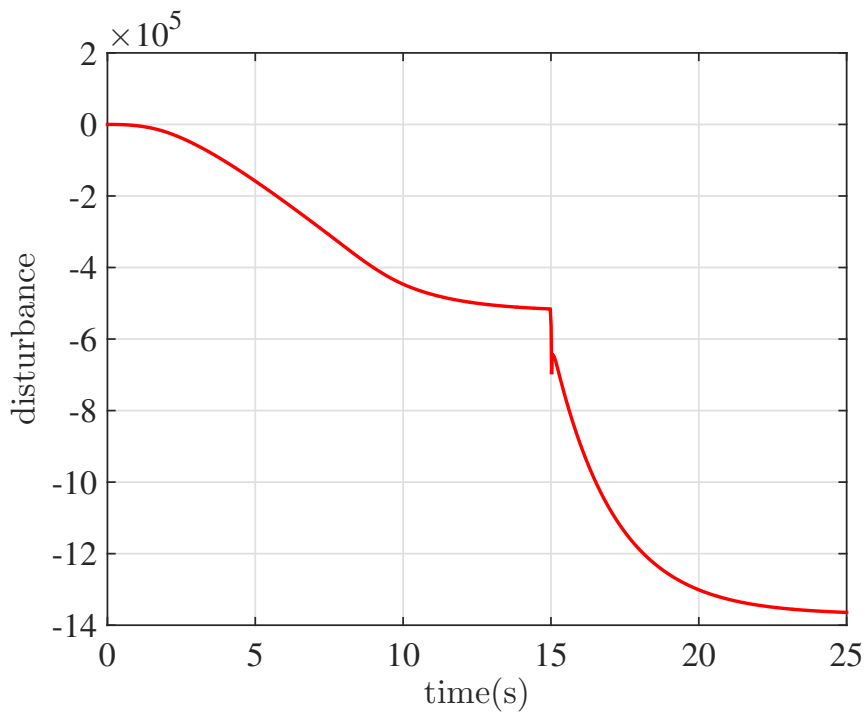


Figure 6.12: Disturbance Vs time when $\omega_0 = 30$ rad/s

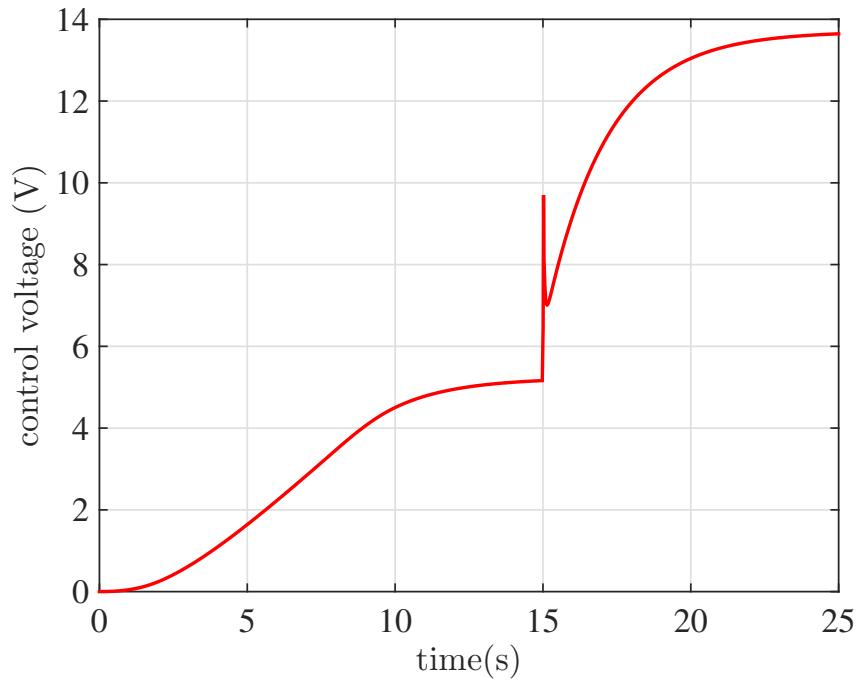


Figure 6.13: Control voltage Vs time when $\omega_0 = 30$ rad/s

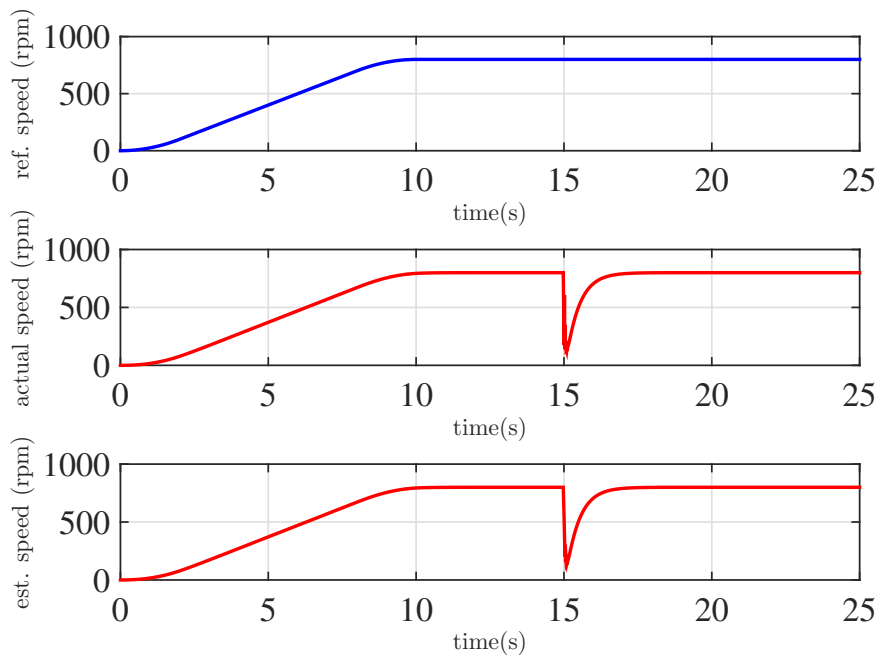


Figure 6.14: Speeds Vs time when $\omega_0 = 55$ rad/s

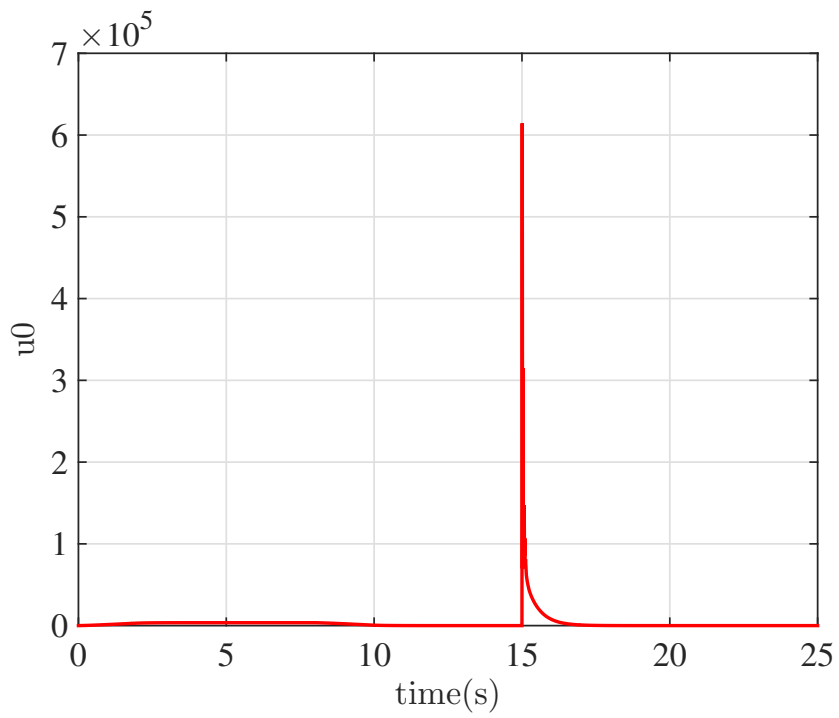


Figure 6.15: u_0 Vs time when $\omega_0 = 55$ rad/s

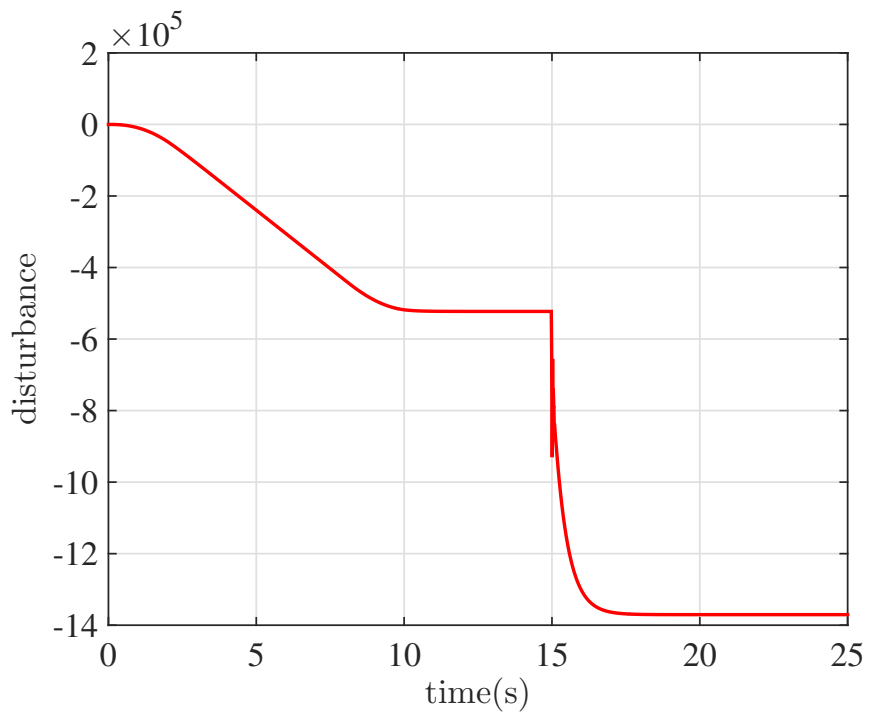


Figure 6.16: Disturbance Vs time when $\omega_0 = 55$ rad/s

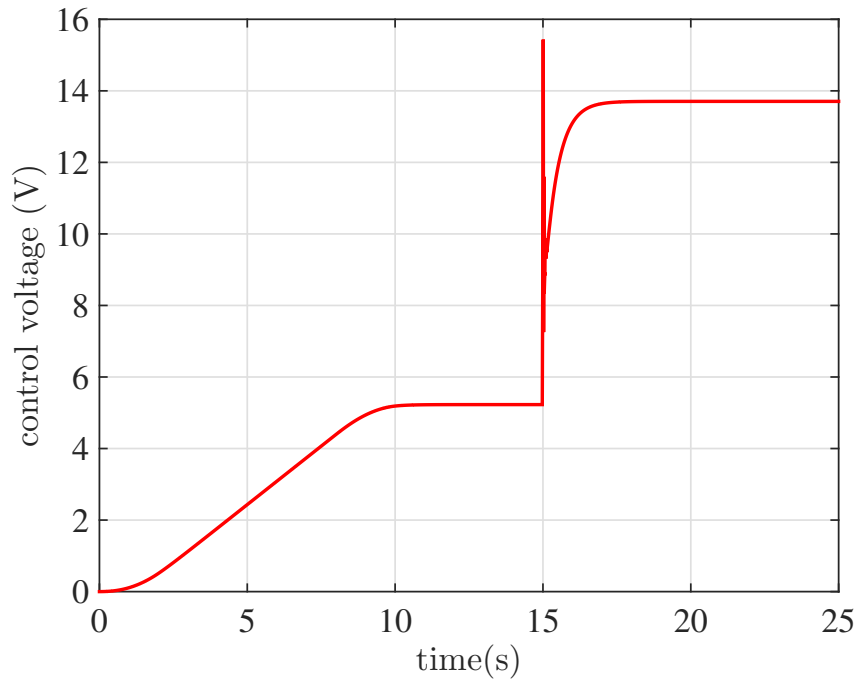


Figure 6.17: Control voltage Vs time when $\omega_0 = 55$ rad/s

A settling time of 1.74s with an accuracy of 0.1% and no overshoot is obtained when $\omega_0 = 70$ rad/s (Figure 6.18). The plots of u_0 Vs time, disturbance estimation Vs time and control voltage Vs time are shown in Figure 6.19, 6.20, 6.21. But as the value of ω_0 increases, it is seen that there is improvement in settling time to 0.013s. However, the tracking takes place with considerable amount of bounded oscillations. As an example $\omega_0 = 74$ rad/s is shown in Figure 6.22. Hence the optimal value of ω_0 is selected as 70 rad/s for which settling time is 1.74s with an accuracy of 0.1%. The standard definition of settling time holds good for 2% and 5% criterion. Hence the choice of 0.1% for % accuracy is justified. When ω_0 exceeds the critical observer bandwidth of 77 rad/s we can note that the estimation is lost which in turn affects the performance of the controller. Figure 6.23, 6.24, 6.25 and 6.26 show the plots of speed, u_0 , disturbance and control voltage versus time for $\omega_0 = 78$ rad/s.

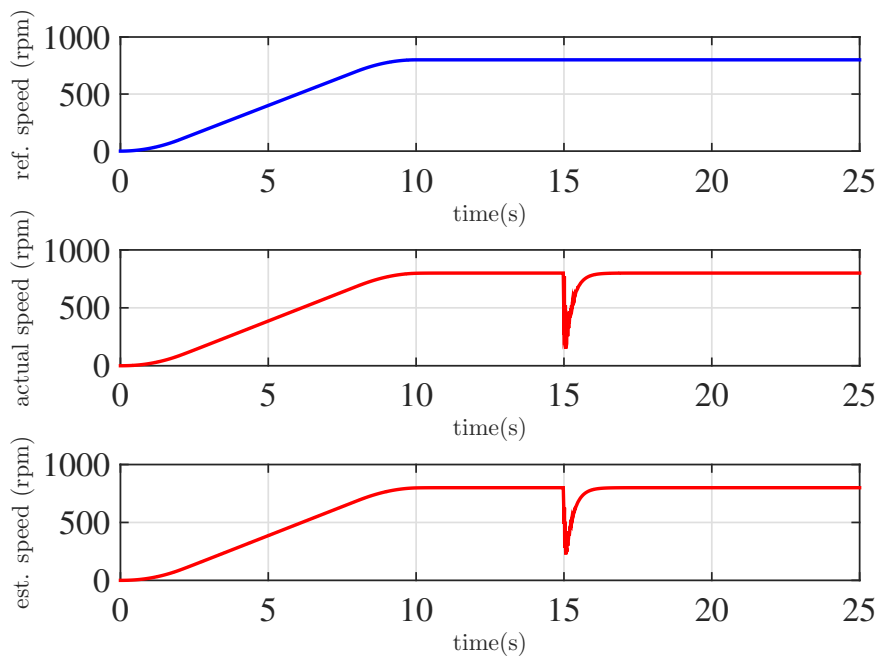


Figure 6.18: Speeds Vs time when $\omega_0 = 70$ rad/s

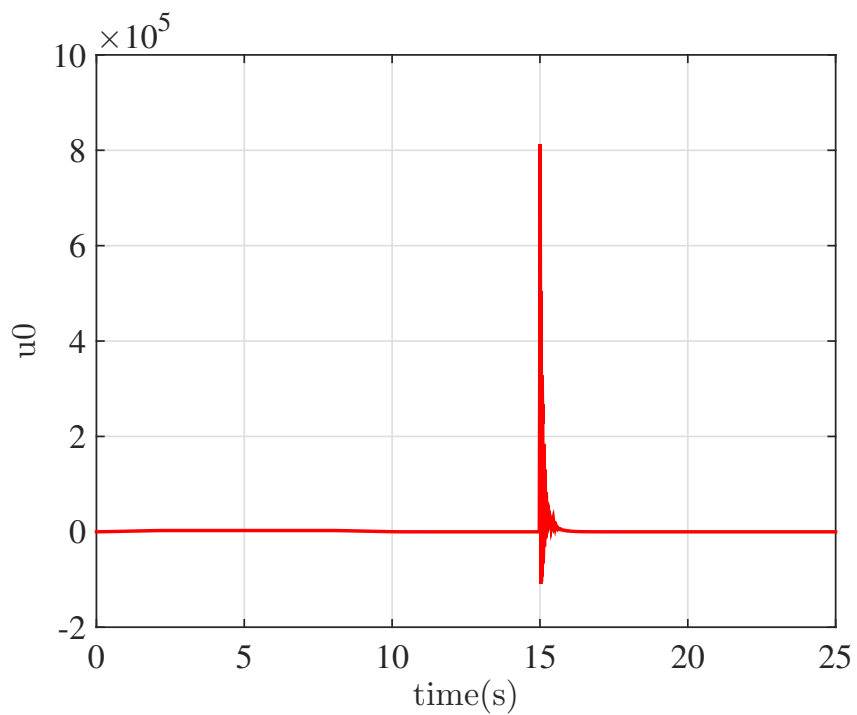


Figure 6.19: u_0 Vs time when $\omega_0 = 70$ rad/s

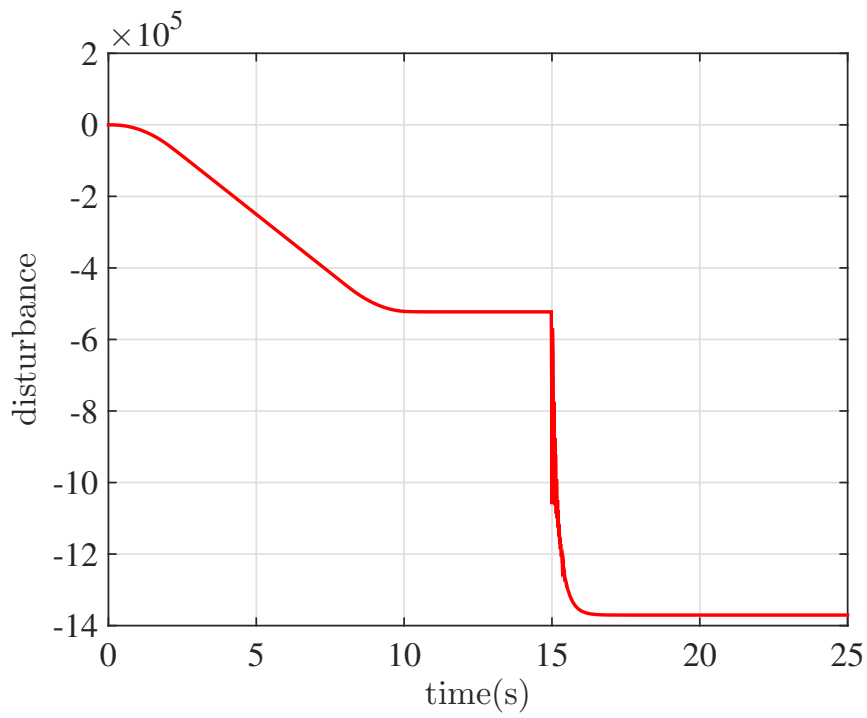


Figure 6.20: Disturbance Vs time when $\omega_0 = 70$ rad/s

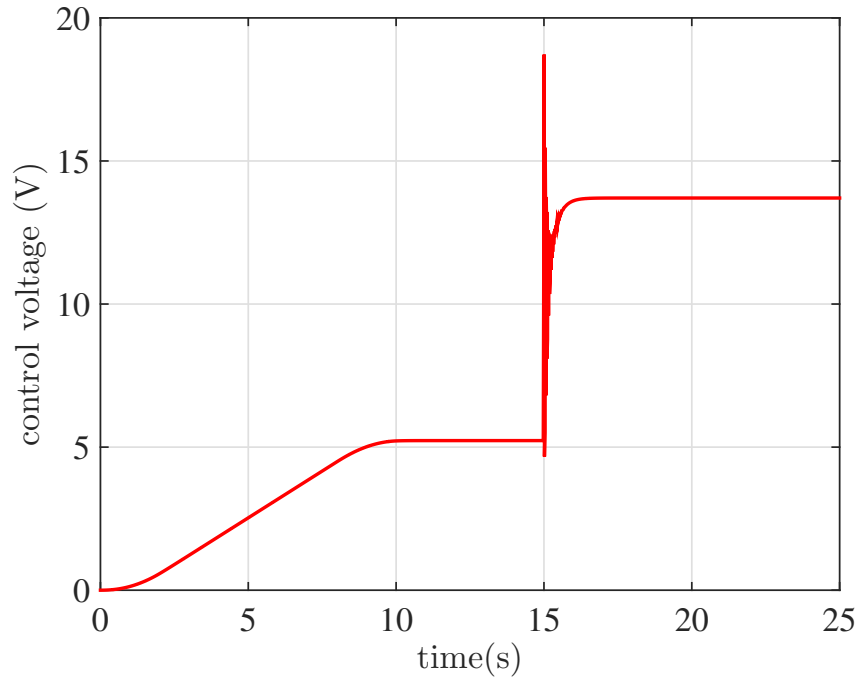


Figure 6.21: Control voltage Vs time when $\omega_0 = 70$ rad/s

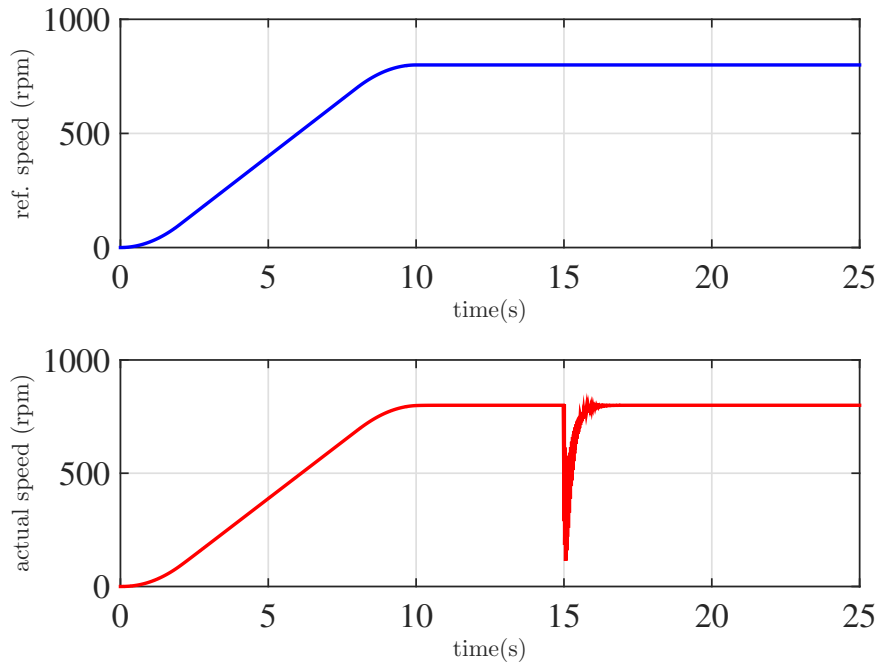


Figure 6.22: Speeds Vs time $\omega_0 = 74\text{rad/s}$

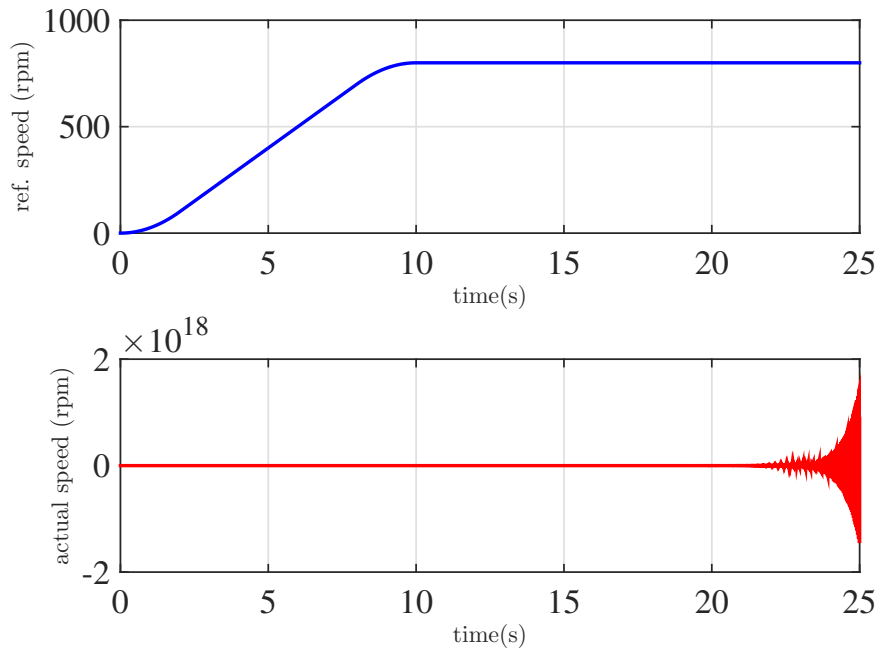


Figure 6.23: Speeds Vs time when $\omega_0 = 78\text{ rad/s}$

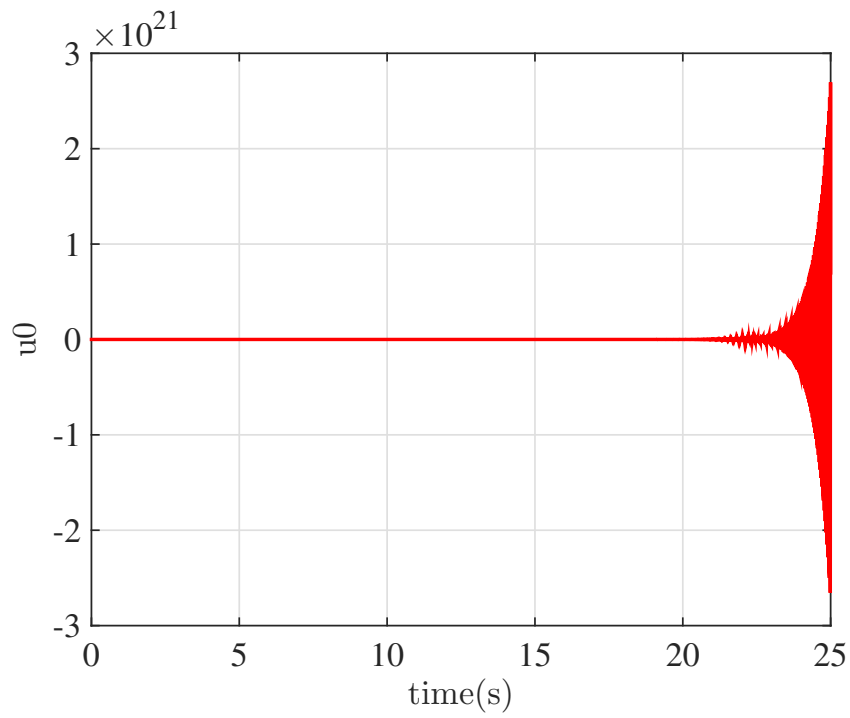


Figure 6.24: u_0 Vs time when $\omega_0 = 78$ rad/s

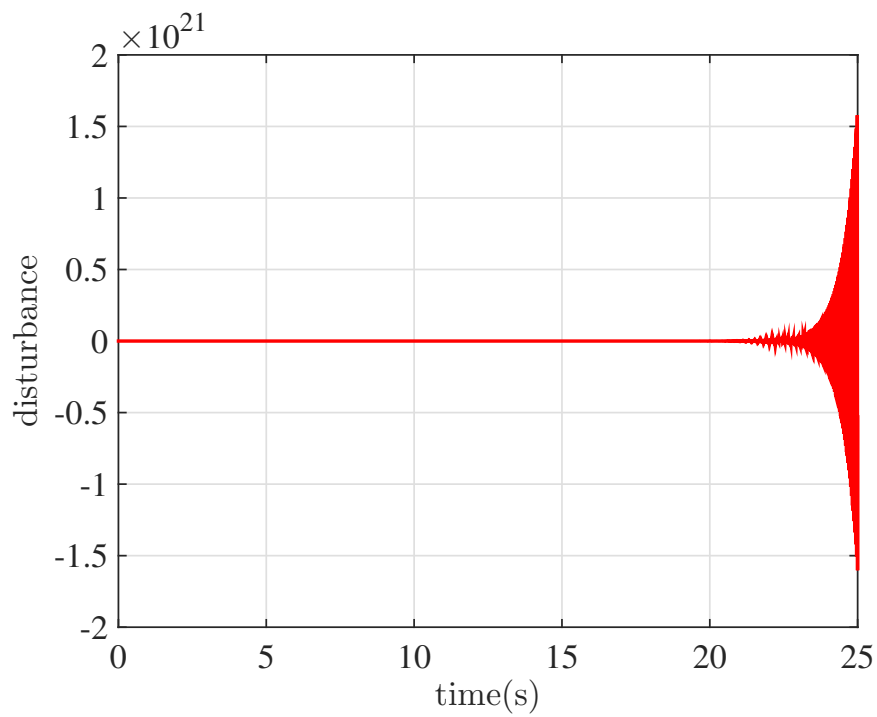


Figure 6.25: Disturbance Vs time when $\omega_0 = 78$ rad/s

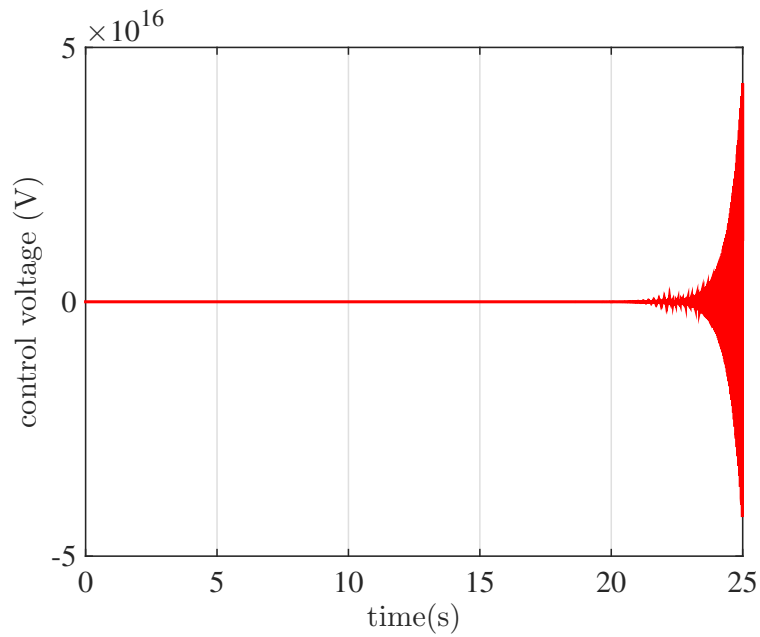


Figure 6.26: Control voltage Vs time when $\omega_0 = 78$ rad/s

6.3 Results and discussions

This chapter discussed the performance analysis of the modified control topology of Active Disturbance Rejection Control (ADRC). The studies reveal that the control performance of ADRC is deeply affected by its counterpart, i.e, the Extended State Observer. Table 6.2 shows that controller performance improves in terms of settling time with an accuracy of 0.1% as the observer bandwidth ω_0 increases when a load is applied to the motor. In Chapter 4, it was noted that the critical observer bandwidth is 77 rad/s. In this analysis also we end up with a similar value of ω_0 as critical observer bandwidth. But in order to ensure reasonable performance of the controller in speed tracking with satisfactory time domain specifications, we select 70 rad/s as the optimal observer bandwidth for the loaded condition, for which the settling time is 1.74s with an accuracy of 0.1% (Table 6.2). Most of the manuscripts use the standard 2% or 5% criterion in estimating the settling time. Hence lesser values of settling time can be noticed in literature. But in this work, in order to establish the potential capability of modified ADRC, the level of accuracy is set high i.e,

Table 6.2: Settling time with an accuracy of 0.1% when a constant torque of 0.6Nm is applied at 15s

ω_0 (rad/s)	settling time (s)
30	> 20
40	> 20
50	3.92
55	3.09
60	2.51
65	2.07
70	1.74
72	1.63
74	0.01
76	0.01
78	does not converge

0.1%. Eventually a value of 1.74s as settling time, seems to be reasonable. Thus the modified topology of ADRC works with reasonable and satisfactory performance. It is established that ADRC is a promising control technique that has only one tuning parameter i.e., ω_0 , the observer bandwidth. The design values primarily depend only on the observer bandwidth (Equation 6.5)

$$\begin{aligned}
 \omega_0 &= 70 \text{ rad/s} \\
 \omega_c &= \frac{\omega_0}{4} \\
 &= 17.5 \text{ rad/s} \\
 K_p &= \omega_c^2 \\
 &= 306.25 \\
 K_d &= 2\zeta\omega_c (\zeta = 1) \\
 &= 35
 \end{aligned} \tag{6.5}$$

For higher values of ω_0 , the disturbance estimation and thereby rejection do not occur properly (Equation 3.13) and we find that the performance of ADRC is affected as a result of performance deterioration of ESO.

CHAPTER 7

HARDWARE IMPLEMENTATION

A performance analysis of ADRC through simulation was detailed in Chapter 6. It was noticed that ADRC is an appropriate replacement for the entrenched PI controller in terms of challenges in tuning and inherent trial and error approach. This chapter reports the details of experiments conducted on ADRC based permanent magnet dc motor, which validates the results obtained in Chapter 6.

7.1 Experimental set up

A testbed to experimentally validate the performance of ADRC in the speed control of a permanent magnet dc motor is developed. Figure 7.1 shows a block schematic representation of the test set up. Hardware unit and Processor unit are the major sections in the implementation.

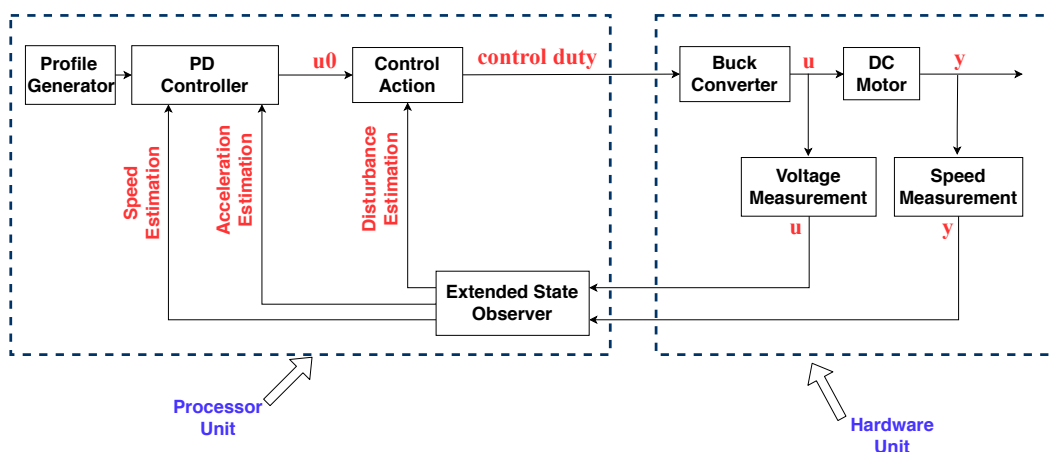


Figure 7.1: Block schematic representation of the test set up

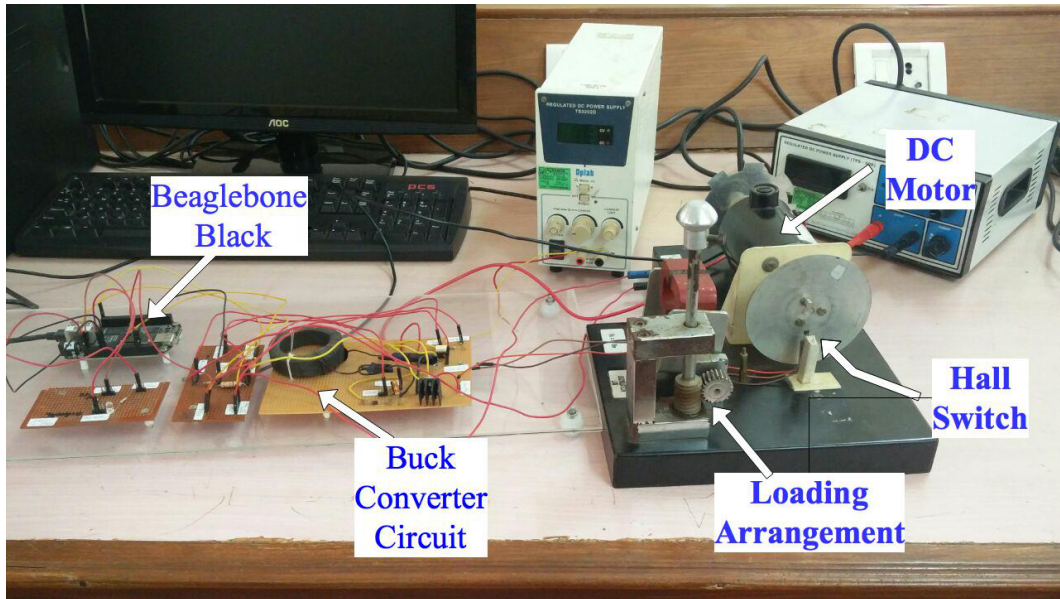


Figure 7.2: Hardware setup

7.1.1 Hardware unit

The entire hardware setup is shown in Figure 7.2. The hardware unit (Figure 7.3) consists of

1. **Permanent magnet dc motor:** A permanent magnet dc motor with a provision for magnetic loading is used as the system whose speed control is analysed (Figure 7.4). The specifications of the dc motor used for the experimental study is given in Sec.5.2. A distinctive feature of ADRC is that it is a model less approach and does not require any motor specification in advance, for the hardware implementation of the controller. It only requires a measure of the control input and the parameter to be controlled.

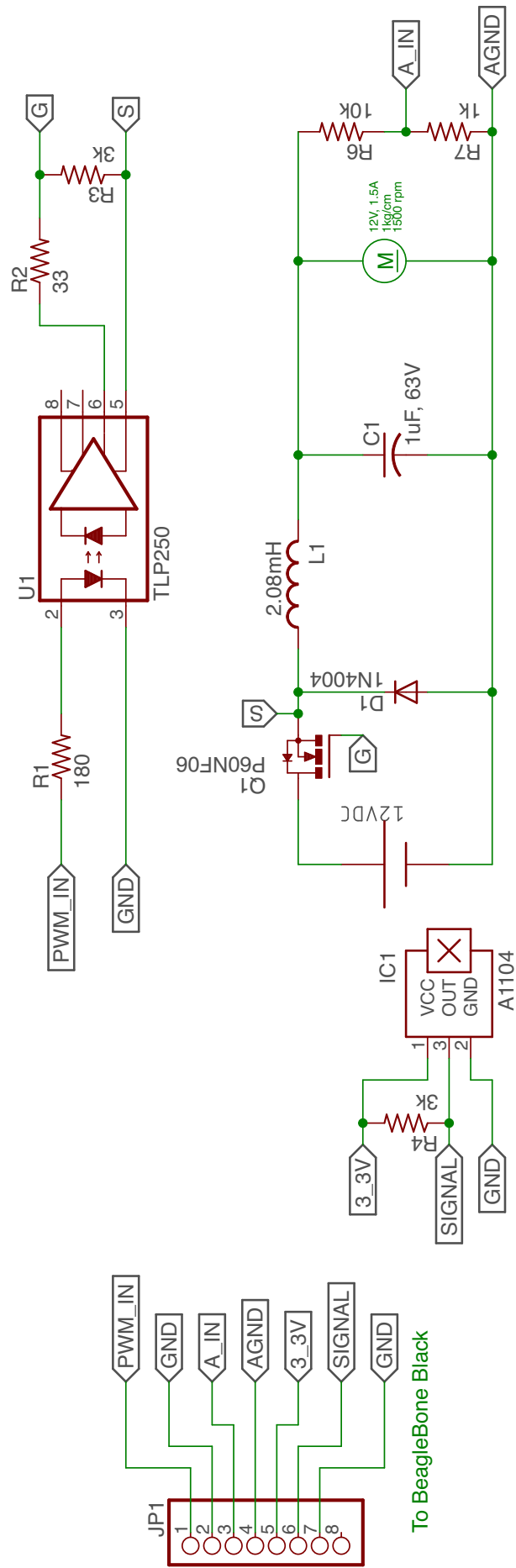


Figure 7.3: Circuit setup for the experimental study

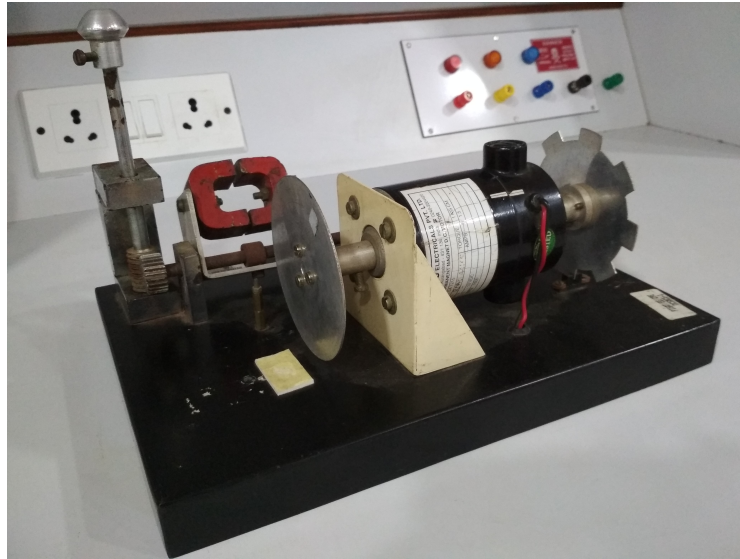


Figure 7.4: Permanent magnet DC motor

2. **Buck converter and its gate driver circuitry:** A buck converter is the simplest non isolated dc-dc converter that can provide required voltage for a dc motor. The circuit set up of the buck converter used in this experiment is shown in Figure 7.5. Here MOSFET P60NF06 is used as the switching device. The input to the buck converter is sourced from a 12V supply. The control signal mathematically calculated (Equation 3.13) by the processing unit, designated as control duty is used for controlling the duty cycle of the semiconductor switch (MOSFET) used in the circuit. This controls the output voltage of the buck converter as given by Equation 7.1.

$$V_o = \frac{T_{on}}{T} * V_s \quad (7.1)$$

The controlled output voltage from the buck converter feeds power to the dc motor.

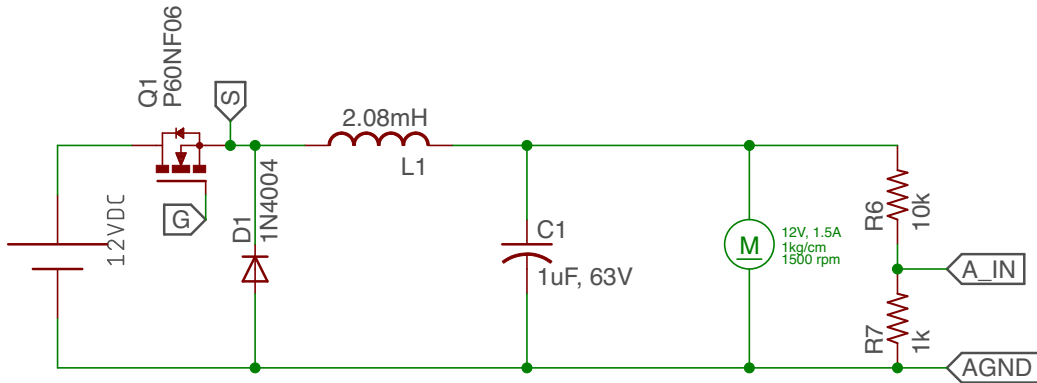


Figure 7.5: Buck converter circuit

The gate of the MOSFET is driven by the processor signal using optocoupler TLP250. This optocoupler isolates the processor unit from the main circuit. A separate power supply is used to power the optocoupler.

3. **Voltage measurement unit:** The control voltage given to the dc motor is measured using a simple potential divider setup (Figure 7.6).

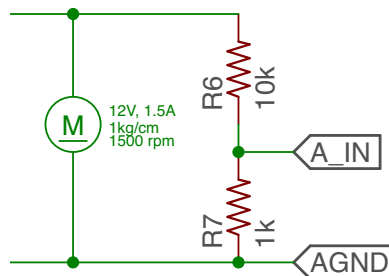


Figure 7.6: Voltage sensing circuit

4. **Speed measurement unit:** A magnetic hall effect digital sensor A1104 (Figure 7.7a) along with neodymium magnet (Figure 7.7b) constitute the speed sensor circuit (Figure 7.8). Hall sensors are transducers that provide output voltage corresponding to the changes in the magnetic field of the sensor. Neodymium magnets are the strongest commercially available magnets (Lucas *et al.*, 2014). The magnet is placed on a disc connected to the shaft of the

motor and the hall sensor is fixed near the magnet so that the magnetic lines properly align with the sensor.



(a) A1104 - hall effect sensor



(b) Neodymium magnet

Figure 7.7: Speed sensing components

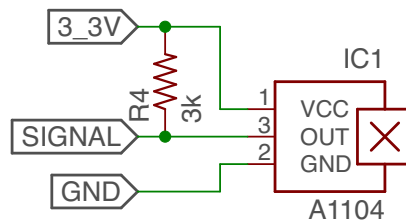


Figure 7.8: Speed sensing circuit

The processor powers the sensor with a voltage of 3.3 V. A pull up resistor is connected between Vcc (pin1) and signal (pin3) to ensure a definite logic level voltage for the processor, even when the switch is open. The signal pin of A1104 is normally held high. When the magnet comes closer to the sensor, the signal level of pin 3 becomes low. This generates a train of pulses which corresponds to the speed of the dc motor. The sensor is calibrated before doing the experiments, using non-contact type tachometer.

These sensor circuits provide necessary inputs to the Extended State Observer (ESO).

7.1.2 Processor unit

The constituent parts of the processor unit are

1. Extended State Observer

2. Profile generator
3. PD controller
4. Control action unit.

The development platform used is Beaglebone Black whose processor unit is a 32 bit ARM Cortex - A8 processor with an operating speed of 1GHz. The sampling period is set as 8ms as it requires ample calculations in every sampling period.

7.2 Realisation of various constituents of Processor unit

For any continuous time state model (Equation 7.2),

$$\begin{aligned}\dot{Z} &= AZ + BU \\ Y &= CZ\end{aligned}\tag{7.2}$$

the solution at $t=T$, is given by Equation 7.3,

$$Z(T) = e^{AT}Z(0) + \left[\int_0^T e^{A(T-\tau)} d\tau \right] BU(0)\tag{7.3}$$

The discrete time state model of Equation 7.2 is given by Equation 7.4, where F and G are discrete time system matrix and discrete time input matrix. The matrices C and D remains unaltered in the the discrete equivalent model. i.e., $C_d = C$ and $D_d = D$.

$$\begin{aligned}Z(k+1) &= FZ(k) + GU(k) \\ Y(k) &= C_d Z(k) + D_d U(k)\end{aligned}\tag{7.4}$$

Let Equation 7.5 gives the solution of the discrete state model after the first sampling, i.e, $Z(1)$, by putting $k=0$.

$$\begin{aligned} Z(1) &= FZ(0) + GU(0) \\ Y(0) &= C_dZ(0) + D_dU(0) \end{aligned} \quad (7.5)$$

Comparing Equation 7.3 and Equation 7.5, we can deduce,

$$\begin{aligned} F &= e^{AT} \\ G &= \left[\int_0^T e^{A(T-\tau)} d\tau \right] B \end{aligned} \quad (7.6)$$

where T is the sampling period. The discussions on ESO and its design in Section 3.6 show that the Extended State Observer is modelled as Equation 7.7 in the continuous time domain (Section 3.6).

$$\begin{aligned} \dot{Z} &= \begin{bmatrix} -g_1 & 1 & 0 \\ -g_2 & 0 & 1 \\ -g_3 & 0 & 0 \end{bmatrix} \begin{bmatrix} z_1 \\ z_2 \\ z_3 \end{bmatrix} + \begin{bmatrix} 0 & g_1 \\ b_0 & g_2 \\ 0 & g_3 \end{bmatrix} \begin{bmatrix} u \\ y \end{bmatrix} \\ \hat{Y} &= \begin{bmatrix} 1 & 0 & 0 \\ 0 & 1 & 0 \\ 0 & 0 & 1 \end{bmatrix} \begin{bmatrix} z_1 \\ z_2 \\ z_3 \end{bmatrix} \end{aligned} \quad (7.7)$$

For the above system, the matrix A and B are

$$\begin{aligned} A &= \begin{bmatrix} -g_1 & 1 & 0 \\ -g_2 & 0 & 1 \\ -g_3 & 0 & 0 \end{bmatrix} = \begin{bmatrix} -3\omega_0 & 1 & 0 \\ -3\omega_0^2 & 0 & 1 \\ -\omega_0^3 & 0 & 0 \end{bmatrix} \\ B &= \begin{bmatrix} 0 & g_1 \\ b_0 & g_2 \\ 0 & g_3 \end{bmatrix} = \begin{bmatrix} 0 & 3\omega_0 \\ b_0 & 3\omega_0^2 \\ 0 & \omega_0^3 \end{bmatrix} \end{aligned}$$

Using the following values for the design (Equation 7.8), F and G are calculated.

$$\begin{aligned}
 \omega_0 &= 70\text{rad/s} \\
 \omega_c &= \frac{\omega_0}{4} \\
 &= 17.5\text{rad/s} \\
 K_p &= \omega_c^2 \\
 &= 306.25 \\
 K_d &= 2\zeta\omega_c(\zeta = 1) \\
 &= 35 \\
 T &= 8\text{ms} \\
 b_0 &= 60
 \end{aligned} \tag{7.8}$$

The entire design depends on the value of ω_0 . Hence the same value of ω_0 is chosen in this hardware implementation too. If ω_0 is fixed, F and G matrices can be calculated in advance, and these matrices can be directly used in the solution (Equation 7.4) to update the states of ESO. This reduces the computational task during the sampling time in the process of control signal generation. For every state vector updation $Z(k+1)$, the inputs required are the previous state vector $Z(k)$ and previous input vector $U(k)$ (Equation 7.4). The previous states and the previous inputs to be used in the solution are properly updated in every 8ms. Here the inputs are control voltage and speed. The estimated outputs z_1 , z_2 and z_3 as in Figure 3.6 are used by the LADRC to implement the control law for u_0 (Equation 3.22). This calculation is also mathematically implemented in the processor. The control action (Equation 3.13) results in a signal which is proportional to the required voltage to be applied to the dc motor. The control action is thus converted to an equivalent duty cycle, which generates a train of pulses with varying duty cycle. The corresponding duty cycle is fed as a train of pulses through the optocoupler to trigger the gate of the switching device in the buck converter. The buck converter gives the equivalent output volt-

age (Equation 7.1). The mathematical equations for ESO, control signal generation of controller and implementation of control law are realised using Python with the support of numpy and scipy libraries.

7.3 Results and Discussions

The reference speed is set as 800rpm in the experimental studies. In Chapter 4 and Chapter 6, $\omega_0 = 70$ rad/s is identified as the optimal observer bandwidth that gives satisfactory hardware and simulated results for ESO and simulated results for ADRC respectively. When ω_0 is 70 rad/s, the estimation time of the response is found to be 0.19s with an accuracy of 0.1% in simulation (Table 4.2). Also, in a time of 0.07s, an accuracy of 0.17% is achieved (Table 6.1). Hence to compare the performance of the controller in simulation as well as experimental studies, ω_0 is selected as 70 rad/s. The speed tracking of the ADRC controlled system when $\omega_0 = 70$ rad/s is shown in Figure 7.9 and Figure 7.10. The error in speed Vs time for the above case is shown in Figure 7.11 and Figure 7.12. The control voltage applied to the motor for this case is shown in Figure 7.13. In all the above results it can be noticed that the simulation and hardware results are well validated.

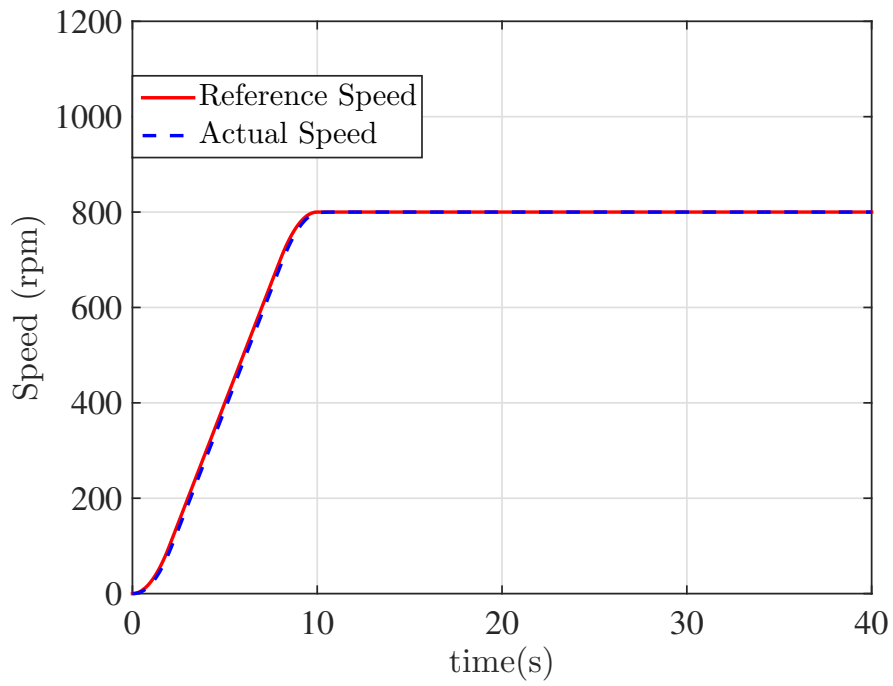


Figure 7.9: Simulation result when $\omega_0 = 70$ rad/s

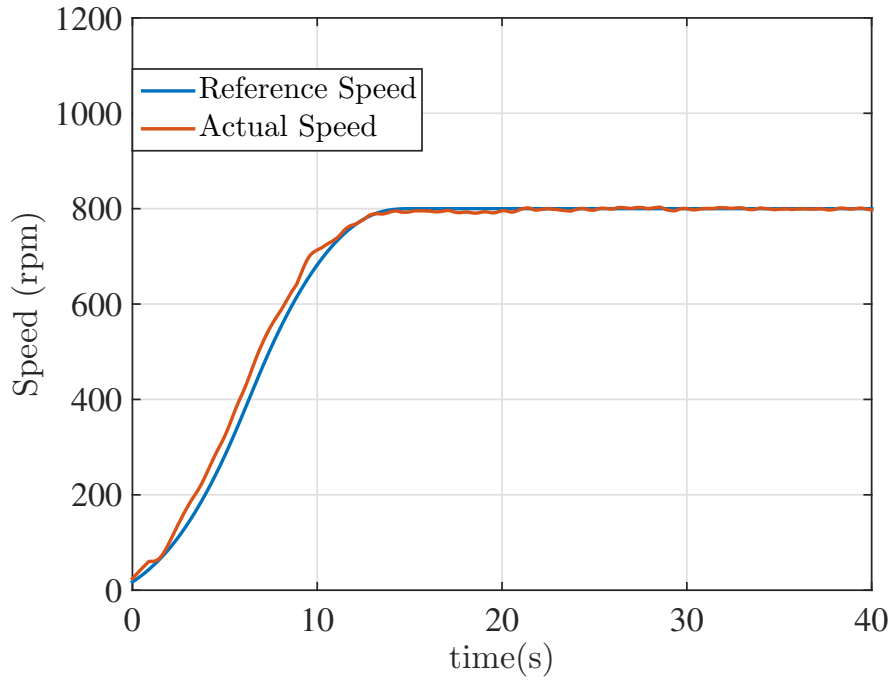


Figure 7.10: Experimental result when $\omega_0 = 70$ rad/s

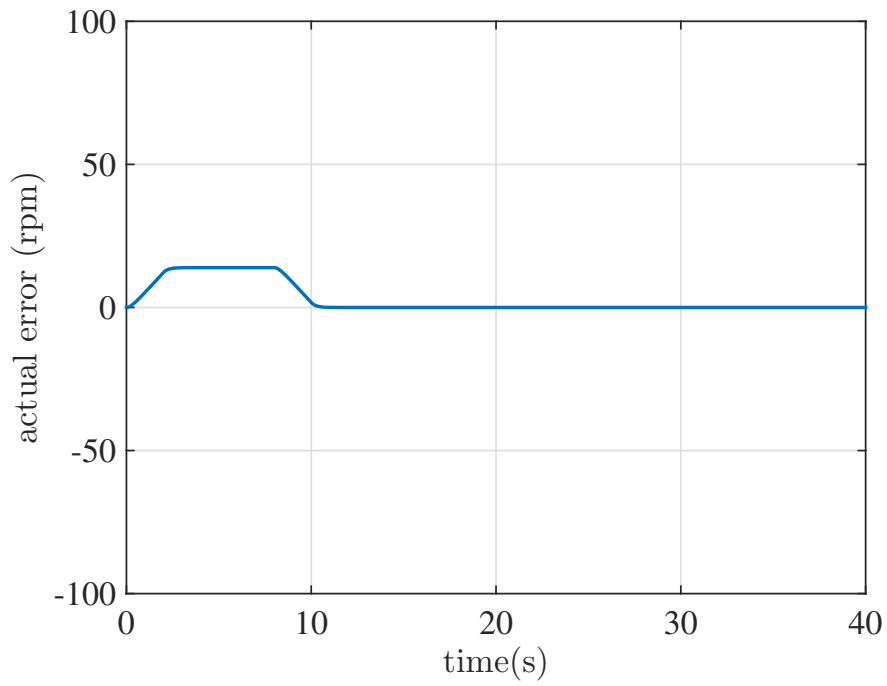


Figure 7.11: Error in speed in simulation when $\omega_0 = 70$ rad/s

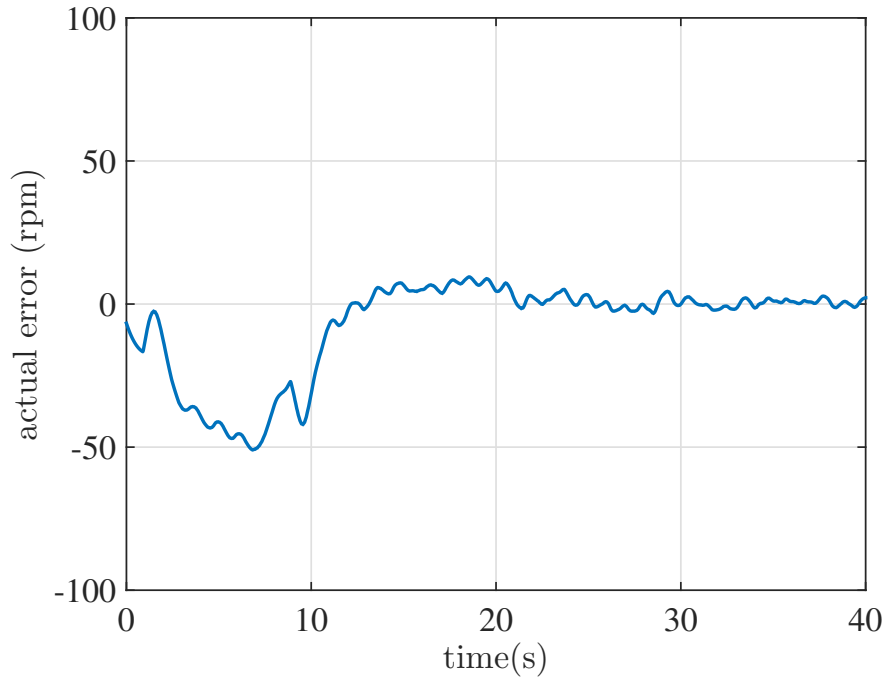


Figure 7.12: Error in speed in experiment when $\omega_0 = 70$ rad/s

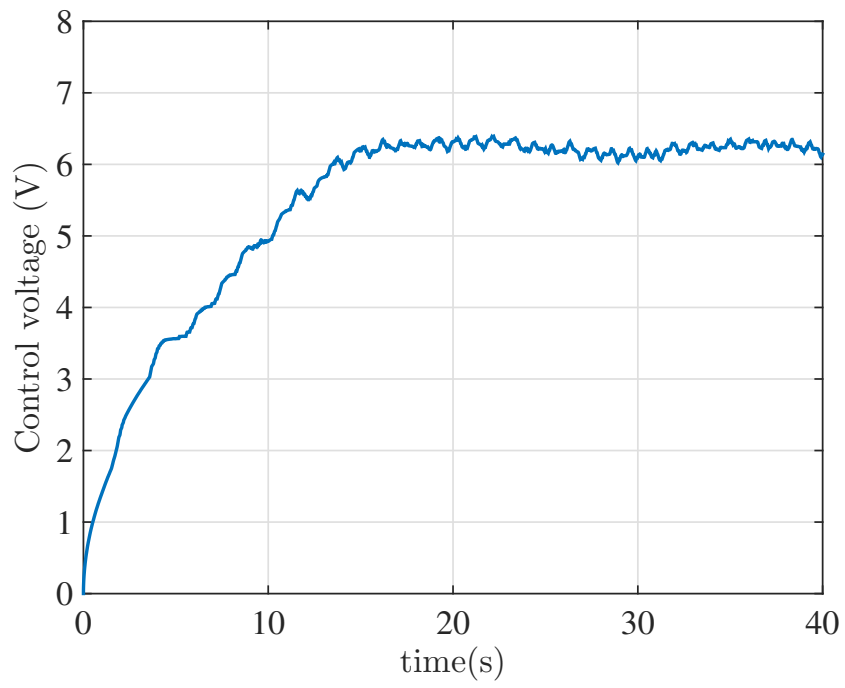


Figure 7.13: Control voltage Vs time

CHAPTER 8

CONCLUSIONS

A promising technology named Active Disturbance Rejection Control is discussed, analysed and applied with modification, in the speed control of permanent magnet dc motor through this research work. The computational capability of Extended State Observer (ESO) to estimate, the external disturbances and uncertainties that would deteriorate the action of the controller, is clearly brought out in this work. One should not overlook the role of ESO in the improved performance of ADRC. Thus the method is found superior to the established PI control, as it a model less, easily tunable approach that easily handles the uncertain dynamics existing in the system and any unwanted external disturbances that creep into system. The feature of ADRC that reduces the complexity in tuning, is a remarkable advancement in industrial control applications.

8.1 Summary

A quantitative performance comparison of ADRC with PI controller through simulations is given in Table 8.1. This reveals that ADRC gives 0% overshoot while PI controller gives 1.25% overshoot for the same system. The 0% overshoot in ADRC is easily obtained by choosing ζ value as 1 in the design of the controller (Equation 7.8). But in Chapter 5 it was noticed that the attempt to reduce the % overshoot resulted in increase of rise time and settling time. Finer tuning may reduce the overshoot of the PI controller but at the cost of increased settling time. But in the case of ADRC it is noticed 0% overshoot and reasonable though larger settling time is obtained with no tuning difficulty.

Table 8.1: A performance comparison of ADRC and PI controller

Particulars	Simulation Results		Experimental Results	
	PI controller	ADRC	PI controller	ADRC
% overshoot	1.25	0	> 40%	0%
settling time	0.04 s	0.07 s	> 50s	0.1s
% error	0.17	0.17	5	1.5
Tuning parameters	2	1	2	1

A controller is developed based on modified Active Disturbance Rejection Control (ADRC) technique for the speed control of a permanent magnet dc motor which can attain the tabulated specifications (Table 8.2). ADRC based system provides an advantage over PI in terms of the effort required in tuning to improve the performance specification, as it is a single parameter tuning approach. The settling time aspect normally reported in literature calculates accuracy for 2% and 5% criterion. Here the maximum % error obtained for estimation is 1.18 % after 0.19 s and that of tracking is 1.5 % after 0.07 s.

Table 8.2: Design Results

SI No	Specification	Simulation	Experiment
1	Observer Bandwidth	70 rad/s	70 rad/s
2	Controller Bandwidth	17.5 rad/s	17.5 rad/s
3	Max % error in estimation after 0.19 s	0.1	1.18
4	Max % error in actual speed after 0.07 s	0.17	1.5
5	% overshoot	0	0

8.2 Observations

The observations unfolded out of this research work are discussed here.

Proper choice of observer bandwidth enhances the performance of ESO and thereby improves the control action of ADRC technique. There is a critical limit for observer bandwidth, beyond which the estimation property of the observer is lost. When ω_0 crosses the critical bandwidth, the speed of estimation becomes too high that, proper estimation of disturbance does not occur. This in turn affects the performance action of the controller which impedes the satisfactory implementation of the control law. When ω_0 increases, faster estimation of uncertainties of the system occurs which easily removes them before it acts on the plant. The % error of the control signal gets improved with an increase in ω_0 , which in turn decreases the % error of the actual speed. An optimal observer bandwidth exists below the critical observer bandwidth, at which sensible transient specifications are met. The present work points to the performance improvement in the time domain specifications in terms of a frequency domain specification, termed observer bandwidth. The performance improvement of ADRC when compared to a PI controller is undoubtedly due to the integration of ESO into the ADRC topology. This is an opening for further studies that relate the frequency domain characteristics and time domain characteristics of ADRC.

8.3 Future scope

Future explorations could be on developing theoretical basis for the boundness of stability of this modified ADRC topology. Further studies can be extended with modifications in the topology of ADRC to increase the robustness of this control technique. Researchers can go further and study on the improvements in performance characteristics by combining ADRC with existing control techniques like

sliding mode control and gain scheduled control. A rough estimate on the order of the system from the fundamental principles is still required for implementing the system. Can we avoid the knowledge of that too in future? From literature it is found that electric power system is not a much explored area where ADRC is applied. It is a vast domain subjected to plenty of unpredicted disturbances. Can ADRC be applied to mitigate the issues resulting out of these unforeseen disruptions? Further research can be done in answering a few questions as mentioned above.

REFERENCES

1. **Anavatti, S. G., F. Santoso, and M. A. Garratt**, Progress in adaptive control systems: past, present, and future. *In Advanced Mechatronics, Intelligent Manufacture, and Industrial Automation (ICAMIMIA), 2015 International Conference on.* IEEE, 2015.
2. **Åström, K. J. and T. Hägglund** (2001). The future of pid control. *Control engineering practice*, **9**(11), 1163–1175.
3. **Basile, G. and G. Marro** (1969). On the observability of linear, time-invariant systems with unknown inputs. *Journal of Optimization theory and applications*, **3**(6), 410–415.
4. **Bellman, R.** (1954). The theory of dynamic programming. *Bulletin of the American Mathematical Society*, **60**(6), 503–515.
5. **Brandin, B.** (1988). A digital approach to the disturbance-accommodation problem. *Transactions of the Institute of Measurement and Control*, **10**(5), 273–280.
6. **Chai, S., D. Li, and X. Yao**, Active disturbance rejection controller for high-order system. *In Control Conference (CCC), 2011 30th Chinese.* IEEE, 2011.
7. **Chandrasekharan, P.**, *Robust control of linear dynamical systems.* Academic Press, 1996.
8. **Chen, X., D. Li, Z. Gao, and C. Wang**, Tuning method for second-order active disturbance rejection control. *In Control Conference (CCC), 2011 30th Chinese.* IEEE, 2011.

9. **Chen, Z., Q. Zheng, and Z. Gao**, Active disturbance rejection control of chemical processes. *In 2007 IEEE International Conference on Control Applications*. IEEE, 2007.
10. **Choi, Y., K. Yang, W. K. Chung, H. R. Kim, and I. H. Suh** (2003). On the robustness and performance of disturbance observers for second-order systems. *IEEE Transactions on Automatic Control*, **48**(2), 315–320.
11. **Csank, J. and Z. Gao**, Uncertainty reduction through active disturbance rejection. *In American Control Conference, 2008*. IEEE, 2008.
12. **Dong, L., P. Kandula, Z. Gao, and D. Wang**, On a robust control system design for an electric power assist steering system. *In Proceedings of the 2010 American Control Conference*. IEEE, 2010.
13. **Dong, L. and Y. Zhang**, On design of a robust load frequency controller for interconnected power systems. *In Proceedings of the 2010 American Control Conference*. IEEE, 2010.
14. **Dong, L., Q. Zheng, and D. Avanesov**, The design and implementation of driving mode control for vibrational gyroscopes. *In 2008 American Control Conference*. IEEE, 2008a.
15. **Dong, L., Q. Zheng, and Z. Gao** (2008b). On control system design for the conventional mode of operation of vibrational gyroscopes. *IEEE Sensors Journal*, **8**(11), 1871–1878.
16. **Dorf, R. C. and R. H. Bishop**, *Modern control systems*. Pearson, 2011.
17. **Dreinhofer, L. H.** (1988). Controller tuning for a slow nonlinear process. *IEEE Control Systems Magazine*, **8**(2), 56–60.
18. **Epstein, A., J. Ffowcs Williams, and E. Greitzer** (1989). Active suppression of aerodynamic instabilities in turbomachines. *Journal of Propulsion and Power*, **5**(2), 204–211.

19. **Esfandiari, F.** and **H. K. Khalil** (1992). Output feedback stabilization of fully linearizable systems. *International Journal of control*, **56**(5), 1007–1037.
20. **Gao, Z.**, Active disturbance rejection control: a paradigm shift in feedback control system design. *In 2006 American control conference*. IEEE, 2006a.
21. **Gao, Z.**, Scaling and bandwidth-parameterization based controller tuning. *In Proceedings of the American control conference*, volume 6. 2006b.
22. **Gao, Z.**, **S. Hu**, and **F. Jiang**, A novel motion control design approach based on active disturbance rejection. *In Decision and Control, 2001. Proceedings of the 40th IEEE Conference on*, volume 5. IEEE, 2001a.
23. **Gao, Z.**, **Y. Huang**, and **J. Han**, An alternative paradigm for control system design. *In Decision and Control, 2001. Proceedings of the 40th IEEE Conference on*, volume 5. IEEE, 2001b.
24. **Goforth, F. J.**, On motion control design and tuning techniques. *In American Control Conference, 2004. Proceedings of the 2004*, volume 1. IEEE, 2004.
25. **Gourishankar, V.**, **P. Kudva**, and **K. Ramar** (1977). Reduced-order observers for multivariable systems with inaccessible disturbance inputs. *International Journal of Control*, **25**(2), 311–319.
26. **Guo, B.-Z.**, **J.-Q. Han**, and **F.-B. Xi** (2002). Linear tracking-differentiator and application to online estimation of the frequency of a sinusoidal signal with random noise perturbation. *International Journal of Systems Science*, **33**(5), 351–358.
27. **Guo, B.-Z.** and **Z.-L. Zhao** (2011). On the convergence of an extended state observer for nonlinear systems with uncertainty. *Systems & Control Letters*, **60**(6), 420–430.
28. **Guo, B.-Z.** and **Z.-L. Zhao** (2013). On convergence of the nonlinear active disturbance rejection control for mimo systems. *SIAM Journal on Control and Optimization*, **51**(2), 1727–1757.

29. **Han, J.** (2009). From pid to active disturbance rejection control. *IEEE transactions on Industrial Electronics*, **56**(3), 900–906.
30. **Han, J.-Q.** (1999). Nonlinear design methods for control systems. *IFAC Proceedings Volumes*, **32**(2), 1531–1536.
31. **Hostetter, G.** and **J. Meditch** (1973). On the generalization of observers to systems with unmeasurable, unknown inputs. *Automatica*, **9**(6), 721–724.
32. **Hou, Y., Z. Gao, F. Jiang,** and **B. T. Boulter**, Active disturbance rejection control for web tension regulation. *In Decision and Control, 2001. Proceedings of the 40th IEEE Conference on*, volume 5. IEEE, 2001.
33. **Huang, Y.** and **W. Xue** (2014). Active disturbance rejection control: methodology and theoretical analysis. *ISA transactions*, **53**(4), 963–976.
34. **Johnson, C.** (1971). Accomodation of external disturbances in linear regulator and servomechanism problems. *IEEE Transactions on automatic control*, **16**(6), 635–644.
35. **Kalman, R. E., P. L. Falb,** and **M. A. Arbib**, *Topics in mathematical system theory*, volume 1. McGraw-Hill New York, 1969.
36. **Kharitonov, V.** (1979). Asymptotic stability of an equilibrium position of a family systems of linear differential equations. *Differential equations*, **14**, 1483–1485.
37. **Kim, J., J. Keller,** and **V. Kumar**, Design and verification of controllers for airships. *In Intelligent Robots and Systems, 2003.(IROS 2003). Proceedings. 2003 IEEE/RSJ International Conference on*, volume 1. IEEE, 2003.
38. **Kotina, R., Q. Zheng, A. J. Van den Bogert,** and **Z. Gao**, Active disturbance rejection control for human postural sway. *In Proceedings of the 2011 American Control Conference*. IEEE, 2011.

39. **Krishnaswamy, P., B. M. Chan, and G. Rangaiah** (1987). Closed-loop tuning of process control systems. *Chemical engineering science*, **42**(9), 2173–2182.
40. **Kuhn, T. S. and D. Hawkins** (1963). The structure of scientific revolutions. *American Journal of Physics*, **31**(7), 554–555.
41. **Kwon, S. and W. K. Chung** (2003a). Combined synthesis of state estimator and perturbation observer. *Journal of dynamic systems, measurement, and control*, **125**(1), 19–26.
42. **Kwon, S. and W. K. Chung** (2003b). A discrete-time design and analysis of perturbation observer for motion control applications. *IEEE Transactions on control systems technology*, **11**(3), 399–407.
43. **Landau, I. D., R. Lozano, M. M'Saad, and A. Karimi**, *Adaptive control: algorithms, analysis and applications*. Springer Science & Business Media, 2011.
44. **Lee, H. S. and M. Tomizuka** (1996). Robust motion controller design for high-accuracy positioning systems. *IEEE Transactions on Industrial Electronics*, **43**(1), 48–55.
45. **Lucas, J., P. Lucas, T. Le Mercier, A. Rollat, and W. G. Davenport**, *Rare earths: science, technology, production and use*. Elsevier, 2014.
46. **Luenberger, D.** (1966). Observers for multivariable systems. *IEEE Transactions on Automatic Control*, **11**(2), 190–197.
47. **Luenberger, D. G.** (1964). Observing the state of a linear system. *IEEE transactions on military electronics*, **8**(2), 74–80.
48. **Marlin, T. E.**, *Process control: designing processes and control systems for dynamic performance*, volume 2. McGraw-Hill New York, 1995.
49. **Maxwell, J. C. et al.** (1868). On governors. *Proceedings of the Royal Society of London*, **16**, 270–283.

50. **Minorsky, N.** (1922). Directional stability of automatically steered bodies. *Journal of the American Society for Naval Engineers*, **34**(2), 280–309.
51. **Müller, P.**, Indirect measurement of nonlinear effects by state observers. *In Nonlinear Dynamics in Engineering Systems*. Springer, 1990, 205–215.
52. **Ogata, K.** and **Y. Yang**, *Modern control engineering*, volume 4. Prentice hall India, 2002.
53. **Ping, Z.** and **Z. Gao**, An fpga-based digital control and communication module for space power management and distribution systems. *In Proceedings of the 2005, American Control Conference, 2005.*. IEEE, 2005.
54. **Pontryagin, L. S.**, *Mathematical theory of optimal processes*. Routledge, 2018.
55. **Profeta, J. A.**, **W. G. Vogt**, and **M. H. Mickle** (1990). Disturbance estimation and compensation in linear systems. *IEEE Transactions on Aerospace and Electronic systems*, **26**(2), 225–231.
56. **Radke, A.** and **Z. Gao**, A survey of state and disturbance observers for practitioners. *In American Control Conference, 2006.* IEEE, 2006.
57. **Schrijver, E.** and **J. Van Dijk** (2002). Disturbance observers for rigid mechanical systems: equivalence, stability, and design. *Journal of Dynamic Systems, Measurement, and Control*, **124**(4), 539–548.
58. **Shamma, J. S.** and **M. Athans** (1992). Gain scheduling: Potential hazards and possible remedies. *IEEE Control Systems*, **12**(3), 101–107.
59. **Slotine, J.**, **J. K. Hedrick**, and **E. A. Misawa** (1987). On sliding observers for nonlinear systems. *Journal of Dynamic Systems, Measurement, and Control*, **109**(3), 245–252.
60. **Su, Y.**, **D. Sun**, and **B. Duan** (2005). Design of an enhanced nonlinear pid controller. *Mechatronics*, **15**(8), 1005–1024.

61. **Sun, B.** and **Z. Gao** (2005). A dsp-based active disturbance rejection control design for a 1-kw h-bridge dc-dc power converter. *IEEE Transactions on Industrial Electronics*, **52**(5), 1271–1277.
62. **Sung, S. W.** and **I.-B. Lee** (1996). Limitations and countermeasures of pid controllers. *Industrial & engineering chemistry research*, **35**(8), 2596–2610.
63. **Tian, G.** and **Z. Gao**, Frequency response analysis of active disturbance rejection based control system. *In 2007 IEEE International Conference on Control Applications*. IEEE, 2007.
64. **Tian, G.** and **Z. Gao**, Benchmark tests of active disturbance rejection control on an industrial motion control platform. *In 2009 American Control Conference*. IEEE, 2009.
65. **Umeno, T.** and **Y. Hori** (1991). Robust speed control of dc servomotors using modern two degrees-of-freedom controller design. *IEEE Transactions on Industrial Electronics*, **38**(5), 363–368.
66. **Utkin, V. I.**, *Sliding modes in control and optimization*. Springer Science & Business Media, 2013.
67. **Veselý, V.** (2013). Robust control methods a systematic survey. *Journal of Electrical Engineering*, **64**(1), 59–64.
68. **Wang, J.**, **L. He**, and **M. Sun**, Application of active disturbance rejection control to integrated flight-propulsion control. *In 2010 Chinese Control and Decision Conference*. IEEE, 2010.
69. **Wang, L.**, **C. Tong**, **Q. Li**, **Y. Yin**, and **Z. Gao**, Disturbance rejection in iron and steel process: problems and current solutions. *In Control Conference (CCC), 2011 30th Chinese*. IEEE, 2011.

70. **Wu, D.** and **K. Chen** (2013). Frequency-domain analysis of nonlinear active disturbance rejection control via the describing function method. *IEEE Transactions on Industrial Electronics*, **60**(9), 3906–3914.
71. **Xue, W.** and **Y. Huang**, On frequency-domain analysis of adrc for uncertain system. *In American Control Conference (ACC), 2013*. IEEE, 2013a.
72. **Xue, W.** and **Y. Huang**, On performance analysis of adrc for nonlinear uncertain systems with unknown dynamics and discontinuous disturbances. *In Control Conference (CCC), 2013 32nd Chinese*. IEEE, 2013b.
73. **Xue, W.** and **Y. Huang** (2015). Performance analysis of active disturbance rejection tracking control for a class of uncertain lti systems. *ISA transactions*, **58**, 133–154.
74. **Yang, K.**, **Y. Choi**, and **W. K. Chung** (2005). On the tracking performance improvement of optical disk drive servo systems using error-based disturbance observer. *IEEE Transactions on Industrial Electronics*, **52**(1), 270–279.
75. **Yang, X.** and **Y. Huang**, Capabilities of extended state observer for estimating uncertainties. *In 2009 American Control Conference*. IEEE, 2009.
76. **Yoo, D.**, **S. S.-T. Yau**, and **Z. Gao**, On convergence of the linear extended state observer. *In 2006 IEEE Conference on Computer Aided Control System Design, 2006 IEEE International Conference on Control Applications, 2006 IEEE International Symposium on Intelligent Control*. IEEE, 2006.
77. **Yoo, D.**, **S.-T. Yau**, and **Z. Gao** (2007). Optimal fast tracking observer bandwidth of the linear extended state observer. *International Journal of Control*, **80**(1), 102–111.
78. **Zhao, C.** and **Y. Huang** (2012). Adrc based input disturbance rejection for minimum-phase plants with unknown orders and/or uncertain relative degrees. *Journal of Systems Science and Complexity*, **25**(4), 625–640.

79. **Zhao, Z.-L.** and **B.-Z. Guo** (2016). On convergence of nonlinear active disturbance rejection control for siso nonlinear systems. *Journal of Dynamical and Control Systems*, **22**(2), 385–412.
80. **Zheng, Q., L. Dong,** and **Z. Gao,** Control and rotation rate estimation of vibrational mems gyroscopes. *In 2007 IEEE International Conference on Control Applications.* IEEE, 2007a.
81. **Zheng, Q., L. Dong, D. H. Lee,** and **Z. Gao,** Active disturbance rejection control for mems gyroscopes. *In 2008 American control conference.* IEEE, 2008.
82. **Zheng, Q., L. Q. Gao,** and **Z. Gao,** On estimation of plant dynamics and disturbance from input-output data in real time. *In 2007 IEEE International Conference on Control Applications.* IEEE, 2007b.
83. **Zheng, Q.** and **Z. Gao** (2005). Motion control design optimization: problem and solutions. *International Journal of Intelligent Control and Systems*, **10**(4), 269–276.
84. **Zheng, Q.** and **Z. Gao,** Disturbance rejection in mems gyroscope: Problems and solutions. *In Control Conference (CCC), 2011 30th Chinese.* IEEE, 2011.
85. **Zheng, Q.** and **Z. Gao** (2016). Active disturbance rejection control: between the formulation in time and the understanding in frequency. *Control Theory and Technology*, **14**(3), 250–259.
86. **Zheng, Q., Z. Gao,** and **W. Tan,** Disturbance rejection in thermal power plants. *In Control Conference (CCC), 2011 30th Chinese.* IEEE, 2011.
87. **Zheng, Q., L. Q. Gaol,** and **Z. Gao,** On stability analysis of active disturbance rejection control for nonlinear time-varying plants with unknown dynamics. *In Decision and Control, 2007 46th IEEE Conference on.* IEEE, 2007c.
88. **Zhou, W.** and **Z. Gao,** An active disturbance rejection approach to tension and velocity regulations in web processing lines. *In 2007 IEEE International Conference on Control Applications.* IEEE, 2007.

89. **Zhou, W., S. Shao, and Z. Gao** (2009). A stability study of the active disturbance rejection control problem by a singular perturbation approach. *Applied Mathematical Sciences*, **3**(10), 491–508.
90. **Zhu, Q. and A. T. Azar**, *Complex system modelling and control through intelligent soft computations*. Springer, 2015.
91. **Ziegler, J. G. and N. B. Nichols** (1942). Optimum settings for automatic controllers. *trans. ASME*, **64**(11).

LIST OF PAPERS BASED ON THESIS

Journals

1. **Parvathy R**, Dr.Asha Elizabeth Daniel and Muhamed Noufal C, Analysis of Extended State Observer and Active Disturbance Rejection Control in the Speed Control of DC motor system, *Mechatronic Systems and Control (formerly Control and Intelligent Systems)*.
2. **Parvathy R**, Dr.Asha Elizabeth Daniel (2014), A Parametric Approach on the Convergence of Controller Parameters in the Design of MIT Rule Based Model Reference Adaptive Controller, *Journal of Innovation in Electronics and Communication Engineering*, 35 - 41.

Conferences

1. **Parvathy R**, Dr.Asha Elizabeth Daniel (2013), A survey on Active Disturbance Rejection Control, *International Multi Conference on Automation, Communication, Computing, Control and Compressed Sensing, Kerala, India*, DOI: 10.1109/iMac4s.2013.6526432.
2. **Parvathy R**, Dr.Asha Elizabeth Daniel (2014), A novel criterion in the design of state observers, *International Conference on Emerging Trends in Instrumentation, Communication, Electrical & Electronics Engineering ICE-ICEE*, organised by Shri Vaishnav Institute of Technology And Science, Indore.
3. **Parvathy R**, Dr.Asha Elizabeth Daniel (2014), A PID controller with sliding model transfer characteristics, 11th *IEEE India Conference INDICON on Emerging Trends And Innovation in Technology, Pune*

CURRICULUM VITAE

PARVATHY R

ASSISTANT PROFESSOR
DEPT. OF ELECTRICAL ENGINEERING
FEDERAL INSTITUTE OF SCIENCE AND TECHNOLOGY (FISAT)
ANGAMALY, KERALA - 683577

Education

Degree	Institution	Period	Remarks
SSLC	Nirmala Bhavan English High School, Thiruvananthapuram	1991 -1992	92.17%
PreDegree	N.S.S College for Women, Neeramankara, Thiruvananthapuram	1992 -1994	79.88%
B.Tech	College of Engineering, Thiruvananthapuram	1994 - 1998	81.36%
M.Tech	I.I.T. Madras	2000 - 2002	8.77 (C.G.P.A)
Ph.D	Cochin University of Science and Technology, Cochin	2010 - 2018	

Fields of research interest

Control Systems, Machine Learning Algorithms

Publications

International Journal	2
International Conference	3
National Conference	4

Personal details

Date of birth	12/11/1976
Gender	Female
Nationality	Indian
e-mail	parvathyrani@gmail.com
Permanent Address	Dwaraka, FISAT Gardens, Mookkannor, Angamaly - 683 577